Progress in Polymer Science 62 (2016) 22–72

Contents lists available at ScienceDirect

Progress in Polymer Science

journal homepage: www.elsevier.com/locate/ppolysci

Recent advances in stereocomplexation of enantiomeric PLA-based copolymers and applications

Zibiao Li[a,1], Beng Hoon Tan[a,1], Tingting Lin[a], Chaobin He[a,b,*]

[a] Institute of Materials Research and Engineering, A*STAR (Agency for Science, Technology and Research), 2 Fusionopolis Way, Innovis, #08-03, Singapore 138634, Singapore

[b] Department of Materials Science and Engineering, National University of Singapore, Singapore 117574, Singapore

ARTICLE INFO

Article history:
Received 7 July 2015
Received in revised form 6 March 2016
Accepted 10 May 2016
Available online 19 May 2016

Keywords:
Stereocomplexation
Biodegradable
Polylactide
Biomedical technology
Material toughening

ABSTRACT

Poly(lactic acid) or poly(lactide) (PLA) is a biodegradable and biocompatible thermoplastic polymer, being derived from renewable resources such as corn and sugar cane. The building block of PLA, lactic acid is chiral and the polymerization of lactic acids (or lactides) leads to isotatic, syndiotatic and atactic/heterotactic PLA primary structures. The stereoselective interaction between two complementary enantiomeric PLLA and PDLA has led to enhanced physical properties such as mechanical properties, thermal resistance and hydrolytic stability compared with the parent polymers. Progress in controlled and/or living polymerization techniques combined with other new synthetic methodologies has facilitated the preparation of PLA-based copolymers with complex architectures such as diblock, triblock, multiblock, star-shape block, comb-shape block and various PLA-grafted structures. The utilization of stereocomplexation strategy to these newly developed copolymers has opened avenues to access a variety of new materials with unique characteristics, including novel chemical functionalities, bioactivities, and smart (responsive to external stimulus) properties tailored for specific applications. This review presents recent advancements in the synthesis of PLA-based block/graft copolymers having complex architectures, with emphasis on the enhanced material performances induced by PLA stereocomplex

Abbreviations: AEBP, 2-azidoethyl-2-bromopropanoate; APCNs, amphiphilic conetworks; ATRP, atom transfer radical polymerization; BBL, β-butyrolactone; Bis A, bisphenol A epoxy; BMA, n-butyl methacrylate; BSA, bovine serum albumin; CAC, critical aggregation concentration; CDI, N,N′-carbonyldiimidazole; CDSA, crystallization-driven self-assembly; CGC, critical gelation concentration; CMC, critical micellization concentration; CPC, cationic polycarbonate; CRP, controlled radical polymerization; DBI, 1,4-diisocyanatobutane; DBU, 1,8-diazabicyclo[5.4.0]undec-7-ene; Dex, dextran; DP, degree of polymerization; DSC, differential scanning calorimetry; EEGE, ethoxyethyl glycidyl ether; F127, PEG-PPG-PEG; FITC, fluorescein isothiocyanate; LCST, lower critical solution temperature; LS, light scattering analysis; MPC, 2-methacryloyloxyethyl phosphorylcholine; mPEG, monomethoxy poly(ethylene glycol); Mw, molecular weight; OVA, ovalbumin; PAA, poly(acrylic acid); PBGMA, poly(benzylidene glycerol methacrylate); PBS, poly(butylene succinate); PCL, poly(caprolactone); PDLA, poly(D-lactic acid); PDMAEMA, poly(N,N-dimethylamino-2-ethyl methacrylate); PEG, poly(ethylene glycol); PEGMA, poly(ethylene glycol) methyl ester acrylate; PG, polyglycerol; PH, poly(L-histidine); PHB, poly(hydroxybutyrate); Phe, L-phenylalanine; pHPMAm, poly(2-hydroxypropylmethacrylamide); PIGMA, poly(isoglycerol methacrylate); PLLA, poly(L-lactic acid); PMTC, poly(methylcarboxytrimethylene carbonate); PNIPAAm, poly(N-isopropylacrylamide); POM, polarized optical microscopy; POSS, polyhedral oligomeric silsesquioxanes; PPG, poly(propylene glycol); PRA, poly(ricinoleic acid); PRX, polyrotaxane; PS, polystyrene; ROP, ring opening polymerization; SA/MPDC, poly(3-methy-1,5-pentylene succinate); sc-CO_2, supercritical carbon dioxide; SET-LRP, single-electron transfer living radical polymerization; SSP, solid-state polycondensation; TEA, trimethylamine; vdW, van der Waals; XRD, X-ray diffraction; γ-PGA, poly(γ-glutamic acid).

* Corresponding author at: Department of Materials Science and Engineering, National University of Singapore, Singapore 117574, Singapore; and Institute of Materials Research and Engineering, A*STAR (Agency for Science, Technology and Research), 2 Fusionopolis Way, Innovis, #08-03, Singapore 138634, Singapore.

E-mail addresses: msehc@nus.edu.sg, cb-he@imre.a-star.edu.sg (C. He).

[1] Both these authors made an equal contribution to this work.

http://dx.doi.org/10.1016/j.progpolymsci.2016.05.003

formation. The origin of the enhanced thermal mechanical property observed in PLA stereocomplex is first discussed. The strong interaction resulted from stereocomplexation in PLA based copolymers could be exploited not only for fabrication of advanced therapeutic delivery carriers and tissue engineering devices, but also for stabilizing colloidal systems in microparticles, micelles and hydrogels, that further broaden the applications of PLA that could not have been attained with single PLLA or its copolymers. The stereocomplexation could also be used to tailor the interface interactions between fillers and PLA matrix that lead to higher strength and toughness of PLA.

Contents

1. Introduction

1.1. Polylactic acid and stereocomplexation

Stereocomplexation between poly(L-lactide) (PLLA) and poly(D-lactide) (PDLA), that occurs in situ at physiological conditions and simple mixing, is of great interest in materials science, as the stereocomplex formed between the left-handed PLLA and right-handed PDLA polymeric helices has been shown to possess improved mechanical and thermal properties when compared with the homochiral polymers [1–3]. In this section, the PLA polymorphs will be reviewed and the origin of enhancement in thermal mechanical property observed in stereocomplex PLA will be discussed. This is followed by the detail discussion in the next few sections on the recent advances in the synthesis of PLA-based copolymers having block- and graft-architectures, with special focus on the significant impact of PLA stereocomplex formation on improving material properties. The exploitation of PLA stereocomplexation towards potential applications in controlled delivery of biologically actives [4–12] as well as cell and tissue engineering scaffolds [13–18], fabrication of stabilized colloidal systems [8,15,19–28] and toughening of PLA in different composites as high performance materials [29–32] will also be discussed.

1.2. Poly(lactic acid) polymorphs

The research interests in PLA arise not only from its environmentally benign synthesis and potential applications, but also from the diversity of its polymer chain architectures and crystal structures – polymorphism. The building block of PLA, i.e., lactic acid (2-hydroxypropanoic acid, $C_3H_6O_3$) is chiral (Scheme 1). Two lactic acid molecules

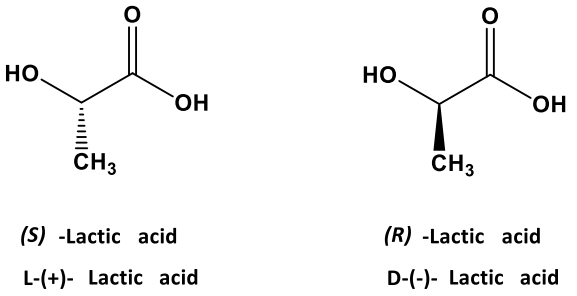

Scheme 1. Two enantiomeric forms of lactic acid: (*S*)- and (*R*)- 2-hydroxypropionic acid.

can be dehydrated to make one lactide, a cyclic lactone. As a result, three stereoisomers of lactide can be formed, namely D,D-lactide (D-lactide), L,L-lactide (L-lactide) and D,L-lactide (or meso-lactide). Polymerization of lactic acids (or lactides) leads to isotatic, syndiotatic and atactic/heterotactic PLA primary structures (Scheme 2). While the atactic PLA is amorphous, both the isotactic poly(L-lactic acid) (PLLA) and poly(D-lactic acid) (PDLA) are highly crystalline. Like many other semicrystalline polymers, polymorphic crystallization has been observed in PLA. For both PLLA and PDLA, at least three polymorphs (α-, β-, and γ-form) have been observed as shown in Figs. 1(a)–(c) [33–36]. The recent discovery that α′-form crystallized at lower temperature has been considered a limiting disordered modification of the α-form [37]. More importantly due to the chirality of PLA, blending of PLLA with PDLA can form stereocomplex – a new crystalline modification (as shown in Fig. 1(d)) with unique properties and high performance [1,3,33,38].

1.3. The origin of enhanced thermal mechanical property

It has been shown experimentally that the formation of stereocomplex between poly(L-lactic acid) (PLLA) and poly(D-lactic acid) (PDLA) significantly improved thermal stability and mechanical properties. Unit cell models of the four different PLA crystal forms have been proposed in the literature based on a comparison of X-ray diffraction (XRD) patterns with classical molecular mechanics modelling. In general PLA is semicrystalline with a melting temperature (T_m) of around 180 °C and a glass transition temperature (T_g) of about 60 °C. In certain conditions, PLLA or PDLA can crystallize in one of the three different single crystalline phases: α-, β- and γ-form [33,34]. More importantly, an equimolar physical blend of PLLA with PDLA creates a new crystal structure – stereocomplex (sc)-form with a T_m of 230 °C, about 50 °C higher than either of the two enantiomeric polymers [38]. Systematic theoretical studies on the energetic, structural, electronic, elastic, vibration and dielectric properties of PLA polymorphs were performed by employing the first-principles method in the framework of density functional theory (DFT) self-consistent field (SCF) calculations within the generalized-gradient approximation (GGA) [39–41]. These computer modelling provide a theoretical understanding on the mechanism behind the observed superior thermal stability of stereocomplexation of PLA and the intermolecular interactions in PLA crystals. The polymorphs of PLA were investigated from a first-principles theoretical perspective to understand the intermolecular interaction in the crystals [41]. Using the unit cell structures obtained by X-ray data as the starting structures for the DFT geometry optimization, the properties of crystalline PLA were then obtained from the DFT optimized unit cells.

The DFT calculation results showed that sc-form is the most energy-favorable among the four identified PLA polymorphs. The sc-form is thermodynamically more stable than α-, β-, and γ-form by 0.3, 1.1, and 1.3 kcal/mol (scaled to one repeat unit of PLA), respectively. The theoretical predicted relative stability trend is well correlated to the melting temperature order reported in the literature:

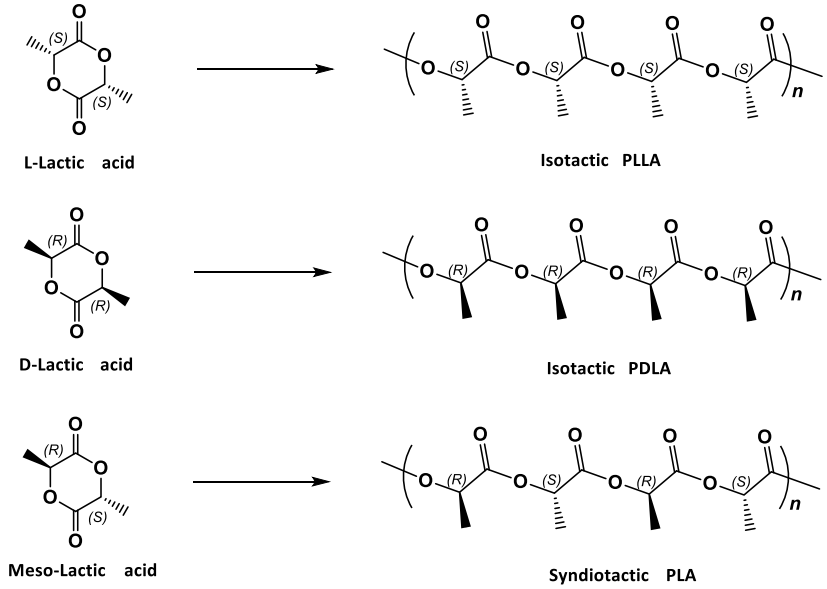

Scheme 2. Three stereoisomers of lactide which lead to distinct PLA structures upon polymerization.

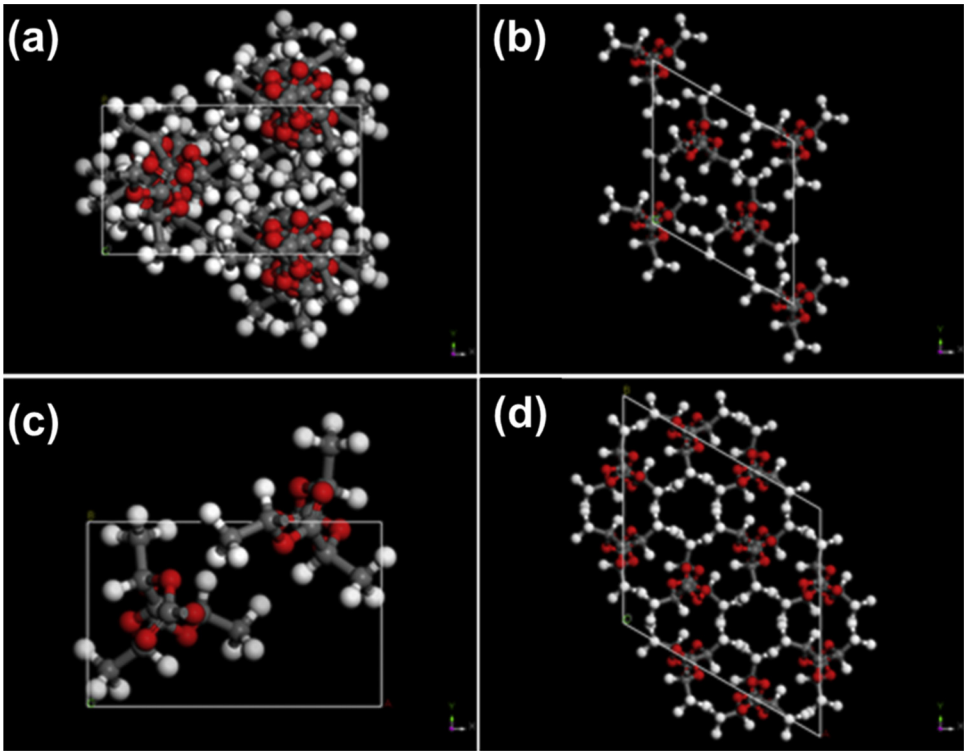

Fig. 1. Three unit cells of PLLA (top view): (a) α-form; (b) β-form and (c) γ-form, (d) sc-form, PLLA:PDLA = 1:1 stereocomplexation unit cell. These PLA crystal unit cells were built by using materials studio based on the previously published crystallographic data [33–36].

sc-PLA (230 °C) > α-PLA (185 °C) > β-PLA (175 °C). By further analyzing non-conventional hydrogen-bonds (H-bond) in the DFT optimized PLA crystalline structures, intermolecular H-bond C^{α}—H···$O_{carbonyl}$ existed in the stereocomplex only, as shown in Fig. 2. Moreover this H-bond had larger angle ∠CHO (obtuse) and shorter distance than those of intramolecular C^{α}—H···$O_{carbonyl}$ H-bond, and was thus much stronger. The enhanced stability of stereocomplex could be attributed to the much stronger and unique intermolecular H-bond network found in this crystal. The stiffness and compliance matrices of α-, β- studied sc-form employing a DFT stress–strain method showed that these tensors are highly anisotropic [39]. The stiffness coefficient along the polymer helix axis direction (c_{33}) is greater than those in the transverse directions (c_{11} and c_{22}). In addition, those of β- and sc-forms are transversely isotropic due to their crystal symmetries. The sc-form has a higher Young's modulus and less compressibility than the β-form on the transverse plane. Contributions from the crystalline phase to the anisotropy of the elastic modulus in a uniaxial oriented PLA fiber were estimated based on a cylindrically symmetric polycrystalline aggregate model. Both symmetry and orientation distribution of the crystals were taken into account. Voigt and Reuss bonds of Young's moduli, shear moduli and Poisson's ratio were also predicted based on the single crystal elastic properties obtained [39]. Furthermore, intrinsic dielectric properties of the PLA crystals were calculated using density functional perturbation theory (DFPT) method [40]. The permittivity and polarizability tensors of these PLA single crystals are anisotropic too. Among the three diagonal components of these tensors, the longitudinal component along the PLA helical axis (parallel to *z* axis) is larger than the two lateral components. The calculated averaged value of DC permittivity of the PLLA α-form is close to the published value of 2.71 measured at 1 kHz. The theoretical birefringence estimated from optical permittivity is also within the experimental range ~ 0.03. A DFPT calculation of IR the spectra of PLLA α-, β-, γ- and sc-forms (Fig. 3) shows that: (1) The carbonyl C=O stretching region (Fig. 3(b)) has only one sharp narrow peak in the stereocomplex while there are five peaks in PLLA α-form and three peaks in PLLA β-form. Moreover, this prominent sc ν(C=O) peak is located at lower wavenumbers; (2) The locations of three distinct bands, $\nu_s(CH_3)$, $\nu(C^{\alpha}—H)$, and $\nu_{as}(CH_3)$ are shown in (Fig. 3(c)). These are characteristic bands of the stereocomplex: the bands in the α-PLLA are spread out whereas the $\nu(C^{\alpha}—H)$ and $\nu_s(CH_3)$ bands overlap and merge into one wide band [40]. This may be due to the more distorted 10_3 helices in the PLLA α-form while sc-form has high symmetry restriction, as shown in Fig. 2.

The strong intermolecular interaction in the PLA stereocomplex, experimentally observed and confirmed via first principle calculation forms a basis for its potential applications ranging from tailoring the filler-matrix interaction in polymer composite to moderating the micelle

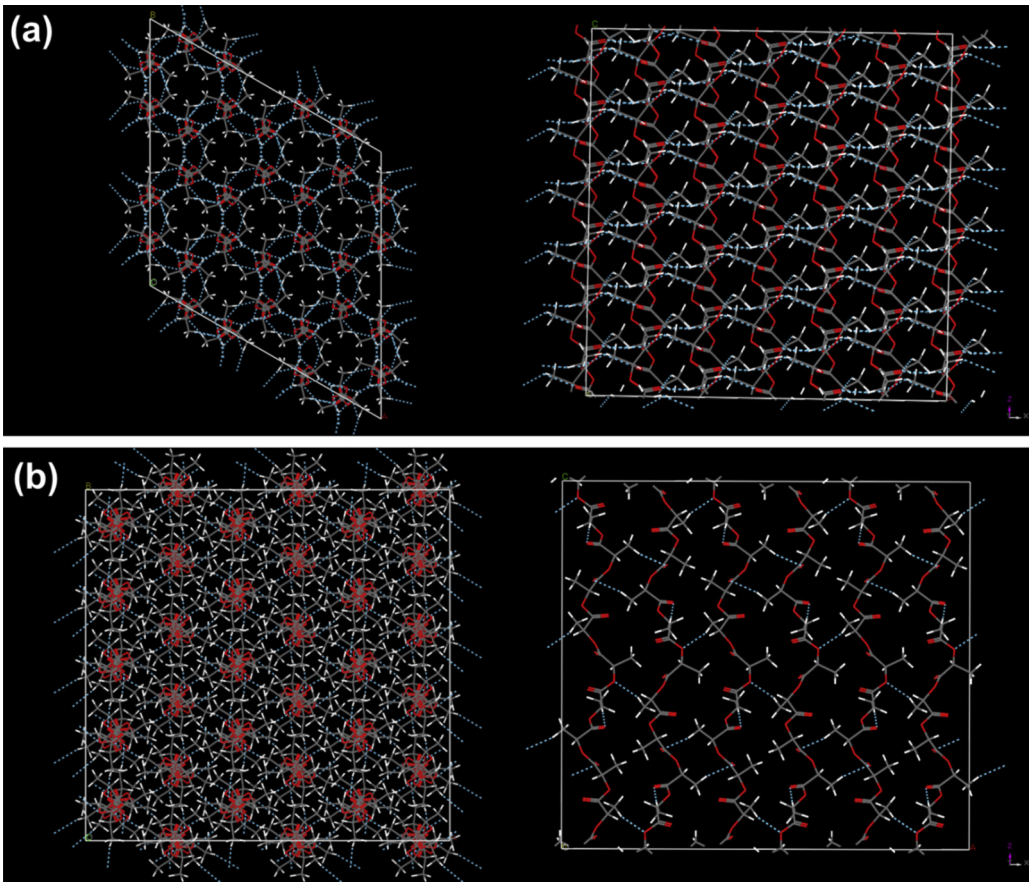

Fig. 2. Three dimensional non-conventional hydrogen bonding C—H. . .O networks (light blue dotted lines, $d_{H\cdots O} < 2.72$ Å, $\angle CHO > 100^{\circ}$) in the PLA crystals: (a) the $2 \times 2 \times 3$ supercell of sc-form; (b) the $3 \times 5 \times 1$ supercell of α-form. Element color codes: red – oxygen, white – hydrogen, and dark grey – carbon. Left panels are top view and right panels are side view of the supercells, helical chain axis along *z* axis [41]. (For interpretation of the references to color in this figure legend, the reader is referred to the web version of the article.)

formation and enhancing its stability, discussed in next few sessions.

2. Stereocomplexation of PLA-based block copolymers

2.1. Amphiphilic PLA-block copolymers

The intrinsic hydrophobicity of PLA and their high hydrolytic stability in tissues remain a challenge for biological and biomedical applications [2]. Copolymerization a wide range of hydrophilic components with PLA to form block or graft copolymers is a promising approach to manipulate its amphiphilic behavior, as well as its mechanical and physical properties. The stereocomplexation between these newly developed copolymers and enantiomers has enabled access to new materials features and expanded the therapeutic applications of PLA. Table 1 shows an overview of stereocomplexation of PLA-based amphiphilic copolymers. In this section, typical stereocomplex formation in well-defined PLA amphiphilic copolymers in various block architectures will be summarized and the improved material properties as induced by stereocomplexation will be highlighted.

2.1.1. PLA/PEG system

2.1.1.1. PLA/PEG diblock copolymer. Enantiopure PLLA-PEG and PDLA-PEG diblock copolymers were prepared by ring-opening polymerization (ROP) of D-lactide and L-lactide in the presence of monomethoxy PEG (mPEG) and stannous octoate (Scheme 3) [4,19,42,43]. The PLA/PEG diblock copolymers obtained through this method have well-defined composition, low polydispersities and more importantly high optical purity. The optical rotation of PLLA and PDLA with 29–104 repeating units is in the range of +142 to +157 and −144 to -152° $cm^3/dm\,g$, respectively [19]. The high optical purity of isotactic stereoisomers could facilitate the stereocomplex formation between enantiomeric PLA.

Leroux et al. demonstrated that stereocomplex block copolymer micelles can be obtained in an aqueous environment by the self-assembly of equimolar mixtures of enantiomeric PLLA-PEG and PDLA-PEG block copolymers (Fig. 4) [19]. The stereocomplex configuration in the

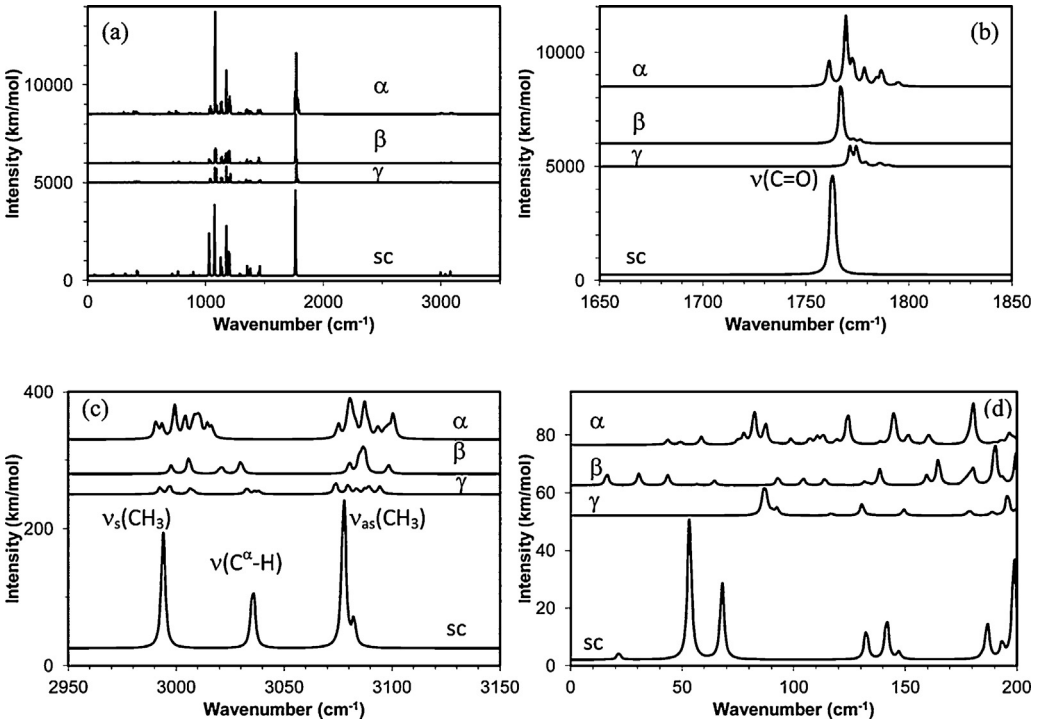

Fig. 3. A comparison of the calculated IR spectra of PLLA α-, β-, γ-form and PLLA/PDLA stereocomplex (sc), Plotted with FWHM = 2 cm^{-1}, graph quality = medium. (a) Full spectra and their expansions in (b) C=O stretching region; (c) C—H stretching region and (d) low wavenumbers/THz region. The spectra have been offset in *y*-axis for clarity [40].

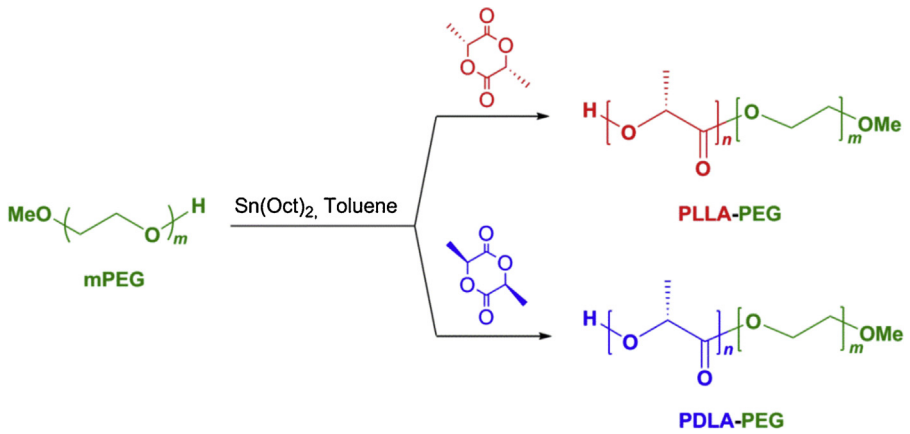

Scheme 3. Synthesis of PLLA-PEG and PDLA-PEG diblock copolymers through ring opening polymerization of enantiomeric lactide using mPEG as macroinitiator.

crystallized micelle cores was evident by X-ray diffraction (XRD), differential scanning calorimetry (DSC) and light scattering analysis (LS). XRD pattern showed characteristic peaks of PLA stereocomplex crystalline structure at 2θ equal to 12.1° and 20.8°, while these peaks were absent in the isotactic counterparts alone [4,19,42]. In addition, the stereocomplex micelles exhibited a higher crystallinity and a melting point ~50 °C above that of enantiomeric components, indicating a better structural organization in the micelle cores. Compared with the PLLA-PEG and PDLA-PEG micelles, the critical micellization concentration (CMC) of the stereocomplex micelles were lower and the sizes of stereocomplex micelles were smaller, with denser chain packing [4]. The compact chain conformation in the core would also lead to a more kinetically stable micelle system than micelles obtained from L- and D-isomers alone that were prone to aggregation during the lyophilization process [19].

The self-assembly of PLA-PEG diblock copolymers in a given solvent is also governed by the chemical compositions of the polymer blocks and temperature. For example, for block lengths of PLLA = 27 kDa and PEG = 20 kDa, the

Table 1
Stereocomplexation of typical enantiomeric PLA-based amphiphilic copolymers and their materials characteristic properties.

Material type	Polymer pair	Synthetic method	Procedure	Stereocomplex properties	References
Block copolymer	PLLA-PEG/PDLA-PEG	ROP of lactides using mPEG-OH as initiator	Solution: H_2O or H_2O/THF	Lower CMC and smaller micelle size; trigger cylindrical to micelle morphological transition.	[4,15,19]
	PLLA-PEG/PDLA	ROP of lactides using mPEG-OH as initiator	Solution: CH_2Cl_2	Nano-ordered surface morphologies.	[43]
	PLLA-PEG-PLLA/PDLA-PEG-PDLA	ROP of lactides using dihydroxylated PEG as initiator	Casting, and solution in H_2O or H_2O/CH_2Cl_2	For microsphere: High encapsulation yields, and more controllable release. For hydrogel: trigger sol–gel transition, enhance mechanical strength.	[7,47,48,55–58]
	PDLA-PEG-PDLA/PLLA	ROP of lactides in melt using dihydroxylated PEG as initiator	Casting	Increase tensile strength, heat resistance and thermal stability.	[49]
	PEG-PLLA-PEG/PEG-PDLA-PEG	Coupling MPEG-PLLA-OH diblock copolymers by HMDI	Solution: H_2O/THF	Induce reversible gel–sol transition, expand gelation window and increase gel strength.	[59]
	mPEG-PH-PLLA/mPEG-PH-PDLA	Combination of ROP, coupling reaction and thiolysis	Solution: H_2O/DMSO	Lower CAC, smaller particle size and high stable dispersion.	[63]
	PEG-PLLA-PDLA (Linear)	Sequential ROP in the presence of mPEG as initiator	Solution: H_2O/THF	Lower CMC, larger size and aggregation number.	[64]
	$(PEG\text{-}PLLA)_m/(PEG\text{-}PDLA)_m$	Coupling PLA-PEG-PLA triblock copolymers by DBI	Solution: H_2O	Trigger sol–gel transition at low CGC, enhance gel strength.	[65]
	PLLA-F127-PLLA/PDLA-F127-PDLA	ROP of lactides using F127 as initiator	Solution: H_2O	Higher gel strength and longer release profile.	[66]
	$(PLLA\text{-}F127\text{-}PLLA)_m/(PDLA\text{-}F127\text{-}PDLA)_m$	Coupling PLA-F127-PLA multiblock copolymers by HMDI	Solution: H_2O	Broader gelation window, lower CGC and higher gel strength.	[67]
	PEG-PLLA-PDLA (Star-shaped)	Sequential ROP using carbonate functionalized PEG as initiator	Solution: H_2O	Lower CMC, higher drug loading capacity.	[8]
	$PEG\text{-}(PLLA)_4/PEG\text{-}(PDLA)_4$	ROP of lactides in bulk using 4-arm PEG as initiator	Solution: H_2O	Trigger sol–gel transition.	[71]
	$PEG\text{-}(PLLA)_8/PEG\text{-}(PDLA)_8$	ROP of lactides in bulk using 8-arm PEG as initiator	Solution: H_2O	Trigger sol–gel transition, enlarge gel window, lower CGC and improve gel strength.	[6,12,72–75]
	PEG-PMTC-PLLA/PEG-PMTC-PDLA	Combination of ROP of cyclic carbonate monomer and subsequent ROP of lactides	Solution: H_2O/CH_2Cl_2	Lower CMC, monodispersed nanoparticles, and constant release profile.	[76]
	A-PEG-PLLA/A-PEG-PDLA/PEGMEA	DBU catalyzed ROP of lactides using PEGMA as initiator, followed by copolymerization with PEGMEA to form APCNs	Solution: H_2O/THF	Provide physical crosslinks in APCNs and enhance gel mechanical strength.	[78]
	PLLA/PDLA-PDMAEMA, or PDLA/PLLA-PDMAEMA	ATRP of DMAEMA using PLA-Br as initiator	Solution: $CHCl_3$	Increase surface smoothness of the electrospun fibers and impart hemostatic and antibacterials activities.	[17]
	PLLA-PDMAEMA/PDLA-PDMAEMA	ATRP of DMAEMA using PLA-Br as initiator	Casting	Increase crystallinity and surface wettability.	[14]
	D-PLLA-D@PEG/D-PDLA-D@PEG	PEG conjugation onto D-PLA-D triblock copolymers using AEBP as a difunctional linker	Solution: H_2O	Lower the CMC, increase micelle swelling ratio and enhance micelle stability.	[20]
	PLLA-PNIPAAm/PDLA-PEG	For PLLA-PNIPAAm: Combination of NMP of NIPAAm and ROP of L-lactide. For PDLA-PEG: ROP of D-lactide using mPEG as initiator	Solution: H_2O	Increase crystallinity and lower CMC.	[82]

Table 1 (*Continued*)

Material type	Polymer pair	Synthetic method	Procedure	Stereocomplex properties	References
	PNIPAAm-PLLA-PNIPAAm/PNIPAAm-PDLA-PNIPAAm	ATRP of NIPAAm using PLA-diBr as initiator	Solution: H_2O/THF	Lower CMC, tunable LCST	[28]
	PLLA-PAA/PDLA-PAA (Linear)	Combination of ROP and RAFT, followed by hydrolysis of PTHPA to PAA	Solution: H_2O/THF	Trigger micelle morphological transition from cylindrical to spherical.	[15]
	PLLA-PAA/PDLA-PAA (Linear-dendritic)	Combination of SET-LRP, ROP and thio–bromo "Click" chemistry	Solution: H_2O/THF	Trigger particle morphological transition from vesicle to micelle.	[84]
	PLLA-PIGMA/PDLA-PIGMA	Combination of ATRP and ROP, followed by acetal hydrolysis	Solution: H_2O/THF	Trigger particle morphological transition from micelle to vesicle.	[27]
Graft Copolymer	PLLA-*g*-PEG (linear and hyperbranched)/PDLA	Grafting onto method through ROP of lactides in the presence of linear and branched PEG as initiator	Precipitation	Supress homocrystal, and increase spherulitic crystal growth.	[79]
	PLLA-*g*-PRX/PDLA-*g*-PRX	Coupling the CDI activated PLA onto α-CD/PEG PRX backbone	Casting	Enhance specific molecular recognition, and form continuous anisotropic phases.	[129]
	PLLA-*g*-Dex/PDLA-*g*-Dex	Coupling the CDI activated PLA onto Dextran	Casting, Solution: H_2O/DMSO, or H_2O	For nanogel: Lower CAC and stronger thermodynamic stability. For film: exhibit mechanically tenacious and tough characters. For hydrogel: induce thermo-reversible transition, program degradation profile.	[5,21,136–141]
	PMBLLA/PMBDLA	Copolymerization of PLAMA with MPC and BMA	Solution: CH_2Cl_3 or CH_3OH/CH_2Cl_2, or H_2O	Trigger sol–gel transition and support cell adhesion.	[16,144–146]
	γ-PGA-*g*-PLLA/γ-PGA-*g*-PDLA	Coupling hydroxylated or amine-terminated PLA onto carboxylated γ-PGA	Precipitation, or Solution: H_2O/DMSO	Lower CAC, stronger thermodynamic stability, larger micelle size and narrower distribution.	[11,148]

crystallization of the PLLA core can direct the self-assembly to form cylindrical micelles. With proper optimization in hydrophilic weight fraction in the copolymers, a pure cylindrical phase with a narrow distribution of length may be obtained [44]. Dove et al. demonstrated that the cylindrical micelles can transform to spherical micelles by mixing homochiral PDLA-PEG and PLLA-PEG diblock copolymer [15]. The competitive crystallization resulted from PLA stereocomplex formation is the reason for the morphological transition. In addition, the stereoselective interaction between PLA enantiomers has also been investigated for surface modification. For example, a unique band morphology was formed by segmental stereocomplex crystallization when PLLA-PEG diblock copolymers were deposited on to silicon-PDLA surface. The specific band surface structure was completely replaced by particulate morphology when the surface was subjected to water soaking [43]. This surface modification technique through stereocomplex binding of enantiomeric PLA-PEG block copolymers endows various biofunctions including

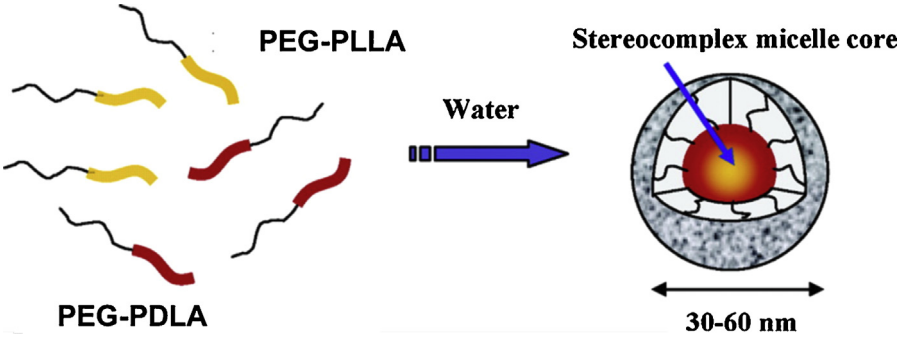

Fig. 4. Self-assembly of stereocomplex micelle from enantiomeric PEG-PLLA and PEG-PDLA diblock copolymers in aqueous solution [19]. Copyright 2005. Reproduced with permission from the American Chemical Society.

wettability, adhesion and roughness for tissue engineering applications [43].

2.1.1.2. PLA/PEG triblock copolymer. For triblock copolymers with PLA and PEG segments, two segmental arrangements are possible, i.e., PLA-PEG-PLA (A-B-A) or PEG-PLA-PEG (B-A-B), where the stereocomplexation between PLA enantiomers in these triblock copolymers architectures exhibits a number of unique material features and properties. The predominant synthetic technique used to produce PLLA-PEG-PLLA and PDLA-PEG-PDLA triblock copolymers are ROP of L- and D-lactide onto a preformed PEG-diol in the presence of catalysts such as stannous octoate, SnO, SnO_2, Sb_2O_3, PhO, GeO_2 and zinc (Scheme 4) [45]. Previously, the stereocomplex formation between PLA/PEG A-B-A triblock copolymers was first established by Feijen's research group in 1995 [46]. The results showed that the crystallization between the two enantiomeric PLA resulted in a much higher melting point compared to the optically pure PLA. In addition, the inclusion of hydrophilic PEG resulted in PLLA-PEG-PLLA and PDLA-PEG-PDLA triblock copolymers that possessed more water absorbing capacity and formed polymeric particles having various sizes and longer blood circulation time. For example, the stereocomplex of a pair of PLLA-PEG-PLLA and PDLA-PEG-PDLA triblock copolymer formed a series of microspheres that were used for bovine serum albumin (BSA) delivery. The BSA was released in a more controlled manner than via the homopolymer microspheres due to the increased water-uptake capacity in the triblock copolymer system [47]. On the other hand, stereocomplex with particle sizes ranging from nanometres to a few microns were also prepared by mixing PDLA and PLLA-PEG-PLLA triblock copolymers [48]. These stereocomplex particles could encapsulate hydrophobic drugs in high yield (77–84%) and promote sustainable release of the encapsulated drugs up to one month [48]. In a similar approach, PDLA-PEG-PDLA triblock copolymers were added into neat PLLA to tune the stereocomplex materials properties [49]. The stereocomplex between PLLA and PDLA in PDLA-PEG-PDLA copolymers could form 3D crosslinking structures that increased the tensile strength, heat resistance and thermal stability of the polymer films. Moreover, the existence of sufficient PEG in PDLA-PEG-PDLA triblock copolymers was proven to promote the slipping of crystallites, and thus increased the elongation at break of the stereocomplex samples (~130%). The balanced mechanical properties with good tensile, toughness and enhanced heat resistance make PLA stereocomplex a promising material for biomedical applications [49].

Another prominent effect of PLA stereocomplexation is the formation of hydrogel from aqueous solutions containing equal amounts of PLLA-PEG-PLLA and PDLA-PEG-PDLA A-B-A triblock copolymers. Hydrogels are a special class of polymers that provide unique swelling behavior and porous network in a 3D structure. Because of its similarity to native tissue, with respect to pharmaceutical delivery and tissue engineering hydrogels have been an attractive topic of extensive research [50–54]. Kimura et al. demonstrated the successful preparation of thermo-sensitive hydrogels mixtures of enantiomeric PLLA-PEG-PLLA and PDLA-PEG-PDLA triblock copolymers [55] Aqueous micelle solutions of PLLA-PEG-PLLA (1300-4600-1300) and PDLA-PEG-PDLA (1100-4600-1100) exhibited sol–gel transition around 37 °C. A gelation mechanism was proposed to occur as an interaction of micelles by exchanging PLA blocks in the micelle core as well as stereocomplex formation between PLLA and PDLA blocks (Fig. 5) [56]. In this regard, the hydrogels constitute of a dynamic and evolvable system because of spontaneous formation and destruction of stereocomplex crosslinks [7]. However, this PLA-PEG-PLA stereocomplex hydrogel showed a relatively low storage modulus at ca. 1000 Pa, that may not be sufficient for many applications as an injectable implant material [55]. Further attempts were made to improve the gelation process to obtain more robust gels. One promising approach is to use the co-micellization of PLLA-PEG-PLLA and PDLA-PEG-PDLA triblock copolymers [56]. The hydrodynamic diameters of micelles formed from enantiomeric PLLA-PEG-PLLA triblock copolymers are primarily influenced by the PEG block length, whereas the micelle size was in the similar range for the premixed PLLA-PEG-PLLA and PDLA-PEG-PDLA block copolymer micelles at different PEG chain lengths, indicating the co-micellization of the two copolymers [56]. The stereo-mixture of the premixed PLLA-PEG-PLLA and PDLA-PEG-PDLA block copolymer micelles at certain Mw exhibited a linear temperature response in sol–gel transition In a particular example, the equimolar racemic mixture of premixed PLA-PEG-PLA triblock copolymers micelles (Mw: 800-2000-800 and 800-3350-800) exhibited a sol–gel transition around body temperature by simply adjusting the copolymer ratio. These mixed PLA-PEG-PLA triblock copolymer micelles showed thermoresponsive properties at physiological conditions and could be used as injectable thermogels. The mechanical properties study showed that upon stereocomplexation, the strength of the gels formed from the racemic PLLA-PEG-PLLA and PDLA-PEG-PDLA mixture was greatly improved with a storage modulus of ca. 6000 Pa, indicating a solid-like and rigid microstructure through structural reorganization [56]. On the other hand, the mixed copolymer micelle solutions from single enantiomer PLLA-PEG-PLLA block copolymers did not exhibit any hydrogel formation under the same experimental conditions. With further optimization of the chemical compositions, stereocomplex hydrogels were also prepared from direct aqueous solutions containing PLLA-PEG-PLLA and PDLA-PEG-PDLA block copolymers without contact of any organic solvents [7,57,58]. In view of the simple approach in the gel preparation, and good biocompatibility of the constituting components, the stereocomplex hydrogel system are promising safe biomaterials for sustained drug delivery and in situ forming implants.

Alternatively, enantiomeric PEG-PLLA-PEG and PEG-PDLA-PEG B-A-B type triblock copolymers with two hydrophilic PEG segments flanking on PLA central block were also explored [59–61]. In one example, PEG-PLLA-PEG triblock copolymers were synthesized by coupling MPEG-PLLA-OH diblock copolymer using hexamethylene diisocyanate (HMDI) (Scheme 5) [59,60]. The obtained PEG-PLLA-PEG triblock copolymer solutions were characterized by the temperature dependent sol–gel transition [60] In a

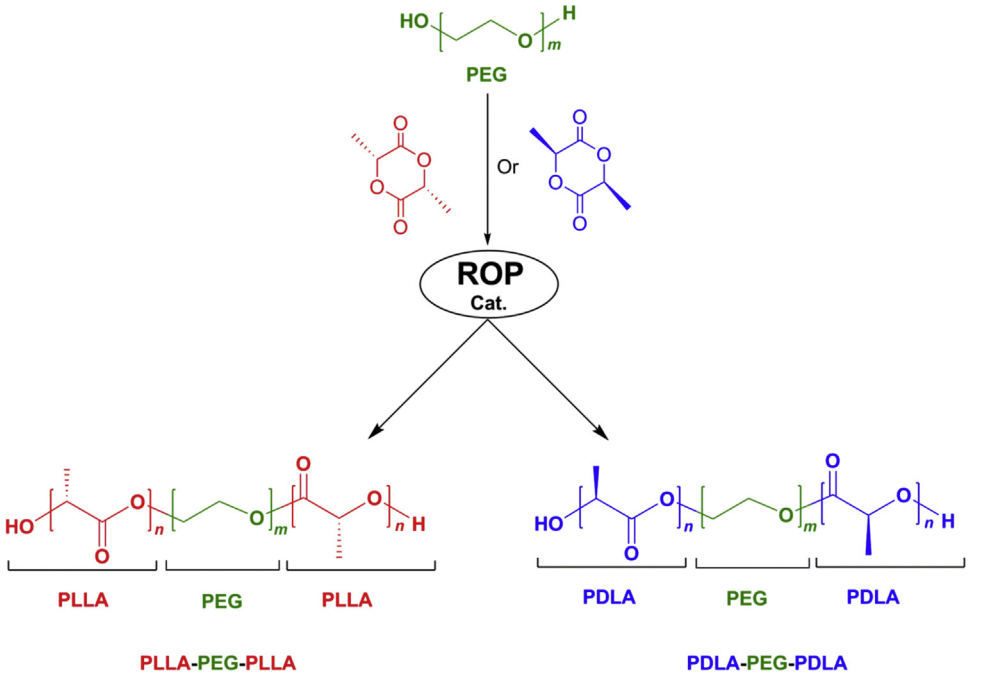

Scheme 4. Ring opening polymerization of L- and D-lactide to produce enantiomeric PLA-PEG-PLA (A-B-A) triblock copolymers.

similar approach, PEG-PDLA-PEG triblock copolymers with different PLA/PEG block lengths were prepared, and hydrogel formation with the enantiomeric PEG-PLLA-PEG was investigated [59]. The enantiomeric mixture could induce reversible gel–sol transition depending on the polymer concentration and temperature whereas the single suspension remained fluid irrespective of the temperature. It should also be noted that for enantiomeric mixture B-A-B triblock copolymer solution, the gel and sol were formed at low and high temperatures, respectively, in a reversible manner. This is quite opposite to the A-B-A system for which gelation was induced with increasing temperature in an irreversible manner [55,59]. Furthermore, the storage and loss modulus (~7 kPa) of the gel formed at lower temperature were dramatically improved compared with those of the gel prepared from the corresponding A-B-A type triblock copolymers (1–2 kPa). The interdigitation of the opposite PEG helical chains as transmitted from the opposite helical senses of PLLA and PDLA was proposed as the gelation mechanism [55,59].

On the other hand, PLA/PEG based triblock copolymers comprising three different segments can be built into the A-B-C triblock architecture. For example, a series of well-defined amphiphilic triblock copolymer methoxy poly(ethylene glycol)-poly(L-histidine)-poly(lactide) (PEG-PH-PLA) were prepared by a three-step reaction combining ROP, a coupling reaction and thiolysis. First, PEG-PH diblock copolymers were prepared by methoxy PEG initiated ROP of N-carboxyanhydride. The PEG-PH diblock copolymers obtained were then coupled with monocarboxylated PLLA and PDLA to yield enantiomeric triblock copolymers. The PEG-PH-PLLA and PEG-PH-PDLA A-B-C triblock copolymers were finally obtained by thiolysis of the triblock copolymers with 2-mercaptoethanol [62,63]. As amphiphilic triblock copolymers, enantiomeric PEG-PH-PLA copolymers could self-assemble into nanoparticles by hydrophobic-hydrophobic interaction as well as by PLA stereocomplexation. Compared with single enantiomer PEG-PH-PLLA nanoparticles, the mean diameter of stereocomplex nanoparticles was smaller (90 vs 110 nm), and the critical aggregation concentration (CAC) was also lower (1 vs 8 μg/mL). This is because PLA stereocomplexation increased the driving force for self-assembly, resulting in the formation of nanoparticles having a more compact hydrophobic core that further leads to a smaller mean diameter and lower CAC [63]. The stereocomplexation could stabilize the nanoparticles in size and morphology for pH from 5.0 to 7.9, that overcomes the drawbacks of aggregation from single enantiomeric PEG-PH-PLA nanoparticles under the same conditions [63]. In another report, PEG-PLLA-PDLA stereo-block copolymers containing short PLLA and PDLA in a single macromolecular chain was synthesized by sequential ROP in the presence of mPEG as an initiator (Scheme 6). Because of the facile interaction of the two enantiomeric PLLA and PDLA block sequence, it readily formed stereocomplex in aqueous solution. The self-assembly properties in terms of micelle formation and structure were investigated and compared with pure PEG-PLA diblock copolymers [64]. The PEG-PLLA-PDLA stereoblock copolymers with similar L- and D-isomer contents could assemble into a stereocomplex core-shell micelle, whereas the isotactic and atactic PEG-PLA copolymers formed the homocrystalline and amorphous micelles, respectively. At a PLA chain length of ~2300 g/mol, the crystallinity of PLA segments in PEG-PLLA-PDLA stereoblock copolymer micelles was smaller than those in the PEG-PLA diblock copolymers, probably attributed to the covalent junction between PLLA

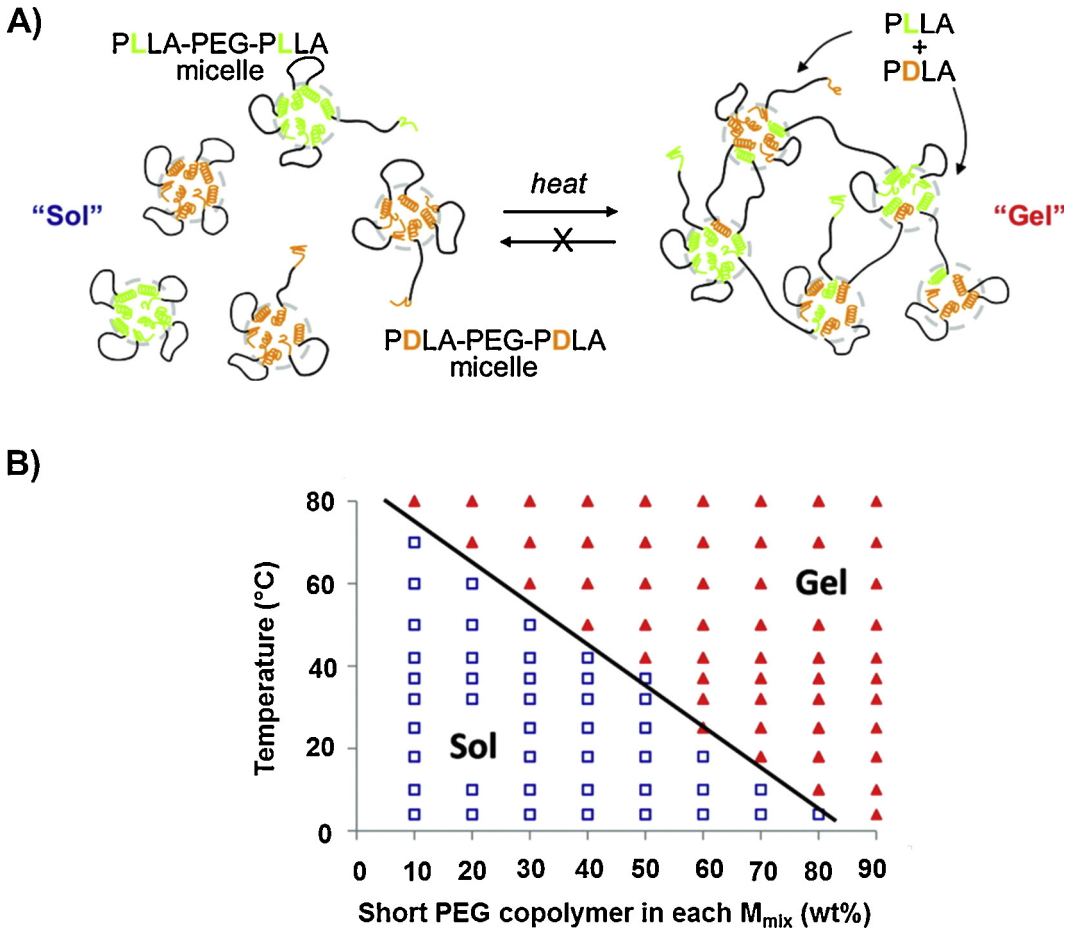

Fig. 5. (A) Proposed stereocomplexed hydrogel mechanism of enantiomeric PLLA-PEG-PLLA and PDLA-PEG-PDLA triblock copolymer mixtures in aqueous solution. The exchange of PLA blocks in the micelle core and formation of stereocomplexation between PLLA and PDLA blocks provided physical crosslinking for hydrogel formation. (B) Sol–gel phase transition diagram showing a linear response in gelation temperature of enantiomerically mixed PLA-PEG-PLA triblock copolymer co-micellization system. PLA-PEG-PLA at two molecular weights of 800-2000-800 and 800-3350-800 were used, and the final micelle concentration was maintained at 10% [56].

and PDLA blocks. However, at similar chemical composition, the stereoblock copolymers showed lower CMC than PEG-PLA diblock copolymers, indicating higher micelle stability. The precise micelle structure as revealed from the synchrotron radiation small-angle X-ray scattering study, showed that PEG-PLLA-PDLA stereoblock copolymer micelles had larger size and aggregation number, but smaller core density and looser packing of PLA chains in the micelle core when compared with the isotactic and enantiomeric mixed PLA-PEG diblock copolymer micelles [64]. The use of stereocomplexation and crystallinity to tailor the physical properties of amphiphilic copolymer micelles have shown flexibility in designing micellar materials with tunable structure and functions.

2.1.1.3. PLA/PEG multiblock copolymer. PLA/PEG based multiblock copolymers can be built up by linking the chain end functional groups of the PLA/PEG copolymers, or by using block copolymer as the initiator in the ROP of LA. Studies show that the stereocomplexation between PLLA and PDLA blocks in PLA/PEG based multiblock copolymers has profound influence in the self-assembly properties For example, enantiomeric PLLA/PEG and PDLA/PEG multiblock copolymers, $(PLLA\text{-}PEG)_n$ and $(PDLA\text{-}PEG)_n$, were prepared by coupling the chain ends of PLA-PEG-PLA triblock copolymers with diisocyanatobutane (DBI) [65]. GPC measurement showed that these multiblock copolymers had molecular weight values 4–5 times higher than the parent triblock copolymers, indicating high coupling efficiency through the urethane technique. Hydrogels were formed in situ upon mixing the two multiblock copolymers aqueous solutions at equal amount in the concentration range of 4–7.5 w/v%. In contrast, no gel formation could be detected from the parent triblock copolymers under the same conditions. Furthermore, the storage modulus increased with increasing crosslinking sites along the multiblock copolymers to produce a stereocomplex hydrogel with a considerably higher storage modulus than the triblock copolymers gels at 37 °C (2200 vs 54 Pa) [65]. In another report, PEG-PPG-PEG (Pluronic, F127) end-capped with D- or L-lactic acid oligomers at various PLA repeat unit of 5 to 18 were synthesized to afford PLA-F127-PLA

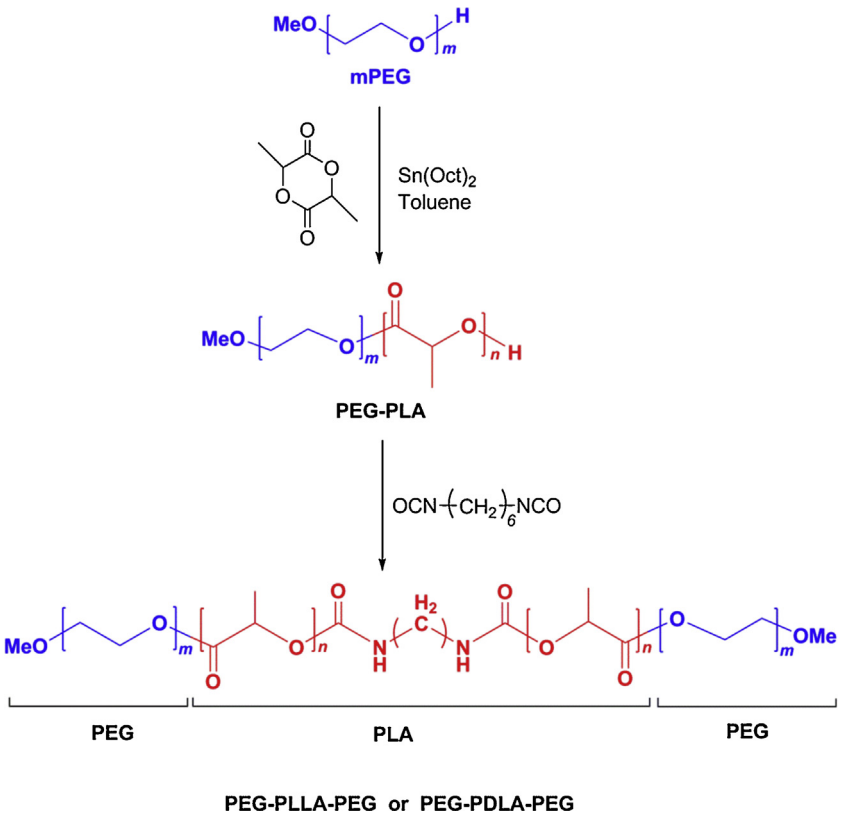

Scheme 5. Preparation of enantiomeric PEG-PLLA-PEG and PEG-PDLA-PEG B-A-B triblock copolymers through the combination of ring opening polymerization and urethane coupling reaction.

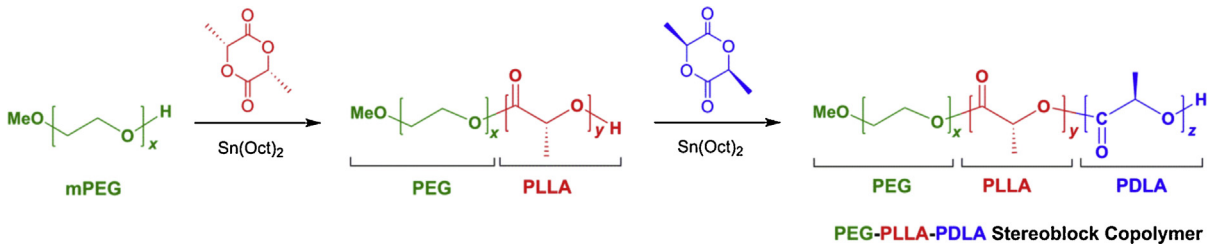

Scheme 6. Synthesis of PEG-PLLA-PDLA stereoblock copolymer through sequential ring opening polymerization of enantiomeric lactide [64]. Copyright 2015. Reproduced with permission from the American Chemical Society.

multiblock copolymers [66,67]. When blended with F127, the stereocomplexation between the enantiomeric oligo(lactic acid) in the multiblock copolymers enhanced the gel stability by providing interlocking crystalline points between the closely packed F127 micelles. As such, the mechanical properties could be optimized by tuning the nanoscale internal networks of the copolymers. At optimal conditions, the well-organized 3D mesh structure could retard gel dissolution and allow a sustained release of encapsulated growth factor hGH for 10 days, compared with the rapid dissolution of F127 gels within 3–5 days [66]. Upon coupling the two terminal hydroxyl groups in PLA-F127-PLA with the corresponding oligo(D- or L-lactic acid) chains, $(PLLA\text{-}F127\text{-}PLLA)_n$ and $(PDLA\text{-}F127\text{-}PDLA)_n$ multiblock copolymers were obtained and the hydrogels prepared from these copolymers showed more robust properties. In the phase diagram study, the stereocomplex hydrogel were far more shifted to the left and exhibited broader gelation temperature ranges, indicating a decreased critical gelation concentration (CGC) compared to the corresponding stereopure $(PLLA\text{-}F127\text{-}PLLA)_n$ gels [67]. In particular, at PLA repeat unit of 18, the stereocomplex hydrogels could be formed at 8.75 wt% compared to 15 wt% for $(PLLA\text{-}F127\text{-}PLLA)_n$ copolymers. The rheological measurements showed that the stereocomplex hydrogels greatly enhanced the mechanical strength compared to the gels prepared from individual copolymers and F127 [67]. It was proposed that the stereopure $(PLLA\text{-}F127\text{-}PLLA)_n$ multiblock copolymer gels were formed by packing of spherical F127 micelles that were simply inter-connected by oligo(L-lactic acid) spacers (Fig. 6). For stereocomplex $(PLLA\text{-}F127\text{-}PLLA)_n$ and $(PDLA\text{-}F127\text{-}PDLA)_n$ multiblock

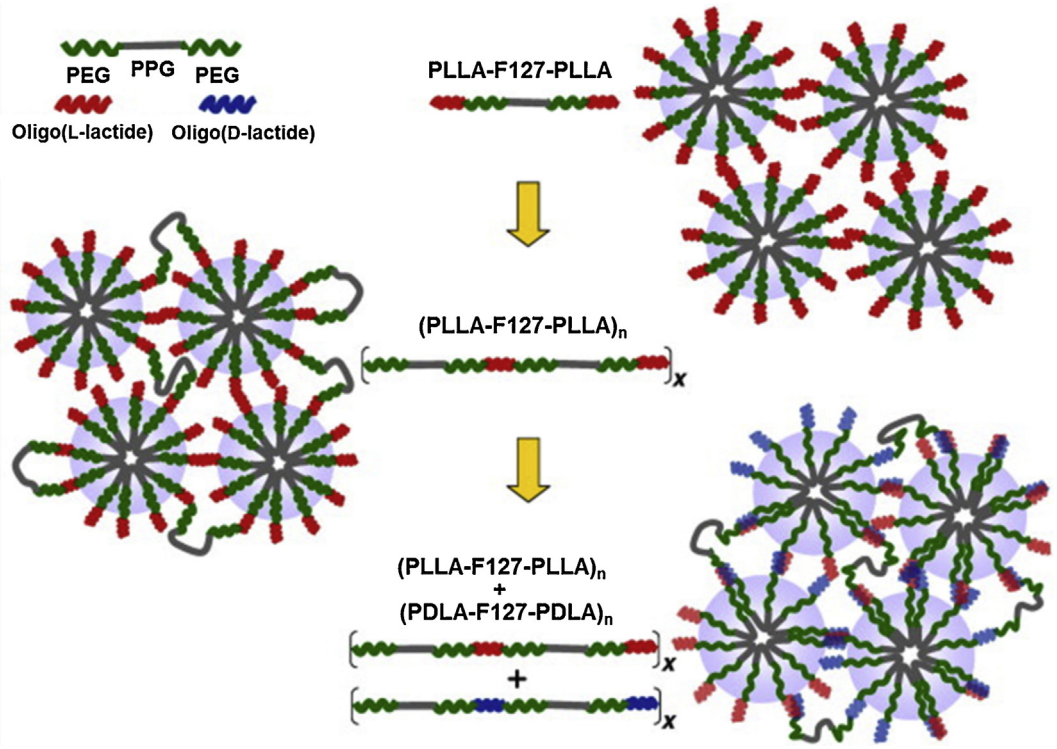

Fig. 6. Schematic illustration for molecular structure of hydrogels formed by PLLA-F127-PLLA, (PLLA-F127-PLLA)n and stereocomplexed (PLLA-F127-PLLA)n/(PDLA-F127-PDLA)n multiblock copolymers [67].

copolymer gels, the stereocomplex crystalline domains generated between the enantiomeric oligo(latic acid) spacers provided additional anchoring and inter-locking sites between the packed F127 micelles (Fig. 6). This would thus stabilize the 3D gel structure and enhance the mechanical strength [67].

2.1.1.4. PLA/PEG star-shape block copolymer. Progress in controlled or living polymerization techniques combined with new synthetic methodologies have facilitated the preparation of new types of polymer with complex architectures and functionality [68–70]. PLA/PEG based star-shape block copolymers have also been reported through several versatile synthetic strategies and their stereocomplex mixtures have shown the feasibility of fine tuning the materials properties in response to specific applications. For example, 3-arm PLA/PEG star block copolymers, also known as miktoarm star copolymer, were prepared from carbonate functional oligomers (Scheme 7). As the key building block, carboxylic acid functional carbonate was first coupled to mPEG-OH followed by ROP of the cyclic carbonate using functional amines. The subsequent two ROP steps of enantiomeric lactides added PLLA and PDLA arms onto PEG, generating the targeted PEG-PLLA-PDLA (A-B-C) miktoarm star copolymers [8]. Similarly, this approach is also feasible in the preparation of PEG-PLLA-PLLA and PEG-PDLA-PDLA (A-B-B) miktoarm star copolymers. The resulting amphiphilic miktoarm copolymers containing enantiomeric poly(D- and L-lactide) formed PLA stereocomplexes, and were also shown to form stabilized micelles in aqueous solution. The role of architecture and stereocomplexation on the micellization behavior was further investigated. The results indicated that stereocomplexation between enantiomeric A-B-B miktoarm copolymers led to a reduced CMC value as compared to the corresponding linear or stereoisomer A-B-B miktoarm copolymers alone due to the formation of a more stable core. A similar trend was also found in the stereoblock A-B-C miktoarm copolymers. Low CMC of amphiphilic micelles is an important parameter for in vivo performance in the large volume of blood. These micelles prepared from miktoarm PLA/PEG star copolymers also showed high capacity of paclitaxel loading without significant initial burst release, demonstrating the useful synthetic platform in the design of stereocomplex macromolecular architectures for controlled drug delivery [8].

Despite the enhanced micellization, no hydrogel formation was observed using miktoarm PLA/PEG star block copolymers. This could be due to the limited accessible arms for PLA stereocomplexation and the hydrophobic to hydrophilic ratio in the copolymers could not fulfil the requirement in the gel networks. On the other hand, enantiomeric 4-arm star-shaped PLA/PEG block copolymers with similar chain lengths were synthesized by bulk ROP of D-lactide and L-lactide, respectively, using 4-arm PEG as a tetra hydroxyl group initiator The stereocomplexation between PLLA and PDLA of the copolymers in aqueous solution promoted in situ hydrogel formation (Scheme 8) [71]. Typical hydrogels can be formed in the concentration range of 18–22 wt%. The gels at higher concentration showed a

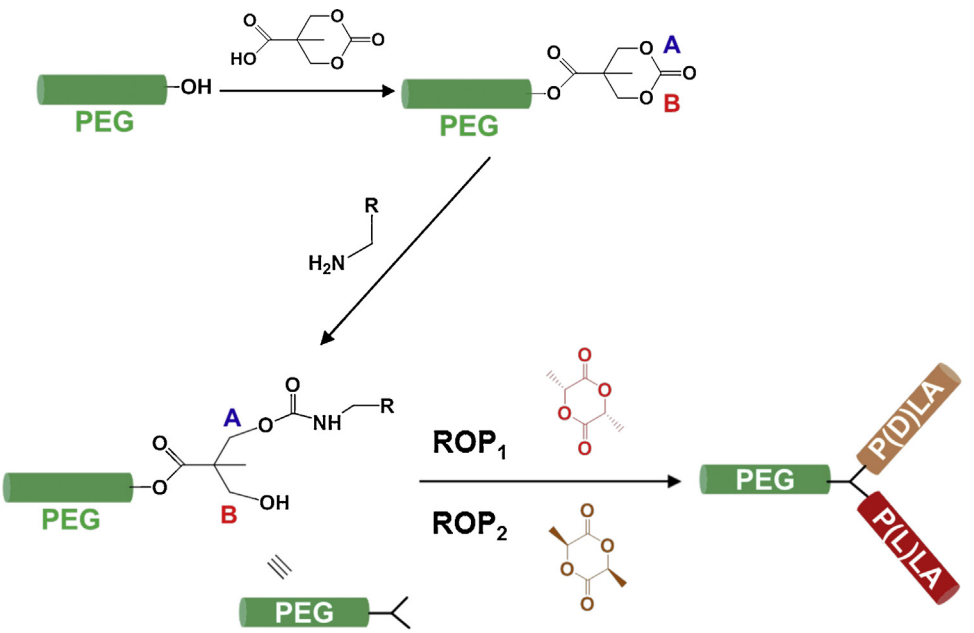

Scheme 7. Synthetic route of PLA/PEG miktoarm star copolymers from carbonate functional oligomers [8].
Copyright 2009. Adapted with permission from the American Chemical Society.

relatively wider range of the stereocomplex region that can be used to modulate the degradation of the hydrogel [71]. Further attempts were made to improve the hydrogel stability by using enantiomeric 8-arm PEG-$(PLLA)_8$ and PEG-$(PDLA)_8$ star block copolymers [6,12,72]. These 8-arm PLA/PEG star block copolymers were synthesized by ROP of either L-lactide or D-lactide at room temperature in the presence of a single-site ethylzinc complex and 8-arm PEG as the catalyst [6,73].

The use of the single site Zn-catalyst allowed excellent control over the degree of polymerization of PLA. PEG-$(PLLA)_8$ and PEG-$(PDLA)_8$ star block copolymers were water soluble when the number of lactyl units per PLA did not exceed 14 and 17 for PEG21800-$(PLA)_8$ and PEG43500-$(PLA)_8$, respectively. Stereocomplexation-driven hydrogel formed on blending equimolar amount of the copolymers. Typically, the stereocomplex hydrogel could be prepared in a polymer concentration range of 5–25 wt% for PEG21800-$(PLA)_8$ star block copolymers and 6–8 wt% for PEG43500-$(PLA)_8$ star block copolymers, respectively. Depending on the aqueous concentration and the PLA block length, the gels were stable in phosphate buffer saline for 5 days, showing an improved gel stability compared with those gels prepared from 4-arm star-shaped PLA/PEG block copolymers [6,71]. Rheological studies showed that stereocomplexed hydrogels in phosphate buffer saline with a range of storage moduli up to 14 kPa could be obtained at 37 °C, with gelation times tuned from instant gelation to ca. 1 h by controlling the PLA/PEG ratio and gel concentrations [6]. The mechanism of the temperature-dependent stereocomplex formation in PEG-$(PLLA)_8$ and PEG-$(PDLA)_8$ star block copolymer hydrogels has been investigated. Results revealed that the stereocomplexation was facilitated at higher temperatures, due to rearrangement in the micellar aggregates exposing more PLA units available for interaction [72]. The highly stable stereocomplexed PLA domains would make the hydrogel as a temperature irreversible gel system [72,74]. In addition, a structure-property relationship study showed that changing the linking unit between PLA and PEG from an ester to an amide group in the PEG-$(NHCO)$-$(PLA)_8$ copolymers, or combining stereocomplexation and photopolymerization in PEG-PLA-MA copolymers could further enlarge the gel windows and improve gel properties [72,75]. For example, the gel degradation time was prolonged considerably to more than 16 weeks after methacrylation of 40% of the PLA hydroxyl end groups in PEG-$(PLA)_8$ star block copolymers [75]. The combination of stereocomplex formation and star-shape structure with different functionalities have endowed PLA/PEG block copolymers having fast gelation behavior under physiological conditions, and exhibiting improved mechanical properties compared to the corresponding gels that were made from enantiomeric mixture of linear PLA/PEG copolymers and others [6,74,75]. The possibilities to form in situ hydrogel and their robustness in mechanical strength could render the new materials suitable for easy immobilization of bioactive reagents and encapsulation of cells for various biomedical applications.

2.1.1.5. PLA/PEG comb-shape block copolymers and others. Amphiphilic comb-shape block copolymers comprised of PEG as hydrophilic component and a poly(methylcarboxytrimethylene carbonate) (PMTC) as a hydrophobic backbone having stereoregular PLA sides chains, PEG-PMTC-*g*-PLLA and PEG-PMTC-*g*-PDLA, have been reported. The synthesis route included a multistage reaction in which an mPEG oligomer was first used as an initiator for the organocatalytic ROP of functional

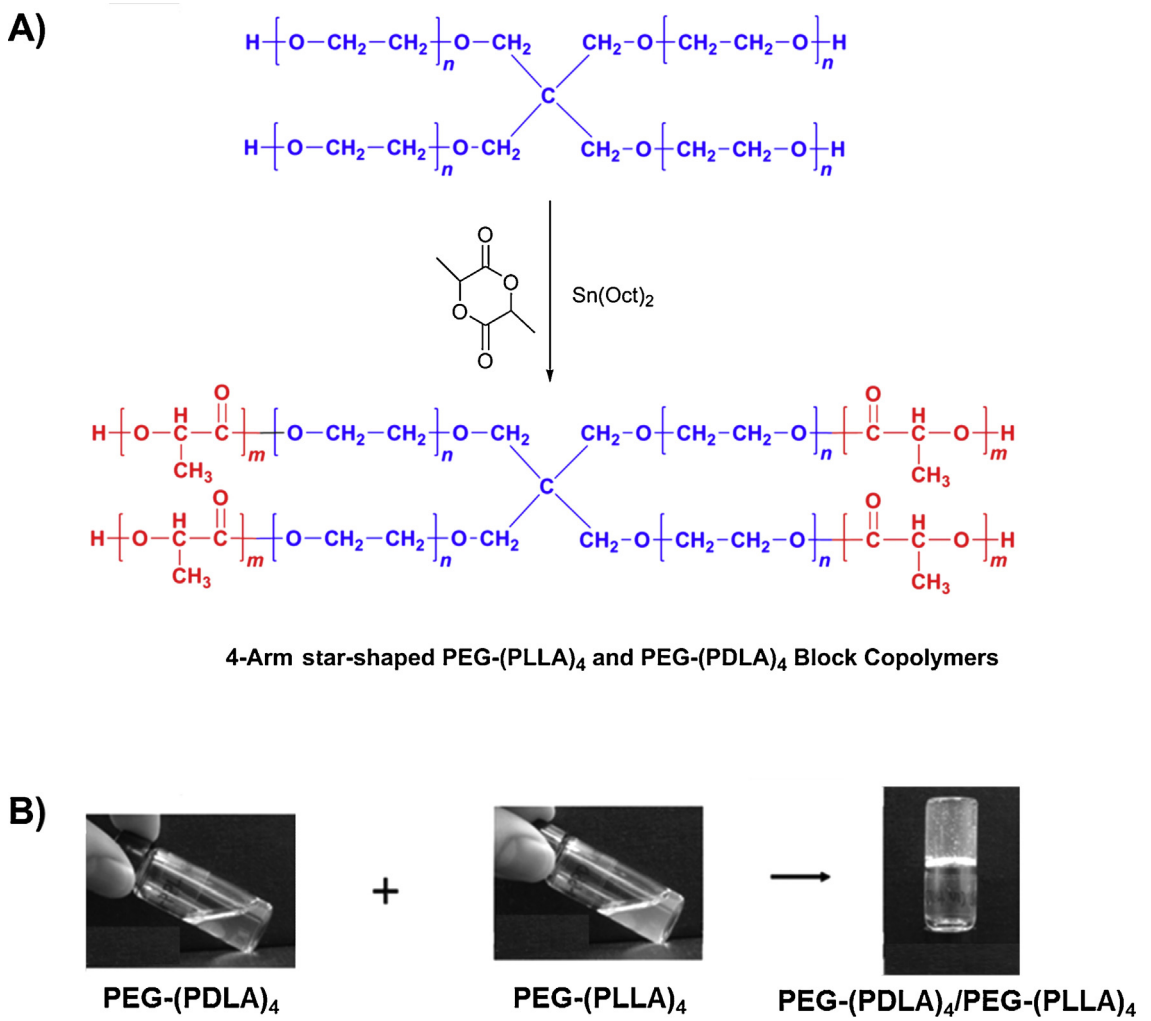

Scheme 8. (A) Synthesis scheme for the preparation of 4-arm PEG-$(PLLA)_4$ and PEG-$(PDLA)_4$ star-shape block copolymers. (B) In situ hydrogel formation by mixing PEG-$(PLLA)_4$ and PEG-$(PDLA)_4$ star at concentration of 20 wt% [71].
Copyright 2008. Reproduced with permission from Springer.

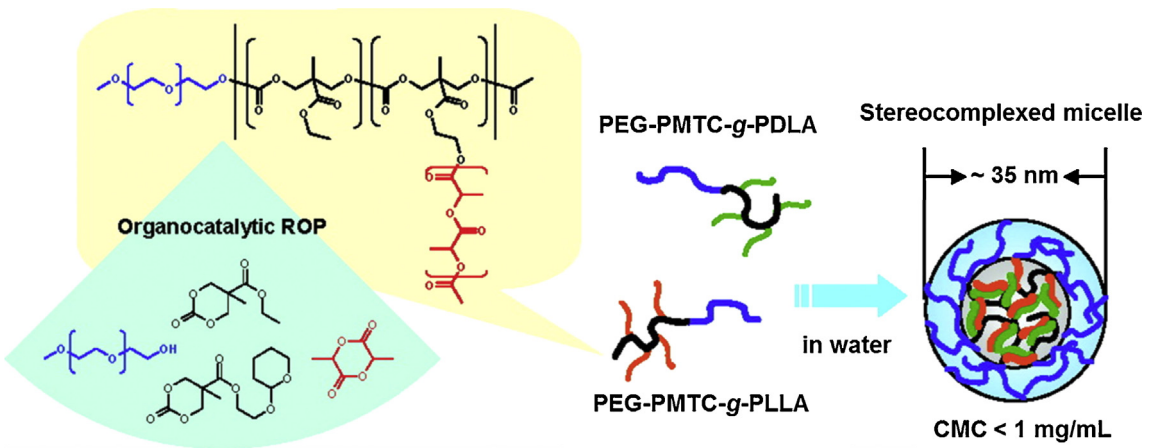

Fig. 7. Aqueous self-assembly of PEG-PMTC-g-PLA comb-shape block copolymers with enantiomeric PLLA and PDLA as the side chains [76].
Copyright 2008. Reproduced with permission from the American Chemical Society.

cyclic carbonate monomers (MTCs) having latent initiator functionalities for the subsequent ROP of enantiomeric lactides [76]. PLA/PEG comb-shape block copolymers of predictable Mw ($1.44–2.31 \times 10^3$ g/mol) and narrow polydispersities (~1.3) were prepared by this method with up to 8-PLA branches (DP 15). The complex architecture that employed stereoregular PLA grafts as complexation sites were investigated by mixing the L- and D-lactide based copolymers. In aqueous solution, PEG-PMTC-*g*-PLA comb-shape block copolymers having stereopure PLA showed strong tendency to self-assemble into micelle formation (Fig. 7). The CMC was in the range of 0.32–1.1 mg/mL, that is desirable for use as a drug delivery vehicle. More importantly, formation of PLA stereocomplex further reduced the CMC to the range of 0.11–0.53 mg/mL because of the more stable formation in the micelle core [76]. In addition, the stereocomplex micelles were monodispersed spherical nanoparticles with a range of sizes from ~20 to 35 nm, that may be a promising carrier for targeted drug delivery via enhanced permeation and retention (EPR) effect [77]. The desirable bio-distribution pattern and constant release profile make PEG-PMTC-*g*-PLLA and PEG-PMTC-*g*-PDLA stereocomplexed micelles a promising candidate for control drug release when compared with micelles formed from conventional block copolymers.

The synthesis of acrylate-terminated copolymers A-PEG-PLLA and A-PEG-PDLA, and their copolymerization with poly(ethylene glycol) methyl ester acrylate (PEGMA) would produce PLA/PEG comb-shape block copolymers has been reported [78]. For the synthesis of A-PEG-PLA prepolymer, 1,8-diazabicyclo[5.4.0]undec-7-ene (DBU) was used as catalyst in the presence of PEGMA as initiator. Compared with the Sn(II) catalyst, DBU can catalyze the ROP of lactide at room temperature, and the side reaction of active acrylate groups in PEGMA can be avoided during the polymerization. More importantly, the PLA stereocomplex formation between A-PEG-PLLA and A-PEG-PDLA could form a di-functional macromonomer, that allowed the acrylate groups to be incorporated into the propagating chain of PEGMEA, leading to a physically cross-linked amphiphilic conetworks (APCNs) (Fig. 8) [78]. The effect of stereocomplexation on the rheology properties of APCNs hydrogels was further investigated. The results indicated that APCN having 5% of stereo-A-PEG-(PLLA-PDLA) had higher storage moduli than the corresponding APCN containing same amount of A-PEG-PLLA. The PLA stereocomplex provided physical crosslinks in the hydrogel conetworks, and the additional hydrogen bond between the stereocomplex would make the hydrogel more stable. Furthermore, the stabilization effect is proportional to the amount of the PLA stereocomplex in the cross-linked macromolecular assemblies [78]. In addition to the above-mentioned studies, another example of comb-shape block copolymers based on functional PLA and PEG was prepared via the combination of anionic and ROP by using PEG/PG (PG: polyglycerol) as backbone and the influence of stereocomplex in copolymer topology was investigated [79]. PLA stereocomplex in other block copolymer architectures such as hyperbranched and H-shape structures containing PLA and PEG as main building blocks had also been reported, showing better physical properties than individual enantiomer polymers, including improved mechanical properties, enhanced thermal and hydrolytic stability [79,80].

2.1.2. PLA/Poly(metha)crylate system

The incorporation of poly(meth)acrylates could render the newly synthesized block copolymers access to tunable properties, such as hydrophilicity, pH- and temperature-induced phase behavior, as well as therapeutic agents encapsulation by simple variation of the functional substitute groups [81]. The general method to synthesize PLA/poly(meth)acrylates amphiphilic block copolymers involves controlled radical polymerization (CRP) of hydrophilic monomers from hydrophobic PLA. In this section, the well-defined enantiomeric PLA/poly(metha)crylate amphiphilic block copolymers will be introduced with special focus on the valuable material features induced by the stereocomplexation of PLA.

2.1.2.1. PLA/PDMAEMA block copolymers. Poly(N,N-dimethylamino-2-ethyl methacrylate) (PDMAEMA) is a water soluble polymer that shows inherent biological activities in many applications [17,50]. Previously, amphiphilic PLLA-PDMAEMA and PDLA-PDMAEMA diblock copolymers were synthesized by a three-steps reaction in the combination of ROP and ATRP, with formation of their stereocomplex films obtained by solvent casting [14]. ROP and ATRP are well-recognized synthesis strategy for tailored design of PLA/PDMAEMA block copolymers with desired macromolecular parameters [14,20]. During the synthesis of PLA-PDMAEMA, PLA was prepared by controlled ROP of L- or D-lactides initiated by $Al(O^iPr)_3$), followed by quantitative conversion of the PLA-OH to PLA-Br, and ATRP of DMAEMA. The presence of PDMAEMA enabled the reduction of the hydrophobicity of the PLA-based copolymers and related stereocomplexes. The surface wettability as measured by static water contact angle showed that there was a sharp decrease of approximately 34° for the PDMAEMA incorporated samples. Stereocomplexation could also occur in mixtures of high Mw PLA homopolymers with enantiomeric PLA-PDMAEMA. The availability of the tertiary amino groups in PDMAEMA also enables further modification of the polymer backbone and could be of special interest in biomedical fields, including hemostatic and antibacterials applications [14,17]. An enantiomeric PDMAEMA-PLA-PDMAEMA triblock copolymers (D-PLA-D) conjugated with PEG (D-PLLA-D@PEG and D-PDLA-D@PEG) was synthesized to further increase the hydrophilicity of the copolymer. The stereocomplexation induced self-assembly property of enantiomeric mixtures in aqueous solution was also investigated [20]. During the synthesis, a bifunctional 2-azidoethyl-2-bromopropanoate (AEBP) linker with bromopropionyl and azide group at the opposite chain termini was designed to facilitate the PEG conjugation reaction. D-PLLA-D@PEG and D-PDLA-D@PEG copolymers were then obtained by sequential quaternization of PDMAEMA chains and azide–alkyne click reaction with alkyne-end PEG (Scheme 9).

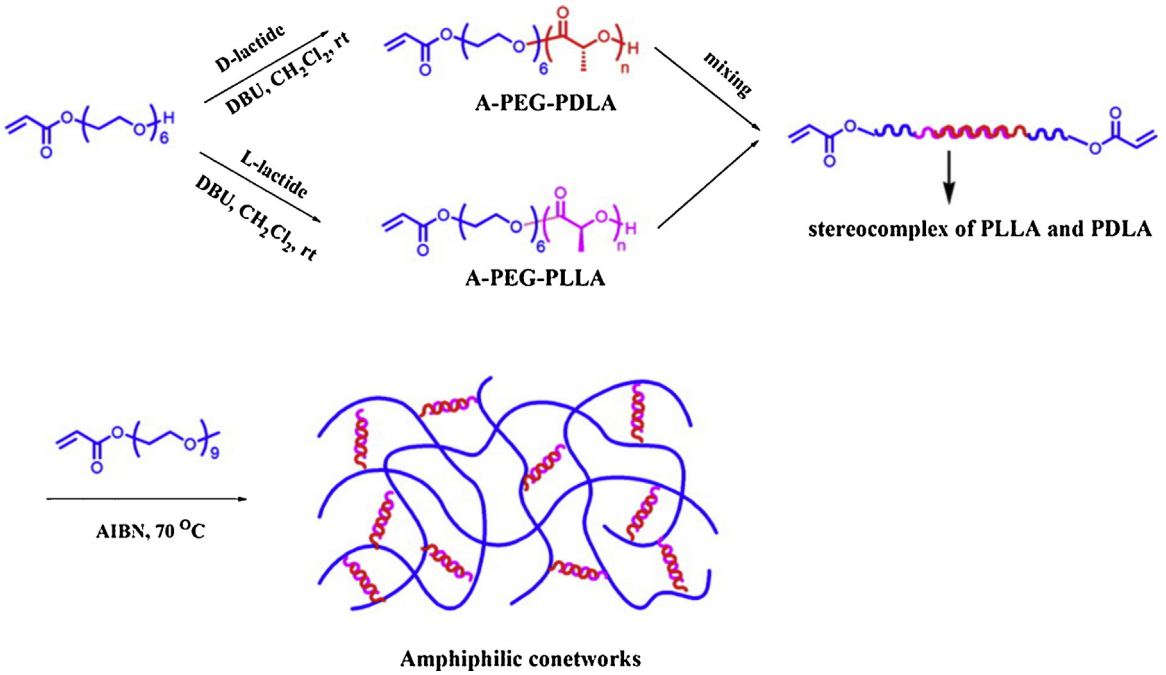

Fig. 8. Synthesis of acrylate-terminated enantiomeric A-PEG-PLA copolymers and illustration of amphiphilic conetwork hydrogels physically cross-linked by PLA stereocomplex [78].
Copyright 2013. Reproduced with permission from the American Chemical Society.

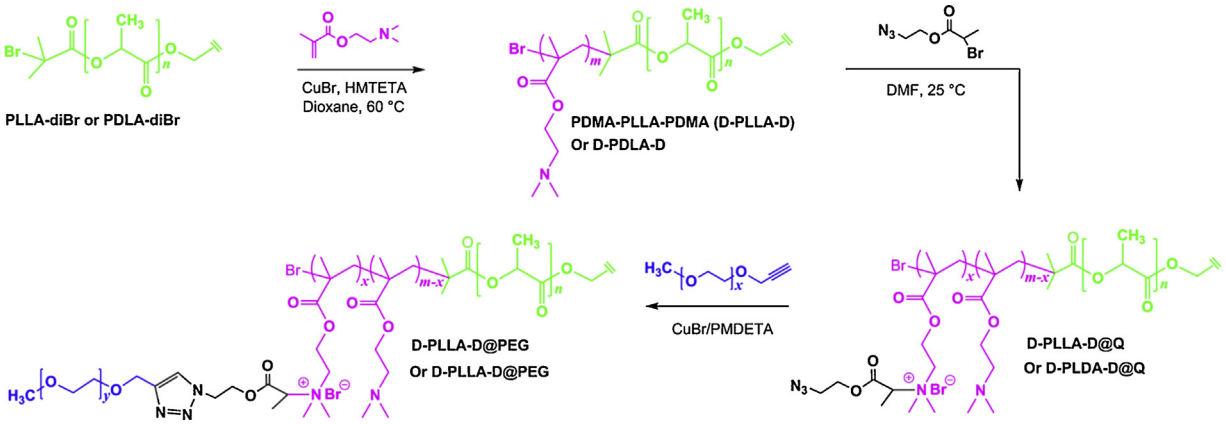

Scheme 9. Synthesis route of PEG conjugated PDMAEMA-PLLA-PDMAEMA@PEG (D-PLLA-D@PEG) and D-PDLA-D@PEG copolymers [20].
Copyright 2015. Reproduced with permission from the American Chemical Society.

Significantly different from the previous reported amphiphilic PLA copolymers that are not soluble directly in aqueous solution due to the high hydrophobicity of PLA and their stereocomplex, the incorporation of PEG in D-PLLA-D@PEG and D-PDLA-D@PEG could facilitate direct dissolution in aqueous media without using any organic solvents [4,15,19,20,63,78]. Furthermore, the presence of PDMAEMA and PEG did not hamper stereocomplex formation. Due to the availability of the functional amine/ammonium moiety in the modified PDMAEMA, the copolymers could form complexes with acidic/anionic substrates. The LS analysis demonstrated that the size of the core–shell micelles was in the range of 58–105 nm, controlled by the pH. At lower pH, the protonation of the PDMAEMA segments could cause the osmotic pressure within the micelle to increase until the micelles reached a maximum size. The micelles formed by 1:1 D/L mixtures showed larger swelling ratios and a hydrodynamic radius that did not change significantly with pH or dilution, as compared to micelles formed from individual D or L forms of the copolymers. These results indicated enhanced micelle stability induced by PLA stereocomplexation. When compared to numerous stereocomplex micellar systems in aqueous solution, that involved the use of organic solvent and tedious post-processing, the simple and versatile dissolution in the micelle preparation and enhanced kinetic

stability of the micelle system could make D-PLA-DPEG copolymer more attractive in application of biomedicine [20].

2.1.2.2. PLA/PNIPAAm block copolymers. Poly(N-isopropylacrylamide) (PNIPAAm) is an extensively studied thermal-responsive polymer with a lower critical solution temperature (LCST) of 32 °C. The distinct LCST of PNIPAAm is close to human body temperature, that allows the properties of this material to be adjusted for specific applications. Previously, Kim et al. demonstrated the stereoselective association between two dissimilar block copolymers PLLA-PNIPAAm and PDLA-PEG. In this study, PLLA-PNIPAAM (Mw: 2–6 K) diblock copolymer was prepared from a dual-headed initiator containing an alkoxyamine and a primary hydroxyl group through nitroxide-mediated polymerization (NMP) of NIPAAm and subsequent ROP of L-lactide [82]. PDLA-PEG (2–5 K) was prepared by using mPEG as an initiator for the ROP of D-lactide (Scheme 3). Mixed micelles of PNIPAAM-PLLA and PEG-PDLA in the size range of 20–40 nm were prepared by dissolving the two block copolymers in deionized water at approximate equimolar ratio (Fig. 9). The CMC of the mixed micelle system was lower than those of single block copolymers at same condition, indicating the stabilized self-association driven by the strong PLA stereocomplexation. In addition, the temperature-responsive behavior of the mixed micelles was not affected by the presence of PEG, showing a LCST at about 20 °C. This could make the mixed biodegradable micelles particularly suitable for delivery of biologically active agents, such as an injectable drug delivery system. One example is in the delivery of anticancer drugs where the drugs could first be loaded into the micelles at 20 °C, followed by the precipitation of the injected drug-loaded micelle system at 37 °C onto the tumor site, and subsequently the sustained release of the drugs to perform its functions. In addition to the PLLA-PNIPAAm/PDLA-PEG system, investigations included the thermal responsive behavior of PNIPAAm in aqueous stereocomplex mixtures of enantiomeric PNIPAAm-PLA-PNIPAAm triblock copolymers [28]. The LCST of a 1:1 PNIPAAm-PLLA-PNIPAAm/PNIPAAm-PDLA-PNIPAAm mixture increased significantly compared with that of individual D or L form of copolymers. For optimized conditions, the LCST of the enantiomeric mixtures reached 38.5 °C, above human body temperature. The particle size measurements indicated a thermally reversible change in micelle size when the temperature alternation crossed over the LCST [28]. The successful manipulation of LCST through adjusting the strength of stereocomplex in PNIPAAm-PLA-PNIPAAm copolymers could be of great potential in developing thermally precise polymeric systems for targeted drug delivery.

2.1.2.3. PLA/PAA block copolymers and others. Stereoregular PLLA-PAA and PDLA-PAA block copolymers have been previously explored to access cylindrical particles through crystallization-driven self-assembly (CDSA). Factors including block length in PLA-PAA copolymer and the ratio of solvent in THF/H_2O mixtures during CDSA were reported to control the dimensions of the cylindrical micelles [18,83]. However, a recent study showed that the cylindrical micelles assembled from a mixture of PLLA-PAA and PDLA-PAA diblock copolymers underwent morphological transition into spherical micelles with a PLA stereocomplex core under the same assembly conditions. It was proposed that the fast crystallization process would lead to the resolution of the mixture to D and L homochiral cylinders, and further produced stereocomplex spheres with higher crystallinity. Two homochiral cylinders mixed under CDSA conditions exhibitied morphological reorganization from cylindrical micelles to stereocomplex spherical micelle formation at the onset of PLA stereocomplexation (Fig. 10). With the presence of an increasing number of spheres, a decreasing dimension of cylinders was detected during the transition process. This indicates that the existence of stereocomplexation in this system can act as driving force to change the crystallization property of PLA in the micelle cores and hence induce a morphology switch [15].

In addition to the conventional linear PLA-PAA block copolymers, linear-dendritic PLLA-PAA and PDLA-PAA block copolymers have been synthesized via the combination of single-electron transfer living radical polymerization (SET-LRP), ROP and thio–bromo "Click" chemistry [84]. Similar to the dendrimer structure, the highly branched molecular architecture in linear-dendritic PLA-PAA block copolymers imparted precise control over the peripheral functional groups and a larger surface coverage by a hydrophilic PAA layer. The unique polymer architecture also led to interesting self-assembly properties in aqueous solution. For example, vesicular aggregates were formed in aqueous solution for individual L and D forms of the copolymer. When a pair of L and D forms of the copolymers was mixed in a 1 to 1 ratio, the corresponding aggregates changed from vesicles to spherical micelles (Fig. 11). This could be attributed to the more dense packing structure and more hydrophobic characteristic of PLA stereocomplex, that favored the formation of micelle morphology. In addition, the stereocomplex formation in the micelle cores was also energetically more stable and the size of the newly formed aggregates could be adjusted by varying the pH values, thus demonstrating pH-dependent swelling and shrinking properties [84]. In another recent report, well-defined block copolymers comprising poly(benzylidene glycerol methacrylate) (PBGMA) and PLA segments were synthesized [57]. The selective acetal hydrolysis of the PBGMA block proceeded smoothly to water-soluble poly(isoglycerol methacrylate) (PIGMA) without affecting the potentially labile ester bonds in PLA. The aggregation behavior in aqueous solution was studied with respect to the stereochemistry of the PLA blocks. The results showed that the uniformly shaped micelles from individual copolymer (20 nm) changed to large vesicles with diameters ranging from 600 to 1400 nm after mixing the D and L types of copolymers at identical amount [27]. Without the requirement of any external stimulus, the simple stereocomplex-driven morphological transition opened new opportunities in biomedical applications for delivery carriers and controlled release to newly designed PLA/poly(metha)crylate system.

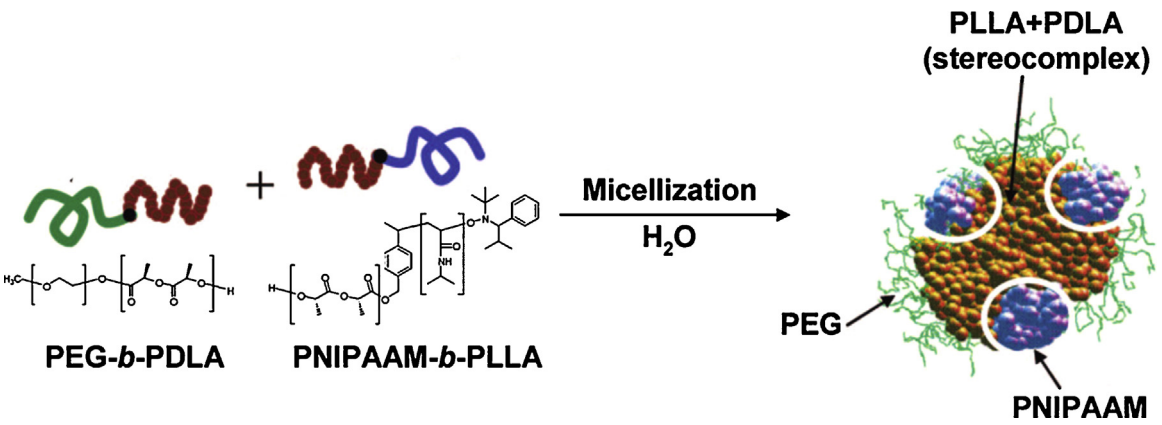

Fig. 9. Mixed micelle formation formed from dissimilar stereocontrolled diblock copolymer mixture of PDLA-PEG and PNIPAAm-PLLA in deionized water [82].
Copyright 2009. Reproduced with permission from the American Chemical Society.

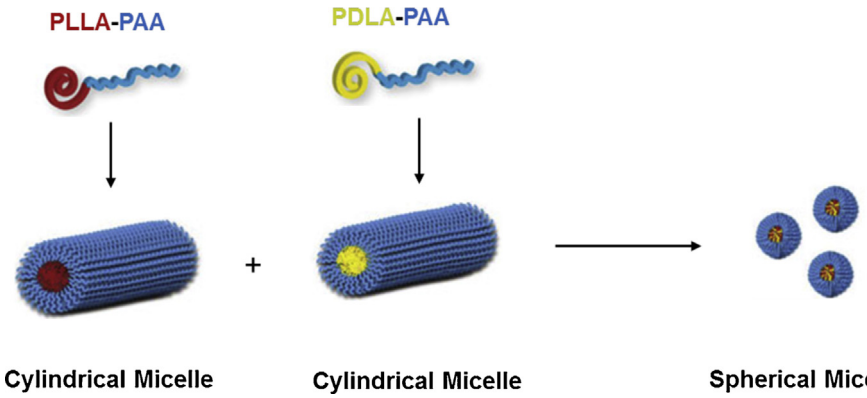

Fig. 10. Schematic illustration of stereocomplex-induced morphological transitions from cylindrical micelles to spherical micelles of enantiomeric PLLA-PAA and PDLA-PAA diblock copolymers mixed solutions [15].
Copyright 2014. Adapted with permission from the Nature Publishing Group.

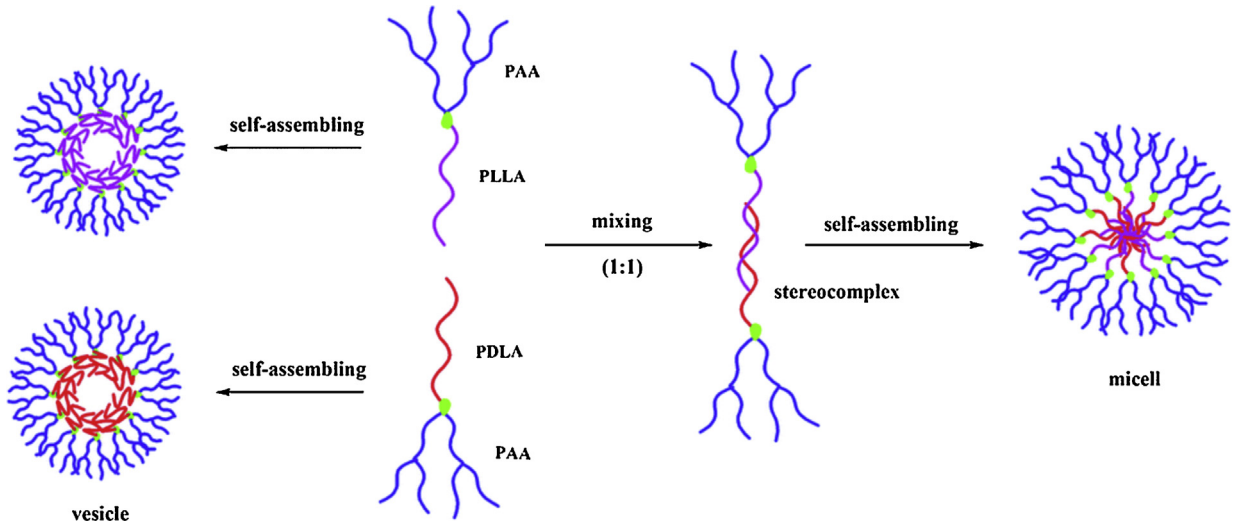

Fig. 11. Schematic draw showing the self-assembly of linear-dendritic PLLA-PAA and PDLA-PAA block copolymers and their vesicles to micelles transition induced by PLA stereocomplexation in aqueous solution [84].
Copyright 2014. Reproduced with permission from the Royal Society of Chemistry.

2.2. PLA-polyester block copolymers

In addition to the PLA-based amphiphilic block copolymers, the stereocomplexation effect in PLA-polyester block copolymers has also been well exploited. By taking the advantages of this strategy, many accessible properties of PLA have been successfully manipulated. In this section, the most recent development of PLA stereocomplex will be summarized with respect to different types of PLA-polyester block copolymers and their difference in materials properties arising from the stereocomplexation will also be discussed.

2.2.1. PLLA/PDLA stereoblock copolymers

Previous studies showed that blends of PLLA and PDLA in either melt or solution formed stereocomplexes, that could provide access to materials with enhanced features, such as higher melting point, higher mechanical strength, and improved thermal and hydrolytic stability [1,3,85]. However, stereocomplexation is often hindered by the concurrent formation of homochiral crystal of the respective polymers, especially at high molecular weight. Recent studies on the formation of PLA stereocomplex have been devoted to the blends of PLA enantiomers with more diversified macromolecular architectures, including cyclic, multi-armed and densely grafted PLAs [86–89]. The structure distinction corresponded to significant impact on the thermal properties and phase behavior, and provided more potential for the applications of PLA stereocomplex materials at higher temperature environments. Although stereoisomers PLLA and PDLA in these new polymer structures showed a strong tendency to interact with each other to form stereocomplexes, there are also certain topological restraints and steric hindrances that resulted in partial participation of the polymer chains in the stereocomplex formation. One effective method to improve stereoselective interaction is to develop PLA stereoblock copolymer, that consists of the enantiomeric PLLA and PDLA in a blocky manner to form isotactic PLLA-PDLA block copolymers [90,91]. The placement of the PLLA/PDLA segments in the neighbourhood can effectively promote the stereocomplexation formation in a molecular level and further improve PLA materials with high-performance properties. For example, Kimura et al. recently demonstrated the synthesis of PLLA-PDLA stereo block copolymers in di, tri, and multi-block structures [92–96]. Significantly different from previous reports, stereoblock copolymers with high molecular weight (M_n > 100 kDa) were prepared by melt-polycondensation of lactic acid, and its combination with solid-state polycondensation (SSP) of melt PLLA/PDLA blends (Scheme 10). The copolymers could be fabricated into films by solution casting or melting methods, and showed exclusive stereocomplexation with little or without homochiral crystallization presented. This indicates that the intimate interaction of PLLA and PDLA in the stereoblock chains could supress the formation of homochiral crystals. In a particular example, the stereocomplex crystallization in PLLA-PDLA stereo-diblock copolymer system was enhanced by blending the copolymers with complementary stereo-sequence. However, the polymer films have been shown to soften at temperature above T_g, that is as low as 60 °C despite showing high T_m at above 210 °C. This is probably due to the low amount of stereocomplex crystal caused by non-equivalent D/L ratios in the copolymer. Further improvement was made by addition of PDLA homopolymer in PLLA-PDLA stereo-diblock copolymer system to compensate the D/L ratio that resulted in prevention of thermal softening effect. This was achieved by supressing the free motion of the abundant enantiomeric chains and increasing stereocomplexibility [93]. As such, the blend samples were found to retain high loss modulus (10^8 dyn/cm^2) above T_g as well as increased heat-stability up to 215 °C. Similarly, PLLA-PDLA-PLLA stereo triblock and multiblock copolymers also preferentially formed stereocomplex crystals unless their PLLA/PDLA block ratio declined to one extreme or the other. The intermolecular stereocomplexation afforded crosslinking points along the polymer chains and induce interesting self-assembly morphologies, such as flower- and cake-shaped stereocomplex particles [97]. Through enantiomeric adjustment of PLLA/PDLA ratio in the stereoblock copolymer blends, stereocomplex crystallinity and thermo-mechanical properties were also significantly enhanced [94–96].

On the other hand, elastomeric soft segment poly(3-methy-1,5-pentylene succinate) (SA/MPD:C) was designed to prepare PLLA-PDLA based stereo pentablock copolymers (PDLA-PLLA-SA/MPD-PLLA-PDLA) [98]. The inner stress was effectively weakened and the brittle nature of PLA stereoblock copolymers was greatly altered by incorporation of the soft segments. For example, the stress–strain study showed that the mechanical properties of the pentablock copolymers can be controlled by changing the block ratios from thermoplastic elastomers to flexible plastics. Meanwhile, the excellent heat stability was preserved owing to the easy stereocomplex formation of the neighbouring PLLA/PDLA in the stereoblock copolymers [98]. All these new materials features could make PLLA-PDLA stereoblock copolymers promising for high-performance applications including structural materials and engineering plastics.

Star-shaped PLLA-PDLA stereoblock copolymers with various arm numbers were also prepared by click coupling of azido-functionalized PDLAs and the ethynyl-functionalized PLLAs possessing different branches ((PLLA)$_x$-(PDLA)$_y$, x and y = 1, 2 and 3) (Fig. 12) [99]. The desired products having Mw of about 10 kg/mol were obtained with high purify. The star-shaped macromolecule structure was confirmed by MALDI-TOF MS. WAXS and DSC studies revealed that the solvent cast samples of (PLLA)$_x$-(PDLA)$_y$ stereoblock copolymers formed preferentially stereocomplex crystals without any trace of homochiral crystallization. The arm numbers in the copolymer affected their T_m and crystallinity, i.e., an increase in arm number caused a decrease in the T_m and crystallinity. A study of stereoblock effect on the polymer stereocomplex properties study showed that T_m of (PLLA)$_x$-(PDLA)$_y$ samples were 5–7 °C higher than that of corresponding (PLLA)$_x$-(PLLA)$_y$/(PDLA)$_x$-(PDLA)$_y$ blend samples, for example, 196 °C for (PLLA)$_2$-(PLLA)$_2$/(PDLA)$_2$-(PDLA)$_2$ and 201 °C for (PLLA)$_2$-(PDLA)$_2$. This indicated that connecting the branched PLLA and PDLA blocks in one molecule to produce star-shaped stereoblock copolymer,

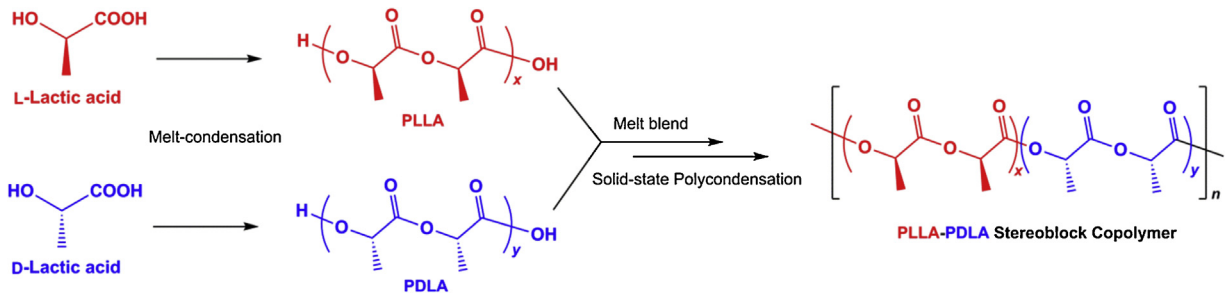

Scheme 10. Synthesis route of PLLA-PDLA stereoblock copolymers by the combination of melt and solid-state polycondensation.

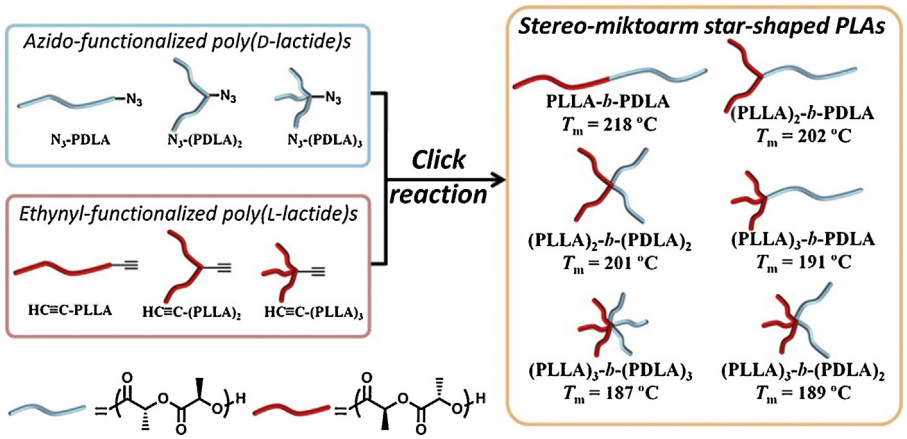

Fig. 12. Synthetic strategy of star-shaped PLLA-PDLA stereoblock polymers by click coupling of azido-functionalized PDLA and the ethynyl-functionalized PLLA [99].

rather than mixing of enantiomers, would result in the formation of stereocomplex with higher T_m [99]. In another example, a pair of macrocyclic PLLA-PDLA stereoblock copolymers with head-to-head and head-to-tail linkages of the PLLA and PDLA blocks were synthesized [100]. The topology effect on T_m of isomeric cyclic PLLA-PDLA stereoblock copolymers having the complementary linking orientations was systematically investigated. The results showed that, upon cyclization, the T_m of the head-to-head PLLA-PDLA stereoblock copolymers increased from 206 to 221 °C, possibly due to the promoted stereocomplex formation by the elimination of the free chain ends during the cyclization. On the contrary, T_m of the head-to-tail counterpart decreased by 5 °C compared with the linear precursor. This could be due to the geometrical restriction of the cyclic topology on the arrangement of the PLLA and PDLA segments in head-to-tail orientation [100].

In addition to star-shaped stereoblock PLAs consisting of PLLA and PDLA arms, Satoh and co-workers also designed brush copolymers consisting of densely grafted PLLA and PDLA side chains, "stereoblock-like PLA brush copolymers", that could behave like stereoblock PLAs, allowing the effective formation of a stereocomplex in the confined space created along the backbone [101]. Random and block copolymerizations of PLLA and PDLA macromonomers having an exo-norbornene group at the α- or ω-chain end (D/L ratio = 1/1, M_n = ca. 5000 g/mol) were performed via ring-opening metathesis polymerization to produce stereoblock-like PLA brush random and block copolymers consisting of parallel or antiparallel aligned PLLA and PDLA side chains on a poly(norbornene) backbone. The stereocomplex properties of the brush random and block copolymers as well as the corresponding blended mixture of enantiomeric brush homopolymers were characterized by XRD and DSC measurements to clarify the effect of the various structural factors, i.e., chain growth direction (backbone to outside or outside to backbone), relative chain direction (parallel or antiparallel), distribution of PLLA/PDLA side chains (random or block), and the backbone length, on the resulting stereocomplex properties. The Mw and PDI of the brush copolymers were in the range of 40,300–458,000 g/mol and 1.03–1.14, respectively. Despite such high Mw, these brush copolymers formed stereocomplex without homochiral crystallization. The T_m and crystallinity of the resulting stereocomplex varied depending on the backbone length, relative chain direction, and distribution of the PLLA/PDLA side chains. The parallel brush copolymers showed significantly higher T_m and crystallinity values than the antiparallel ones, demonstrating that the PLLA/PDLA side chains aligned parallel on the poly(norbornene) backbone facilitated the formation of a thermodynamically stable stereocomplex crystallites, as illustrated in Fig. 13. The stereocomplex properties of the parallel brush random copolymers were insensitive to the backbone length. However, there was a significant negative effect of the backbone length on the

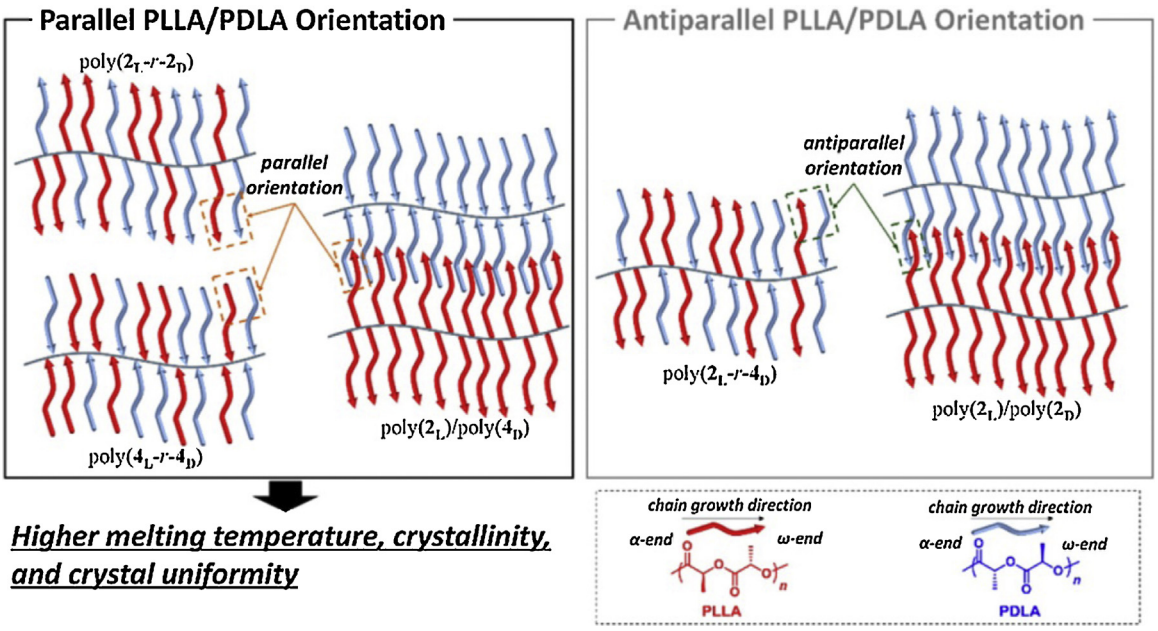

Fig. 13. Schematic representation of parallel and antiparallel orientations in the stereocomplex crystallite formed from PLLA and PDLA brush homopolymers and blends of enantiomeric homopolymers consisting of poly(norbornene) backbone having PLLA and PDLA side chains [101].
Copyright 2014. Reproduced with permission from the American Chemical Society.

$T_{m,sc}$ and crystalline uniformity of the antiparallel random copolymers. The difference in the dependence of backbone length on stereocomplex properties could be due to the slower crystallization kinetics for the antiparallel series than for the parallel series [102–105]. Okihara et al. [106] proposed that the PLLA and PDLA helices are ordered in the parallel orientation in the stereocomplex crystallite, while Brizzolara et al. [107] pointed out that both parallel and antiparallel orientations are possible because of the similar interaction energy and packing structure. In terms of improving the material properties of the stereocomplex PLAs, the antiparallel orientation should be excluded from the crystallite. Indeed, Tezuka et al. realized the preferred parallel orientation of the PLLA and PDLA chain in macrocyclic stereoblock PLAs, that revealed that the parallel orientation in the stereocomplex crystallite gives rise to a higher T_m value than for the antiparallel one [100].

Grubbs et al. reported that the blend of a similar high molecular weight ($1.07–2.55 \times 10^6$ g/mol) stereoblock-like PLA brush copolymers with a linear PDLA, formed stereocomplex without homochiral crystallization, while the stereocomplex formation in the blend of the enantiomeric PLA brush copolymers was highly restricted [87]. They demonstrated that by using the tendency for stereocomplexation between PLLA and PDLA as a driving force, complementary linear polymer is capable to interdigitate into densely grafted molecular brush copolymers to form a stereocomplex, as depicted in Fig. 14. Due to the adequately strong stereocomplex driving force, brush polymers can allow diffusion of macromolecules into their side chains, such that at sufficient distance from the brush polymer main chain, some entanglement may begin to take place at the ends of the side chains. However, stereocomplex formation between complementary brush copolymers

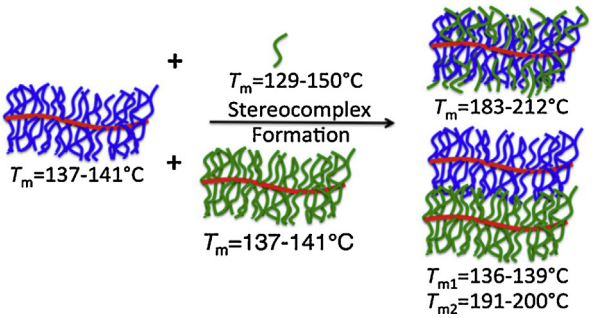

Fig. 14. Schematic representation of stereocomplex formation between stereoblock-like PLLA brush copolymer with a linear PDLA as well as the stereocomplex formation in the blend of the enantiomeric PLLA and PDLA brush copolymers [87].
Copyright 2014. Reproduced with permission from the American Chemical Society.

is restricted and only partially observed when the side chains are of a critical Mw (Fig. 14). These results add to the intriguing properties of brush polymers and may aid in extending the scope of applications for these macromolecules.

2.2.2. PLA/PCL block copolymers

In addition to PLA, PCL is another type of biodegradable and biocompatible polyester that has been extensively studied. Because of the synthetic versatility and presence of reactive groups, PCL and its derivatives have been widely reported for block copolymer development in most biomedical applications [50–52,108]. Block copolymers from LA and caprolactone (CL) containing highly crystalline and amorphous components could afford materials with

interesting phase behavior. It was previously reported that stereocomplex formation occurs by binary blend of PLLA-PCL and PDLA-PCL block copolymers. The enantiomeric blends showed improved performance that could not be achieved by their parent polymers [24,109]. For example, Portinha et al. studied the aggregation behavior of PLLA-PCL and PDLA-PCL diblock copolymers in THF solutions [22]. The results showed that the hydrodynamic radius of cocrystallization induced assemblies in enantiomeric blended solutions were 200 nm, higher than that for the individual L or D-forms of copolymers in solution. The enantiomeric blend also exhibited sharper distribution in hydrodynamic radius than that of non-blended polymer solutions [22]. Further investigation on the self-assembly properties revealed that, at higher concentrations, such as 10 g/mL, stereocomplexation was in competition with a solvophobically driven aggregation, whereas at lower concentrations, stereocomplexation was the only process involved [24]. In addition, PCL block in the copolymers could improve the colloidal stability by steric repulsion and limit the growth of the particles [23]. At a PLA length of ~2800 g/mol, the driving force for self-assembly is reduced as compared to PLA with higher Mw. However, the PLLA-PCL/PDLA-PCL particles formed through stereocomplex were stable for months, even in dilute solutions. From AFM phase images, the particles were in well-controlled anisotropic cylindrical shape and were harder than the background, that is compatible with the crystalline nature of the stereocomplex [23] In another example, thermal properties of PLA/PCL di and triblock copolymers were examined by the corresponding blends. The stereocomplex occurred in all enantiomeric polymer pairs when the mixtures were precipitated from a dichloromethane solution into methanol. An increase of approximately 55 °C in the T_m of PLA phase was detected in the blends as compared to individual enantiomeric PLA copolymers. There are no significant differences between the di and tri-block systems [110].

Although solvent casting and melt processing have been widely used to produce stereocomplex PLA, these two methods have major disadvantages, including generating low degrees of stereocomplexes, long processing time and a limited Mw range of PLLA and PDLA. Supercritical carbon dioxide (sc-CO_2) was explored to improve these shortcomings, demonstrating easy combination of molecular units and achieving fast stereocomplexation. High mass transfer between PLA helical conformations and low cost could be another advantages of this method. For example, Kim et al. reported the stereocomplex formation between random PLLA-*r*-PCL and PDLA-*r*-PCL block copolymers at high Mw ($M_n > 10^5$ g/mol) by sc-CO_2 modified co-solvent system [111]. The specimen obtained exhibited higher thermal stability that significantly enhanced the degree of stereocomplex after melting, indicating that the presence of flexible CL units could increase the mobility of the PLA chains during stereocomplexation. Further study by the same group showed that the increase in chain mobility was caused by methylene groups within CL fragments that acted as soft segments in the copolymer chain [112]. In addition, the blends functioned as soft stereocomplex materials with improved properties. Typically, the tensile strength was about 2.5 times higher than those of commercial PLGA [111]. In addition, the degradation rate could be controlled by the CL content in the copolymers. A comparison study showed the blends of random PLLA-*r*-PCL and PDLA-*r*-PCL possessed faster degradation than PLLA-PCL and PDLA-PCL stereocomplexed block copolymers [113]. The random PLA-*r*-PCL blends also showed a higher elongation at break than that of PLA-PCL blends, whereas the tensile moduli were reversed. When the PDLA-*r*-PCL was blended with neat PLLA, the increased chain mobility could assist PDLA fragments to confront with PLLA to form stereocomplex and further enhanced the melt stability by neighbouring participation [112]. Blending PLA-PCL block copolymers with the corresponding enantiomeric derivatives resulted in mechanical improvement, thermal stability and also controlled degradation. This would thus lead to formation of new materials with high potential in both industrial and medical fields.

2.2.3. PLA/PHB block copolymers and others

Poly(hydroxybutyrate) (PHB) is another example of biodegradable polyesters that has different isomeric structures [114]. Specifically, poly(2-hydroxybutyrate) (P2HB) is known to form hetero-stereocomplex with PLA when two optically active polymers with the opposite configurations are blended. Tsuji et al. reported the crystallization behavior of block copolymers with substituted and non-substituted PLAs, i.e., P(D-2HB)-PLLA and P(D-2HB)-PDLA [115]. The results showed that only hetero-stereocomplex crystallites were formed in P(D-2HB)-PLLA when the samples were subject to the temperature range of 60–160 °C and the formation of P(D-2HB) and PLLA homocrystallites was not detected. At equilibrium, the T_m of P(D-2HB)-PLLA was 189 °C, that was higher than the 171.3 °C for PDLA homocrystallites in P(D-2HB)-PDLA. This indicated that the block copolymerization is a very effective method to increase PLA thermal stability by forming hetero-stereocomplex crystallites between P(D-2HB) and PLLA [115]. On the other hand, PLLA-P(*R,S*-3HB)-PDLA stereo triblock copolymers were synthesized through a sequential living ROP of lactides and β-butyrolactone (BBL) with dinuclear indium $[(NNO)InCl]_2(\mu\text{-OEt})(\mu\text{-Cl})$ as catalyst (Scheme 11). A comparison of thermal properties showed that copolymers with atactic PHB as the middle block, displayed only one melting temperature, indicating formation of exclusive stereocomplex crystallites. In addition, the T_m of triblock copolymers with PLLA and PDLA at each end was much higher compared to the copolymers with PLLA at each end, and the longer L- and D-blocks in PLLA-P(*R,S*-3HB)-PDLA would result in a higher melting temperature [116]. Rheological studies indicated that PLLA-P(*R,S*-3HB)-PDLA copolymers barely flowed and exhibited solid-like behavior even at temperature above the stereocomplex formation. However, the elastomeric nature of P(*R,S*-3HB) would render PLLA-P(*R,S*-3HB)-PDLA copolymers significant improvement in elongation at break. Typically, the elongation at break increased by a factor of 5−10 times in comparison to the copolymers having PLLA only, showing the important impact on the mechanical properties [116].

In addition, the stereocomplexation effect in other types of PLA-polyesters block copolymers has also been well

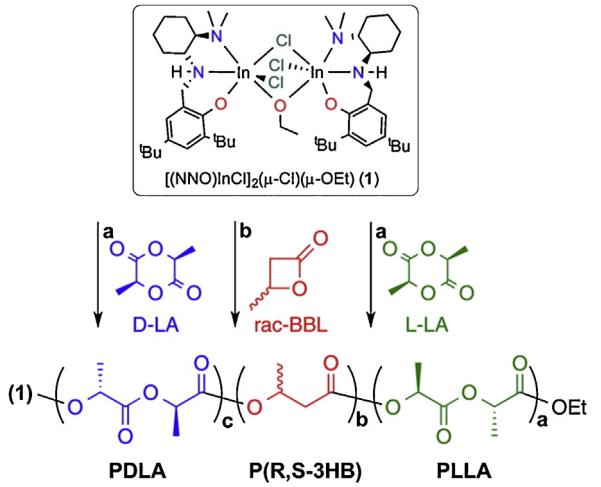

Scheme 11. Synthesis of PLLA-P(R,S-3HB)-PDLA stereo triblock copolymers through a sequential living ROP of lactides and β-butyrolactone with dinuclear indium as catalyst [116].
Copyright 2013. Reproduced with permission from the American Chemical Society.

established to achieve new materials properties, including PLA-PBS [PBS: Poly(butylene succinate)] and PLA/PRA [PRA: Poly(ricinoleic acid)] block copolymers. For example, when mixing equivalent amounts of enantiomeric PLA-PBS-PLA copolyester pairs in acetonitrile solution at 60 °C, in situ self-assemblies occurred and the PLLA/PDLA block lengths in the copolymers was a crucial factor in mediating self-assembly properties [117]. It was shown that the interactions stemming from stereocomplexation, induced the stable stereocomplex to aggregate together and self-organize to form molecular clusters or microparticles with uniform distribution and core-shell structure. In another example, L-lactic acid and ricinoleic acid were copolymerized to yield PLA-PRA block copolymers with different macromolecular structures [118]. Stereocomplexes were formed spontaneously during the precipitation of polymer from solution or by melt mixing, and showed different physical properties in terms of solubility, film forming properties, and melting temperature when compared to films formed without sterecomplex. The resultant pasty PLA-PRA block copolymers could be used as carrier for drugs and polymeric scaffolds for tissue engineering [118].

2.3. Other PLA-based block copolymers

The PLA-polyester block copolymer systems discussed in the preceding provided stereocomplexes with enhanced materials performance and demonstrated good potential in many interesting applications. Other block copolymer systems consisting of PLA sequences have also been reported to form similar stereocomplexes. For example, bisphenol A epoxy copolymerized with PLA chains (PLA-Bis A),[119] PLA-poly(sebacic acid)-PLA ester-anhydride (PLA-PSA-PLA) triblock copolymers,[9] and PLA-polymenthide-PLA (PLA-PM-PLA) [120] are particularly interesting as they showed altered physical properties with respect to melting temperature and mechanical strength. Another interesting example is PLA-PS diblock copolymer [PS: polystyrene]. The different stabilities or degradability between the PS and PLA blocks could afford a possible route to prepare novel functional structural hierarchies [121,122]. PLA-PS bearing similar lengths of respective PLLA and PDLA blocks were synthesized through controlled ATRP of styrene, and a subsequent living ROP of enantiomeric LA monomers [121]. The in situ aggregation behavior of the copolymer mixtures in a non-selective solvent was investigated and the different material properties induced by PLA stereocomplex were highlighted by comparing with other polymer combinations of PLLA-PS/PDLA and PLLA-PS alone. Unlike the individual PLLA-PS system, the interplay of stereocomplexation between the PLLA and PDLA blocks was the sole driving force for self-assembly, that gradually biased the well-dissolved copolymer coils to interlock and self-assembled into THF insoluble cores comprising more stable racemic crystals. The THF-soluble PS block segments were surrounded by the less mobile cores to form the well-defined core–shell structural aggregate, that gradually associated to increase their sizes to a highly uniform extent until exceeding the solvability of PS. On the contrary, the relatively poor affinity between PLLA and PS in PLLA-PS diblock copolymer induced the formation of micelle-like particles in THF without further association. The sizes of these micelle-like particles increased only by absorbing more free chains with PLLA homochiral crystals as the main internal component (Fig. 15) [121].

In another aspect, polyhedral oligomeric silsesquioxanes (POSS) are the smallest possible silica particles containing nano-sized inorganic cores, made of silicon and oxygen atoms linked together in a cubic form [123]. It is of great interest to design new POSS-polymer hybrids to combine the nanosize level of active inorganics and organics in a single material, that would create entirely new compositions having truly unique properties [124–127]. The synthesis of PLLA-P(MA-POSS) and PDLA-P(MA-POSS) block copolymers and evaluated their self-assembly in solution via PLA stereocomplexation has been reported [25]. Stereocomplexed nanoparticles in solution were formed by simply mixing two solutions of copolymers containing complementary PLLA and PDLA blocks. Similar to the PLA-PS system, stereocomplexation proved to be the only driving force for self-assembly. Further study showed that the size and stability of the nanoparticles could be controlled by the inorganic P(MA-POSS) block lengths. As illustrated in Fig. 16, the experimental findings were supported by the density functional theory (DFT) simulation. The results demonstrated that at fixed PLA block length, the optimized van der Waals (vdW) volumes, surface areas and cross sectional area in PLA-P(MA-POSS) increased with increasing number of POSS units. This would make it difficult for the neighbouring complementary PLA to form a stereocomplex, and subsequently decreased the size of the aggregates formed in solution [25]. All these results indicated that with careful design of the copolymer structure and chemical compositions, new functional aggregates bearing desirable sizes, morphologies and stabilities can be obtained through PLA stereocomplexation.

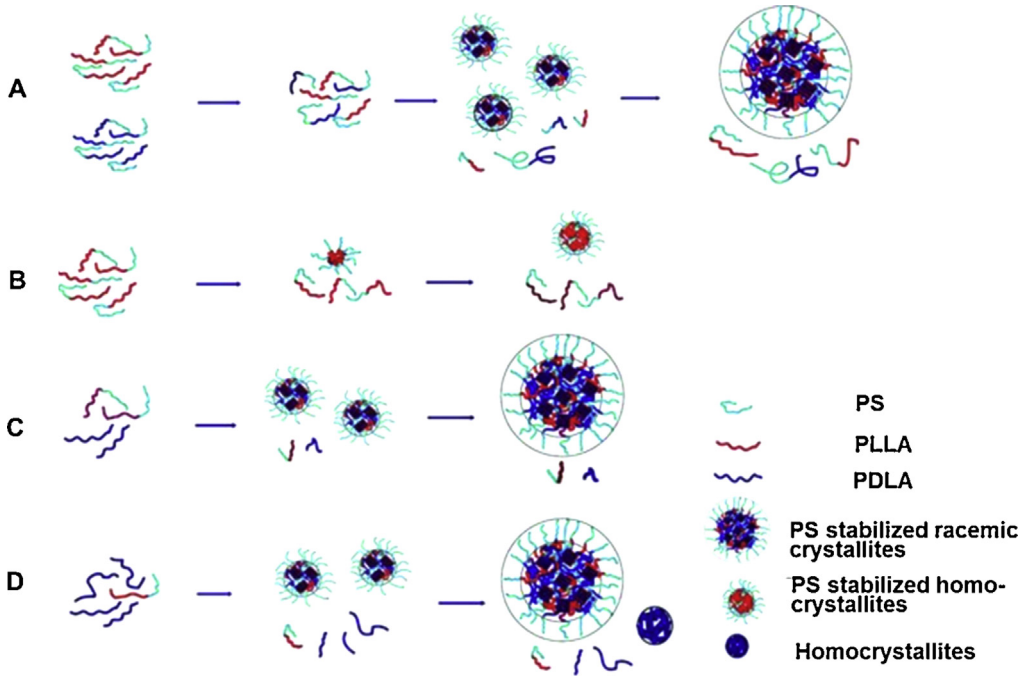

Fig. 15. In situ aggregation mechanism of (A) enantiomeric PLLA-PS and PDLA-PS diblock copolymer, (B) PLLA-PS, and (C) PLLA-PS/PDLA at 1:1 and (D) other enantioermic ratios [121].

3. Stereocomplexation of PLA-graft copolymers

Stereocomplexation is also an effective method to produce stable structures from various PLA graft copolymers. Compared to PLA linear block copolymers, the advent of stereocomplexation in PLA-graft copolymers has become more prominent in the last ten years. The development of advanced synthesis techniques has enabled the grafting of various materials onto PLA, to give hydrophilic polymers, inorganic materials and carbon-rich materials. Thus the exploitation of PLA stereocomplexation in these various graft copolymers provides an alternative route, besides PLA block copolymers, to develop materials with enhanced properties, that will be reviewed in this section.

3.1. PLA-graft amphiphilic copolymers

To date, various groups have attempted to regulate the hydrophobicity of PLA by grafting hydrophilic polymers, such as PEG, polysaccharides (pullulan, dextran, and amylose), phospholipid and poly(glutamic acid) onto the hydrophobic PLA either via a "grafting from" or "grafting onto" strategy to produce amphiphilic PLA grafted copolymers. In this section, different types of amphiphilic PLA-grafted copolymers that have been used to exploit PLA stereocomplexation will be reviewed. The representative examples and new stereocomplex properties are also summarized in Table 1.

3.1.1. PLA/PEG graft copolymers

The group of Coughlin and Frey performed a systematic comparison between graft PEG-*g*-PLA copolymers with different topologies and studied the influence of polymer architecture on PLA stereocomplex crystallization [79]. Two "topological isomers," a linear PEG copolymer and a branched PEG copolymer with varying glycerol content were used as backbone polymers to synthesize graft or hyperbranched copolymers via the "grafting from" (or core-first approach) followed by controlled ROP of lactide on the multifunctional PEG used as an initiator backbone polymer as shown in Scheme 12. For linear graft-copolymers, the macroinitiator is synthesized from ethylene glycol (EG) and ethoxyethyl glycidyl ether (EEGE). Acidic removal of the ethoxyethyl protecting group yielded linear P(EG-*co*-G) that, compositionally, is a linear PEG with a varying number of hydroxyl groups where lactide polymerization can be initiated. On the other hand, the hyperbranched macroinitiator is prepared via direct copolymerization of glycidol and ethylene glycol. Depending on the amount of hydroxyl functionalities and lactide monomer to hydroxyl group ratio, the number of PLA side chains and PLA chain lengths can be varied, respectively.

When blending the graft-PEG/PLLA with PDLA homopolymers, it was discovered that stereocomplex crystals formed preferentially over the homopolymer crystals in all the graft and hyperbranched PLLA and PDLA stereocomplex blends [79]. For the 25% hyperbranched copolymer blend, stereocomplex formation is impeded due to the increased steric hindrance, and both homopolymer crystallization and stereocomplex crystallization occurred [79]. In addition, the crystalline morphology and the spherulitic growth process of the graft and hyperbranched PEG-PLA were compared with morphology and growth of PLA-PEG-PLA triblock copolymers using polarized optical

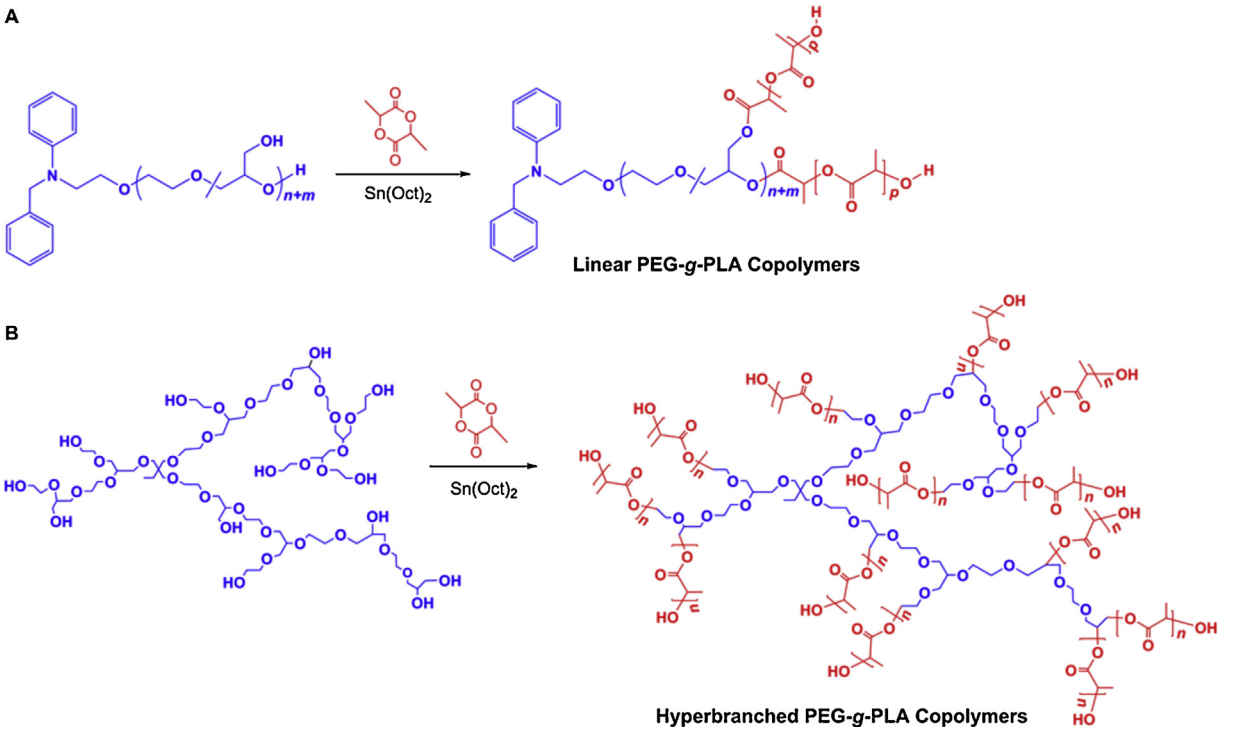

Scheme 12. Synthesis of PLA-g-PEG copolymers in (A) linear and (B) hyperbranched topology [79].

microscopy (POM) [79]. The results showed that most of the graft and hyperbranched PEG-PLA blend samples had a typical spherulitic morphology as compared to the triblock copolymer blends that did not show clear spherulitic morphologies. Instead, the PLA-PEG-PLA triblock copolymer blends formed typical dendritic morphologies because of the presence of large amounts of PEG in this blend, where the PEG could form covalent bonds with PLLA and would be trapped in the interlamellar and interfibrillar regions of stereocomplex crystals. Numerous inter-spherulitic amorphous regions are also found in the triblock copolymer blend that translates to stereocomplex crystals dispersed in a continuous amorphous phase. The lower content of PLLA in the triblock copolymer blends compared with the hyperbranched and graft copolymer blends resulted in fewer nucleation sites for stereocomplex crystallization in the former, leading to a different morphology in comparison with the other blends [79,128].

Nagahama and co-workers designed PRX-based graft copolymers (PRX: polyrotaxane), in that PLLA or PDLA side chains were grafted onto α-CDs threaded on a PEG main chain [129]. They successfully exploited the stereocomplex formation between enantiomeric PLLA and PDLA grafted copolymers to enhance specific molecular recognition on a movable polyrotaxane platform in the bulk whereas PLLA or PDLA homo crystals were not. Based on this unique stereocomplex self-assembly, the obtained films formed continuous anisotropic phases over a wide temperature range [129]. Because PLA and PRXs of PEG and CD are biocompatible polymers, PRX-*g*-PLAs with unique phase structures and softness offer a new opportunity in the field of biomaterials for the human body.

3.1.2. PLA-g-dextran copolymers

PLA-grafted dextran (PLA-*g*-Dex) based copolymers are another type of amphiphilic polymer, widely exploited to develop unique stereocomplex structures, mainly as biomedical materials [130–135]. Hennink and co-workers [5,136–138] and later Nagahama et al. [21,139] developed a controlled synthesis method based on the "grafting onto" approach to couple PLA to dextran via the activation of the hydroxyl group on PLA with N,N′-carbonyldiimidazole (CDI), followed by the coupling of the activated compound to dextran and subsequently yielding Dex-*g*-PLA (Scheme 13). The teams demonstrated that they could vary the degree of grafting/coupling of the activated PLA onto dextran from 30% to 85% by controlling the molar feed ratio of activated hydroxyl compound to dextran as well as the coupling reaction time and temperature.

Nagahama reported that it is possible to obtain monodisperse stereocomplex nanogels that are stable against destabilizing agents such as surfactants simply by mixing aqueous solutions of the enantiomeric PLLA-*g*-Dex and PDLA-*g*-Dex [21]. The self-assembled stereocomplex nanogel possessed partially crystallized cores of stereocomplex PLA and a hydrophilic dextran shell. The stereocomplex nanogel also exhibited a significantly lower CAC value as well as stronger thermodynamic stability compared to those of the corresponding L- or D-isomer nanogels. The group also prepared stereocomplex films to produce materials exhibiting mechanically tenacious and

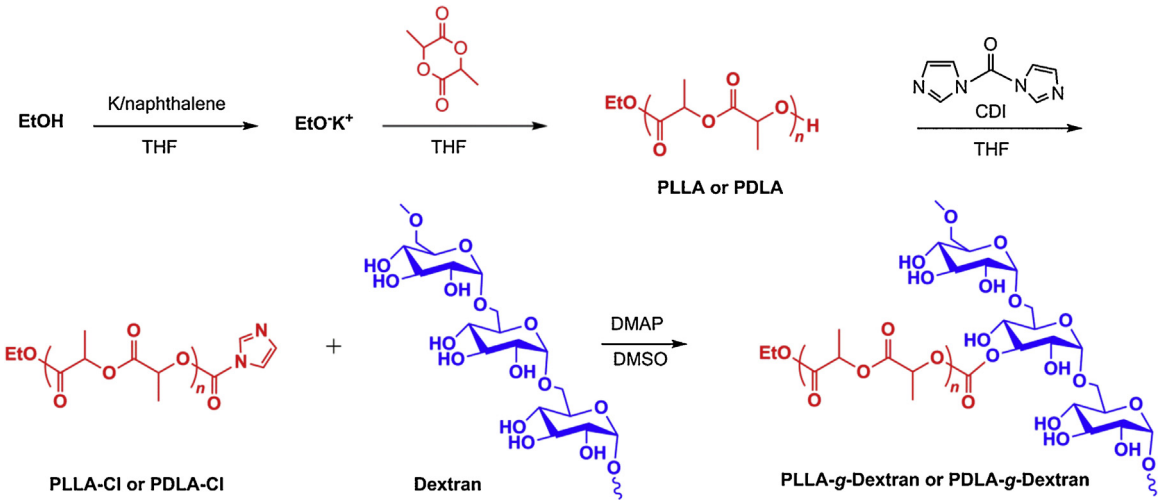

Scheme 13. Synthesis of PLLA-*g*-Dex and PDLA-*g*-Dex copolymers through "graft onto" strategy [21].
Copyright 2007. Reproduced with permission from the American Chemical Society.

tough characters in the wet state [139]. The stereocomplex blend films showed lamellar-type microphase-separated structures. When swollen with water, these blend films showed the same level of tensile strengths and Young's modulus as the films in the dry state.

In addtion to the ability to form stable nanogels in dilute solutions and stereocomplex blend films, it has been demonstrated that equimolar mixture of the aqueous solutions of PLLA-*g*-Dex and PDLA-*g*-Dex can form hydrogels in an aqueous environment for cargo release (Fig. 17) [5,136–138]. The cross-linking in hydrogel was created by stereocomplex formation between enantiomeric PLLA and PDLA grafted to dextran as confirmed by FTIR and XRD analysis [137,138]. As revealed in the rheological measurement, the storage modulus of the obtained hydrogel strongly decreased upon heating to 80 °C, while it was restored upon cooling to 20 °C, demonstrating the thermo-reversibility and the physical nature of the crosslinks.

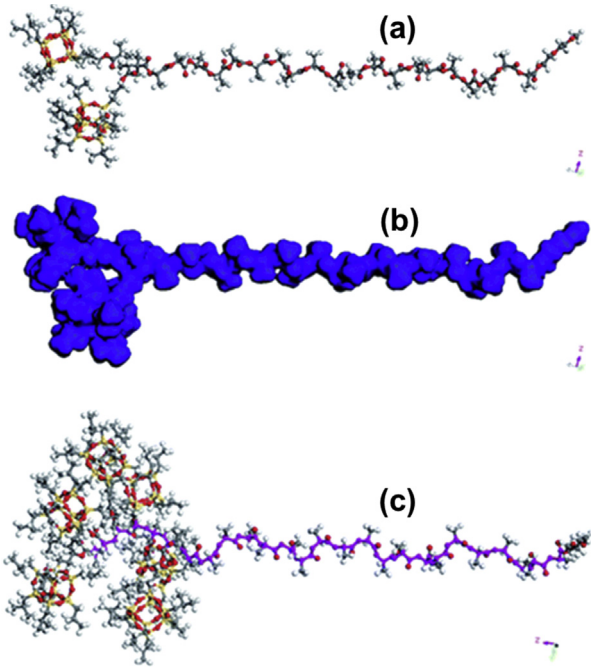

Fig. 16. DFT simulation of (a) the optimized geometry and (b) van der Waals surface area of PLA-P(MA-POSS) with 2 repeat unit of MA-POSS, and (C) optimized geometry of PLA-P(MA-POSS) with 6 repeat unit of MA-POSS [25].
Copyright 2013, reproduced with permission from the Royal Society of Chemistry.

In addition, rheological experiments with monodisperse lactic acid oligomers grafted to dextran showed that the DP of the lactic acid oligomers must be at least 11 to obtain a hydrogel [5,136,137]. The hydrogel characteristics may be modulated by varying the DP, degree of substitution (DS, number of lactic acid side chains per 100 glucopyranose units) of the PLA-*g*-Dex copolymers and water content of the PLA-*g*-Dex solutions. Stronger gels were obtained by increasing the DP and DS, and by decreasing the water content. It was further discovered that under physiological conditions, the gels and blend stereocomplex films formed from stereocomplex PLA are fully degradable in aqueous systems [5,21,139]. This implies that when the stereocomplex hydrogels and films are applied in vivo, it is very likely that they are fully degradable and no crystalline stereocomplex fragments will remain. The degradation properties of stereocomplex PLA-*g*-Dex nanogels could be tuned by varying the number of grafted PLA chains, the length and polydispersity of the grafts and the initial water content. It is hypothesized that the degradation of the stereocomplex hydrogel starts with hydrolysis of the carbonate ester, that links the lactate graft to dextran. Similar hydrolytic degradation properties were also obtained in stereocomplex hydrogels from poly(2-hydroxypropylmethacrylamide) (pHPMAm)-*g*-L- and D-lactic acid oligomers that can be readily tailored from 1 week to almost 3 weeks by changing the grafting density of the polymers and the structure of the terminal group of the side chains [140]. The enantiomeric mixture of

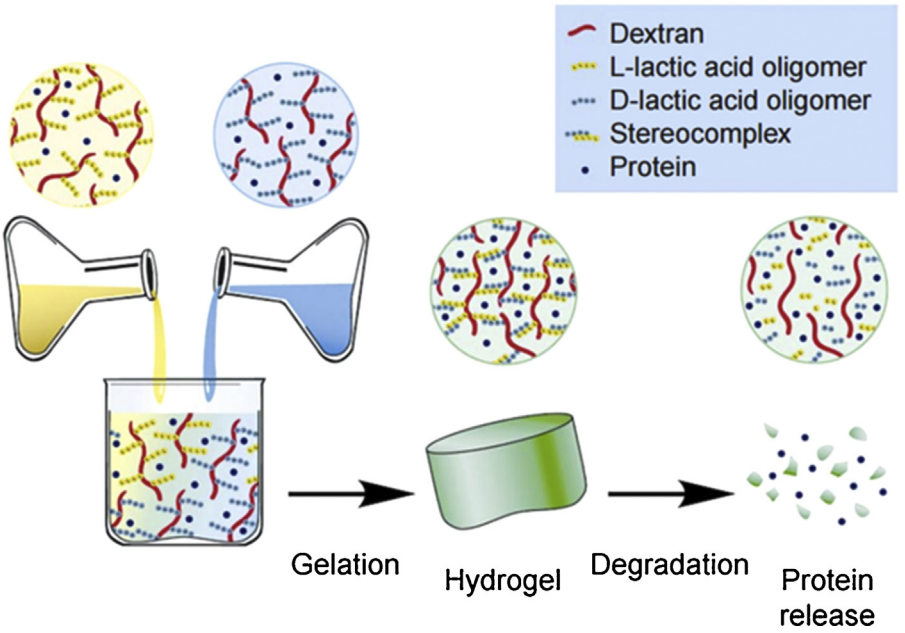

Fig. 17. Schematic pictures illustrating the preparation of stereocomplex hydrogel for protein release by using PLA-g-dextran copolymers containing either L- or D-lactic acid units as grafts [140].

PLA-*g*-Dex to form stereocomplex should be a good candidate for an implantable biocompatible material exhibiting favorable mechanical properties and degradation behavior. More studies on the application of stereocomplex PLA-*g*-Dex hydrogels for loading and delivery of actives will be discussed in Section 4.1.

3.1.3. *PLA-g-phospholipid copolymers*

Stereocomplexation of PLA has also been exploited in PLA grafted phospholipid based copolymers for enhancement of cell adhesion. Particularly, the 2-methacryloyloxyethyl phosphorylcholine (MPC) copolymers, that is a type of phospholipid, were widely investigated and used as excellent biomaterials that suppress not only protein adsorption [141] and cell adhesion [142], but also the inflammatory reaction for attached cells [16]. Ishihara and co-workers grafted PLLA and PDLA onto MPC copolymers via the "grafting onto" approach to produce a novel PLA grafted phospholipid copolymer (PMBLLA and PMBDLA) composed of MPC, n-butyl methacrylate (BMA) and the PLLA or PDLA macromonomer (Scheme 14) [16,143,144]. The PLLA and PDLA macromonomers containing methacrylate functional groups were first synthesized before proceeding to the graft copolymerization with MPC and BMA [16,143,144]. As revealed from the ^{1}H-NMR results, the DP corresponding to each building components in PMBLLA and PMBDLA could be tailored by changing the monomer ratio. The stereocomplexed PMBLLA and PMBDLA could be used as a functional coating material to support a better cell adhesion while the reference copolymer composed of the MPC and BMA units showed low cell adhesion. The group also prepared a porous scaffold from the stereocomplex formation between the PLLA and PDLA segments on the graft copolymers. The porous scaffold obtained from the PLA phospholipid copolymer was confirmed by wide-angle XRD and DSC and is of great importance as novel cell-compatible materials for tissue engineering.

The same group went on to develop an injectable hydrogel matrix by designing water-soluble biocompatible and biodegradable grafted copolymers composed of MPC and poly(L- or D-lactic acid) macromonomers [145]. Compared to the stereocomplex PLA/PEG block copolymer hydrogel system, the properties and functions of stereocomplex PLA grafted phospholipid copolymers (PMBLA) can be easily regulated through simple random copolymerization with changes in both the composition and the chemical structure of the monomer units [145]. Aqueous solutions containing the MPC polymers with PLLA and PDLA chains underwent spontaneous gelation when mixed together, due to the formation of a stereocomplex between the PLLA and PDLA side chains that act as crosslinking components in the hydrogel. The gelation time of the stereocomplex gels depended on the concentration of the polymers. For example, a mixture of 20 wt% polymers in the solution required 8.7 min for gelation, while a 15 wt% polymer solution required over 100 min. The hydrogels degraded in a buffer solution by hydrolysis of the side chain, and it is suggested that the stereocomplex hydrogels degrades under physiological conditions in the body. The degradation of the hydrogels was monitored by measuring the fluorescence intensity of the hydrogel containing phosphate buffer saline along with the FITC-labelled BSA as a function of time and pH. The fluorescence intensity became saturated at conditions corresponding to 100 h, 37 °C and pH 7.4 and the degradation rate increased in media with a higher pH. From these results, it is suggested that the polymer system could be applied as an injectable,

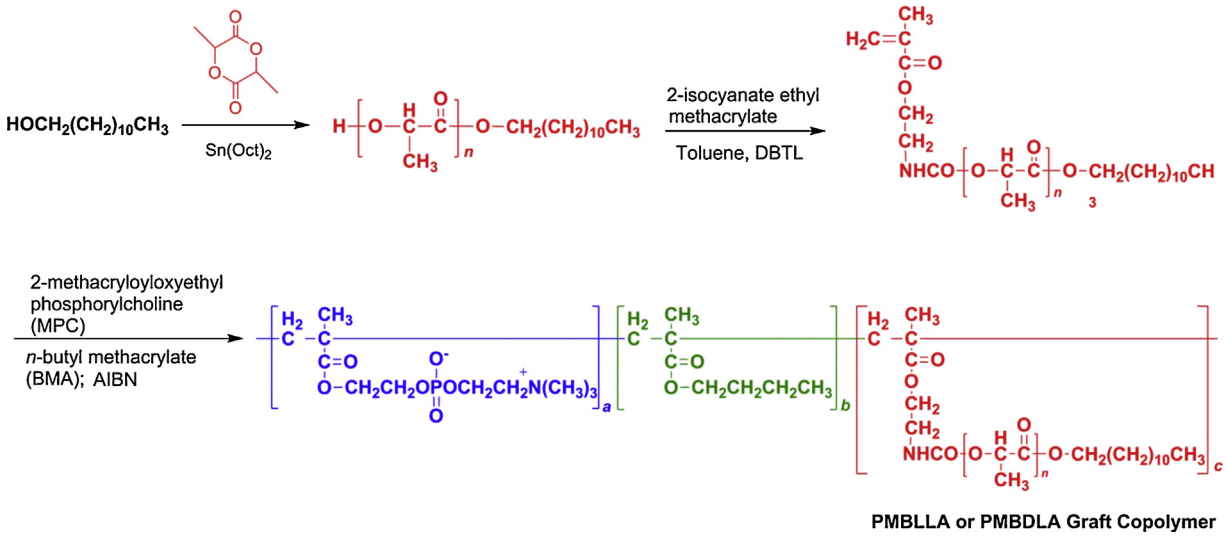

Scheme 14. Synthetic route of PLA grafted phospholipid copolymers PMBLLA and PMBDLA [16].

biocompatible, and degradable hydrogel system to serve as a reservoir of bioactive molecules in drug delivery systems and as a scaffold in cell-based tissue engineering [145]. The fibroblast cell adhesion on the graft-type PLA phospholipid copolymer-coated surface and the utilization of PLLA and PDLA stereocomplexation to prepare a porous scaffold and injectable hydrogels from the graft-type PLA phospholipid copolymers will be reviewed in Section 4.1.

3.1.4. PLA-g-poly(γ-glutamic acid) copolymers

Another water soluble polymer that has benefitted from the grafting of PLA and the corresponding stereocomplex interaction between the enantiomers PLA copolymers is poly(γ-glutamic acid) (γ-PGA) [11]. γ-PGA is a polyamide that is synthesized by certain strains of Bacillus. The polymer is made of D- and L-glutamic acid units linked through α-amino and γ-carboxylic acid groups, respectively, and its α-carboxylate side chains can be chemically modified. γ-PGA is water soluble, biodegradable, edible, and non-toxic for humans and the environment [146]. Furthermore, it is reported that high-molecular-mass γ-PGA can mediate antitumor immunity and initiate innate immune responses, suggesting that γ-PGA may warrant consideration as a therapeutic agent for cancer and other diseases [146]. However, γ-PGA still have some problems for in vivo applications, such as a relatively low drug-loading efficiency on the surfaces, poor stability of γ-PGA against dilution and difficulty in controlling the degradation process. Akashi et al. attempted to regulate the hydrophobicity of γ-PGA by grafting hydrophobic polymers, such as PLLA and PDLA onto the hydrophilic PGA backbone ("grafting onto" approach) to produce γ-PGA-*g*-PLLA and γ-PGA-*g*-PDLA copolymers.

In this "grafting onto" approach, 1-ethyl-3-(3-dimethylaminopropyl)-carbodiimide was used to introduce carboxylic groups in γ-PGA followed by the coupling reaction between the terminal hydroxyl group in PLA and the carboxylic groups in γ-PGA to produce γ-PGA-g-PLA graft copolymers with different grafting degree of PLA [147]. The group also synthesized amine-terminated PLAs by the ring-opening polymerization of L- and D-lactides using N-Boc-ethanolamine as an initiator, followed by removal of the Boc protection group from the PLA-NH-Boc [11]. The grafting of this amine-terminated PLAs (PLA-NH) onto γ-PGA was then carried out by the coupling reaction between the terminal amine group in PLA and the carboxylic groups in γ-PGA under similar reaction conditions as reported above for the hydroxyl terminated PLA (Scheme 15). The number of the PLA chains grafting was controlled by altering the feed ratio between γ-PGA and PLA in the reaction system [11,147]. The content of PLA units in the graft copolymer increased from 20% to more than 30% when the coupling reaction was carried out using amine-terminated PLAs (PLA-NH) compared to hydroxyl terminated PLA that was mainly due to the higher reactivity of the amine-terminated PLAs than hydroxyl-ended PLAs [11,147]. Self-assembly studies in aqueous solution demonstrated that both the individual γ-PGA-g-PLLA and γ-PGA-g-PDLA as well as equimolar mixture of enantiomeric γ-PGA-g-PLLA and γ-PGA-g-PDLA were able to form nanoparticles in aqueous solution [11]. The mean diameter, degree of stereocomplex crystallinity and degradation behavior of the stereocomplex nanoparticles could be controlled by changing the grafting degree of the copolymers and the preparation methods. Compared to nanoparticles formed by γ-PGA-*g*-PLLA and γ-PGA-*g*-PDLA only, the size of stereocomplex nanoparticles formed by an equal molar mixture of PLLA and PDLA copolymers was larger and the size distribution was narrower. The increased size implied that the number of copolymer chains involved in the self-assembling process was increased. In addition, the stereocomplex nanoparticles exhibit a lower CAC as well as stronger thermodynamic stability compared with the corresponding nanoparticles formed from enantiomeric L or D form only of the graft copolymers [147]. Further studies on

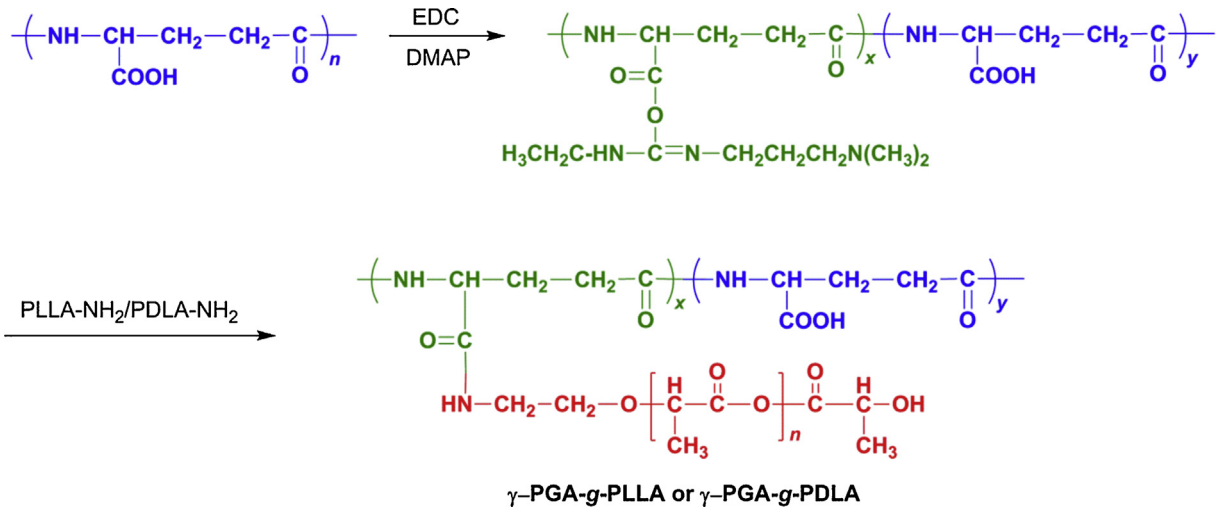

Scheme 15. Synthesis of γ-PGA-g-PLLA and γ-PGA-g-PDLA copolymers by coupling reaction between amine-terminated enantiomeric PLA and the carboxylic groups in γ-PGA [11].
Copyright 2014. Reproduced with permission from Wiley-VCH.

surface-functionalized ability and protein encapsulation capacity of the stereocomplex nanoparticles as potential targeting protein carriers will be reviewed in Section 4.1.

3.2. PLA-inorganic graft copolymers and others

While significant attention has been paid to the stereocomplexation of PLA organic based copolymers, the recent exploitation of stereocomplexation between the PLLA and PDLA segments of hybrid (organic/inorganic) copolymers indicates that stereocomplexation is also playing an important role in advancement of PLA/inorganic grafted copolymers [26,29–32,87,101,148–150] that will be reviewed in this section.

Polyhedral oligomeric silsesquioxane (POSS) is an increasingly popular inorganic component to impart new functionalities to stereocomplexed PLA hybrid copolymers [25,26,31,150]. POSS has a well-defined cage-like nanostructure made of silicon and oxygen atoms linked together in a cubic form, usually functionalized with organic functional groups at each corner to facilitate miscibility and/or covalent incorporation into organic polymers [123,125,151,152]. POSS nanoparticles have been extensively used to enhance various thermal and mechanical properties of organic polymers at the molecular level and more importantly, it is biocompatible as well [123,125,151,152]. The utilization of POSS nanocage as the core to grow PLA arms and the synthesis scheme of the resultant hybrid star polymers POSS-star-PLLA and POSS-star-PDLA synthesized via ring-opening polymerization is shown in Scheme 16.

Differential scanning calorimetry (DSC) and wide-angle X-ray scattering (WAXS) measurements in the solid state confirmed the formation of stereocomplex in the mixture of POSS-star-PLLA and POSS-star-PDLA (50:50 wt%). In a solution of the same mixture in tetrahydrofuran, stereocomplexation leads to formation of hybrid nanoparticles having CAC values that are approximately ten times lower than the values for individual POSS-star-PLLA or POSS-star-PDLA in THF. Moreover, the size distribution of the nanoparticles is much narrower in the case of the mixture sample than in the case of the individual polymers, suggesting the formation of a more compact and uniform nanoparticle induced by the stronger stereocomplex interaction. In the case of the individual polymers, the individual PLLA and PDLA star polymers self-assembled via weak solvophobic interactions that consisted of a balance between two competing forces, i.e., the Van der Waals forces between the PLA arms and the interaction between polymer chains and the solvent environment. Because the difference between the two competing forces is narrow, small fluctuations in local environment could lead to significant differences in agglomeration state and hence the size of the nanoparticle that explains the broad size distribution observed for nanoparticles in individual star polymer solutions [26]. In terms of stability of the hybrid nanoparticles against dilution, the size of the nanoparticles formed in the mixture sample is almost constant when diluted by a dilution factor as high as 5 (from 0.2 to 0.04 mg/mL), proving that the nanoparticles are very stable with dilution. Similar finding have been reported on the stability of the stereocomplex nanoparticles formed by enantiomeric PLA block copolymers in THF using small-angle neutron scattering (SANS) and static light scattering (SLS), where the nanoparticles remained stable over months and are not sensitive to dilution [22–24]. However, when similar stability experiments were performed on the individual PLA star copolymer, the size of the nanoparticles decreases by more than half from ~158 to ~67 nm when diluted by a dilution factor of 5, i.e., from 1.5 to 0.03 mg/mL. This finding clearly suggests that unlike the stereocomplex nanoparticles, the solvophobically driven nanoparticles in individual star polymer solution are dynamic and reversible in nature and kinetically unstable (not frozen) that tended to disintegrate into smaller nanoparticles on dilution. On the basis of the light scattering, ^{1}H NMR and transmission

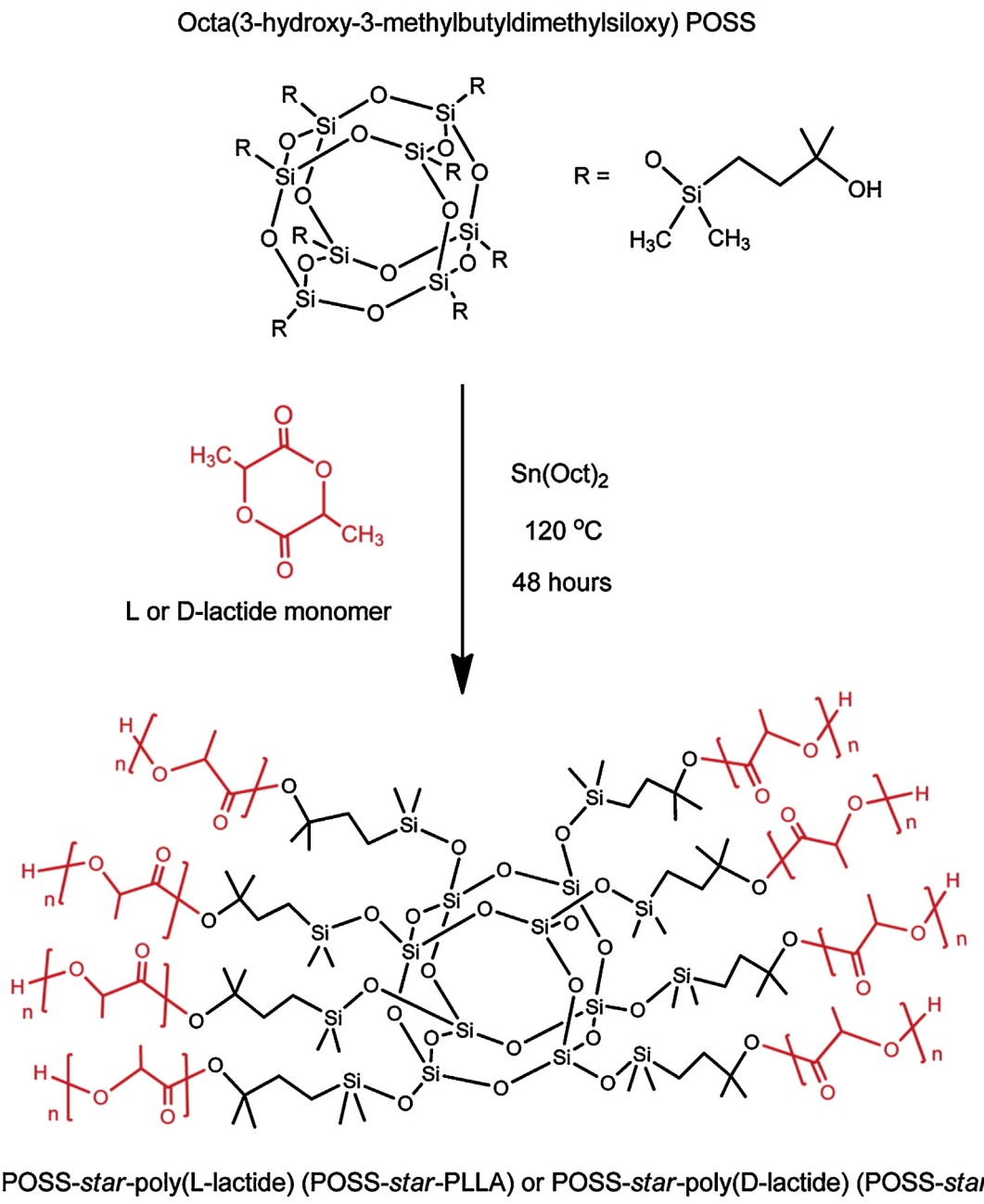

Scheme 16. Synthesis of POSS-star-PLLA and POSS-star-PDLA star polymers by ring opening polymerization [26].

electron microscopy (TEM) results, the conformations of the nanoparticles in the individual star polymer and mixture solutions at different concentrations can be schematically illustrated as shown in Fig. 18. Fig. 18(a) shows that above the CAC, the star polymers in the individual solutions self-assemble via weak solvophobic interactions to form loosely packed multimolecular nanoparticles made up of individual star polymers. In the case of solutions containing the mixture, Fig. 18(b) illustrates the formation of a dense and compact nanoparticle structure due to the strong stereocomplex interaction between the PLLA and PDLA arms that shrinks away from the solvent environment.

The use of a fully biodegradable PLA core-shell rubberlike particles, is illustrated in Scheme 17 [31], in that the novel core-shell rubberlike particle has a three-layer structure: (1) the inner core consists of POSS with eight corners having alkyl alcohol functional groups that could initiate the subsequent ROP of ε-caprolactone (ε-CL) and lactide monomers; (2) the middle layer is a random copolymer of poly(caprolactone-co-lactide) (PCLLA) synthesized via ROP to serve as the rubberlike phase, that is covalently

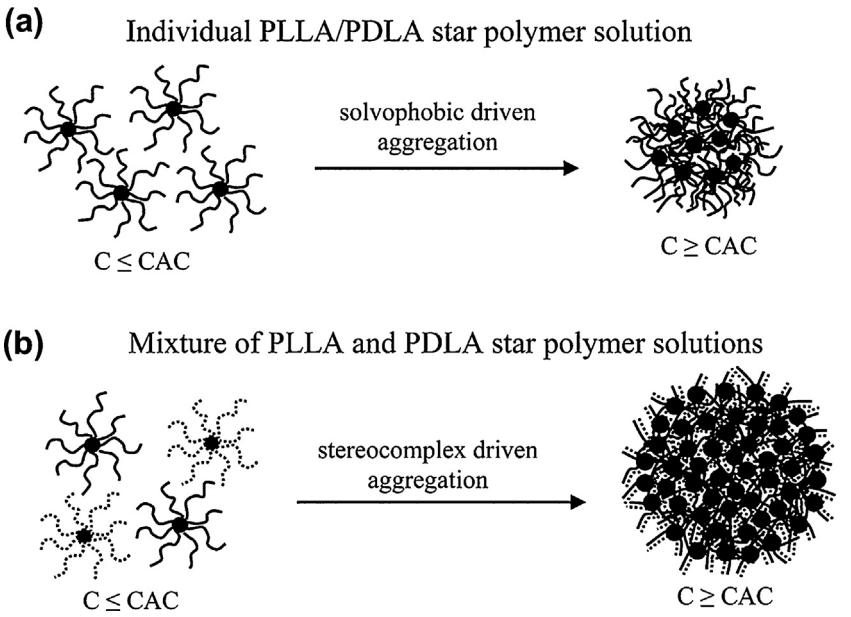

Fig. 18. Schematic representations of the conformations of the nanoparticles formed in (a) the individual star polymer solution and (b) a mixture solution at polymer concentrations below and above the CAC [26].
Copyright 2011. Reproduced with permission from the American Chemical Society.

linked to POSS cage and later to the outer layer; and (3) finally the outer layer consisting of PDLA grafted onto the rubber-like middle shell. For POSS grafted with PCLLA without the outer layer of PDLA, the resulting POSS-rubber particles exhibit a T_g at about −7 °C, revealing the rubbery characteristic of POSS-rubber at room temperature. For PDLA grafted onto the POSS-rubber particles to form POSS-rubber-D, only one T_g was detected at 37 °C, between T_g of POSS-rubber (−7 °C) and pure PDLA (51 °C for M_n 6000). The effect of the outer PDLA on the T_g of PCLLA could be 2-fold: First, the PDLA chains are directly linked with the rubber-like chains, that reduces mobility of the rubber phase and moves the rubber T_g to a higher temperature. Second, in addition to homocrystallites, stereocomplex is also observed in POSS-rubber-D, indicating that the PDLA chains interact with the L-lactyl blocks of PCLLA copolymer to form stereocomplex. The formation of homocrystallites and stereocomplex would further confine the rubber-like phase and could lead to an increase in T_g of the rubber-like phase while reducing the T_g of PDLA. When the synthesized core–shell rubber-like particles were blended with commercial PLLA, FT-IR, DSC and WAXD analysis confirmed the stereocomplex formation between PLLA matrix and POSS-rubber-D [31].

DLS and SLS measurements indicate that the POSS-rubber-D has a R_g/R_h ratio of 0.28 in chloroform solution, below the "hard sphere" value of 0.75 [31] and could suggest that the PDLA chains of POSS-rubber-D are dangling in ambient chloroform and produced a much softer decay in segment density. On the other hand, PLLA has a R_g/R_h ratio of 1.14, presenting a random coil structure. When PLLA and POSS-rubber-D are mixed together, in a weight ratio of 90:10, R_g/R_h becomes 0.83, closer to the "hard sphere" value that indicates the formation of more

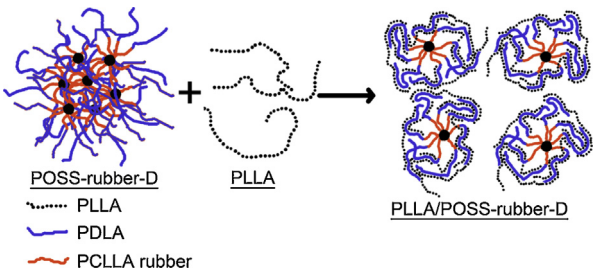

Fig. 19. Schematic representation of the particle conformations in chloroform solutions [31].
Copyright 2013. Reproduced with permission from the American Chemical Society.

compact particles induced by the cross-linking stereocomplexation between PLLA and the dangling PDLA chains of POSS-rubber-D. The R_h of the aggregates of the stereocomplex formed between POSS-rubber-D aggregates and PLLA polymer decreases significantly to ~400 nm compared to the R_h of POSS-rubber-D aggregates only (~930 nm). The POSS-rubber-D particles in solution could have strong interparticle interactions due to stereocomplexation to form an interdigitated structure (Fig. 19) having a large R_h. Stronger stereocomplexation could occur for PLLA polymer blended with the POSS-rubber-D particles, due to longer PLLA chains, that could form a more stable stereocomplex with the PDLA of POSS-rubber-D, as evidenced by the much larger stereocomplex heat of fusion in DSC measurements for the stereocomplex than that of POSS-rubber-D alone. Consequently, the R_h of the aggregates of POSS-rubber-D particles was reduced when blended with commercial PLLA, as illustrated in Fig. 19 [31]. This is important for

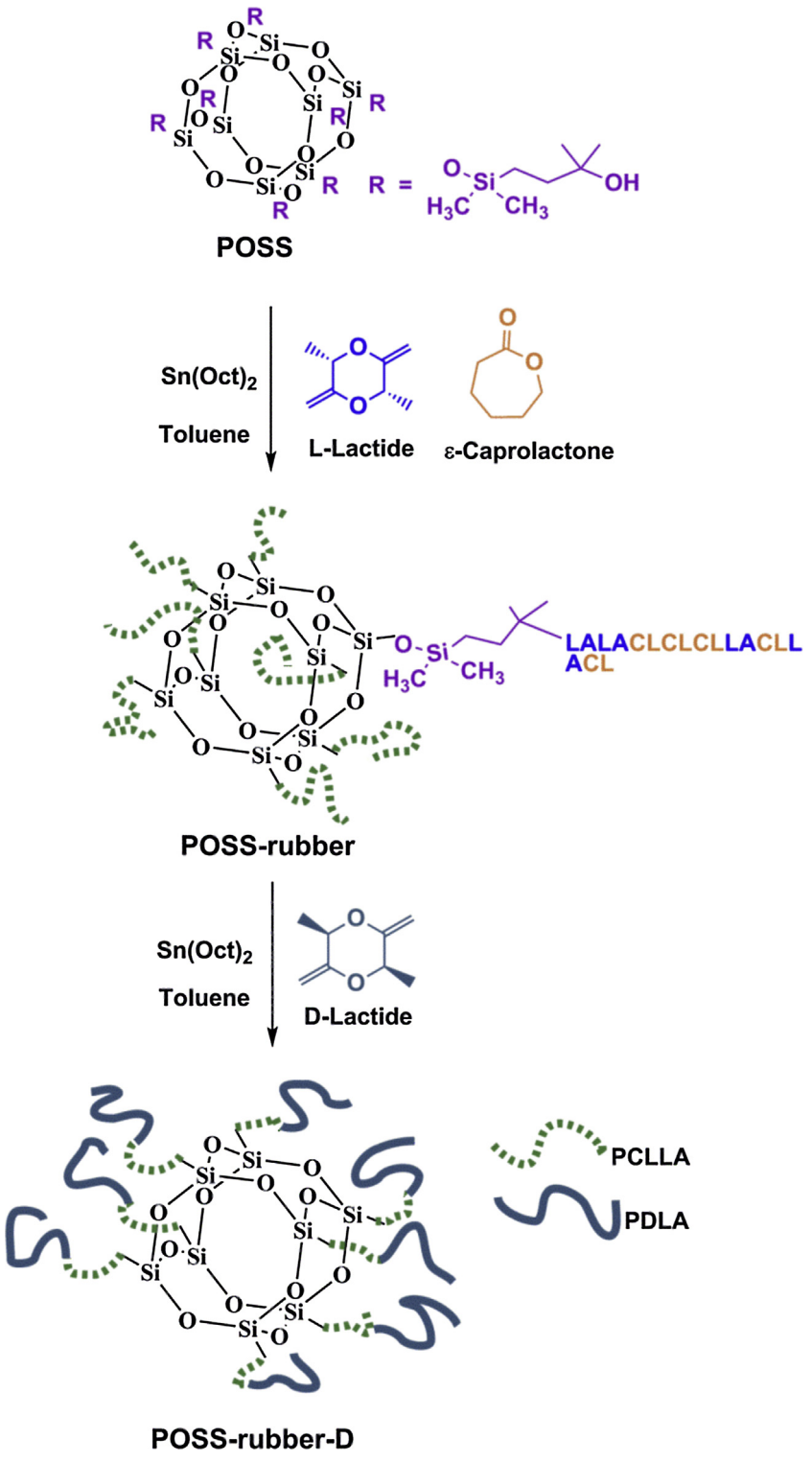

Scheme 17. Synthesis of POSS-Rubber-D core–shell particles by ring-opening polymerization [31].

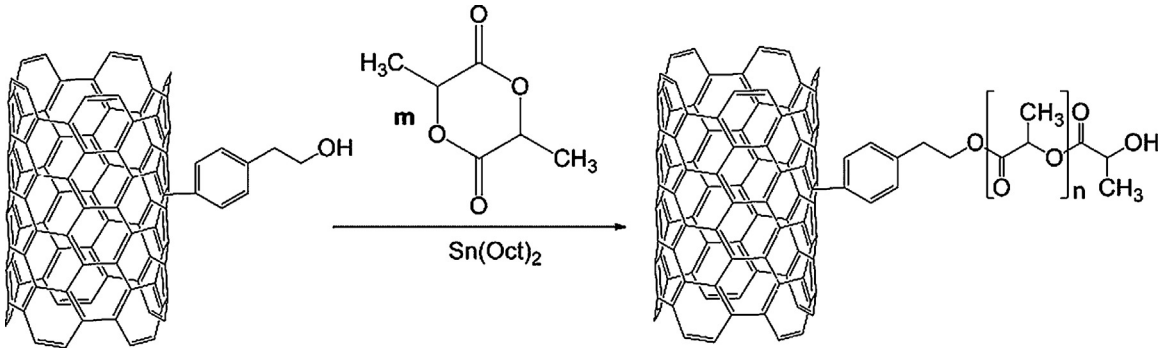

Scheme 18. ROP of LA in the Presence of MWCNT−OH [150].
Copyright 2012. Reproduced with permission from the American Chemical Society.

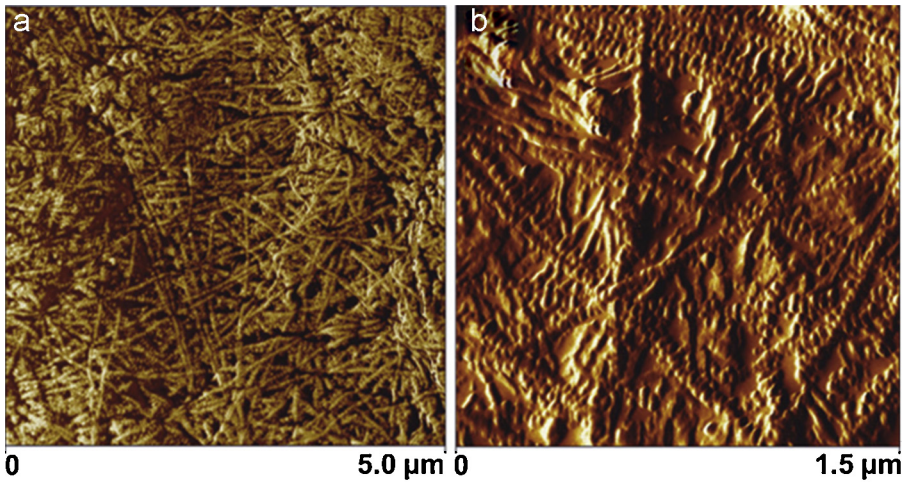

Fig. 20. AFM phase image of the shish-kebab morphology of stereocomplex thin films: (a) AFM phase mode and (b) zoomed image of the AFM amplitude mode [150].
Copyright 2012. Reproduced with permission from the American Chemical Society.

preparation of nanocomposites based on POSS-rubber-D particles.

Similar biodegradable PLA rubber-like particles have been developed, but with the poly(caprolactone-*co*-lactide) (PCLLA) rubbery layer was grafted on lignin (instead of POSS) via ROP, followed by the polymerization of PDLA outer segments to produce lignin-rubber-PDLA (lig-rubber-D) [153]. Lignin is an abundant renewable lingo-cellulosic biomass extracted from agricultural waste [154] and has been added to PLA to achieve biodegradable and renewable composites [155]. For blends of lig-rubber-D with commercial PLLA in chloroform, FTIR, DSC and WAXS measuremnts demonstrated that stereocomplexation occured between lig-rubber-D and PLLA matrix, facilitating good dispersion of lig-rubber-D in the matrix, resulting in strong matrix/filler interfacial interaction [153].

Carbon nanotubes (CNT) are another inorganic component that have attracted the attention of researchers for imparting new functionalities to stereocomplex PLA hybrid copolymers, due to the unusual properties of CNTs such as high aspect ratio, high mechanical strength and high thermal and electrical conductivity [156,157]. In addition, CNTs are also known to be good nucleation agents, and have been used as additives to reinforce the mechanical strength of various composite materials [158,159]. Biela and coworkers developed a simple method for the preparation of linear, high-molar-mass, thermally stable PLA stereocomplexes with multiwalled carbon nanotubes (MWCNTs) covalently attached to enantiomeric PLA chains. The MWCNTs modified with organic spacers terminated with —OH groups were used as initiators for the ring-opening polymerization (ROP) of enantiomeric L- and D-lactides via a "grafting from" approach to obtain MWCNT-*g*-PDLA and MWCNT-*g*-PLLA as depicted in Scheme 18. Stereocomplexes were prepared either by precipitation from solution or as a film via solvent evaporation. Stereocomplexes formation was fully reversible. This is a crucial result, especially for the preparation of stereocomplex films because it was not previously possible via casting from solution. To evaluate the influence of PLA-grafted MWCNTs on the thermal properties of stereocomplex PLA, different mixtures of PLLA/PDLA were prepared with MWCNT-*g*-PLA, MWCNT-OH and unmodified MWCNT. With only a single enantiomer of PLA in stereocomplexation mixture attached to MWCNTs (0.5%MWCNT-*g*-PLA), peaks

characteristic for PLA stereocomplex crystallites were observed in the first and second DSC heating run. Heterocrystallites (stereocomplexes), homocrystallites were also observed in the second DSC heating run. Addition of MWCNTs and MWCNT-OH to a mixture of L-PLA and D-PLA did not significantly improve the thermal properties of formed stereocomplexes. The presence of PLA covalently attached to MWCNTs strongly affected the thermal stability of the PLA-carbon nanotubes stereocomplex nanocomposites, even at very low concentrations of MWCNT-*g*-PLA. AFM showed shish-kebab morphology of stereocomplex thin film (Fig. 20) with very thin (<50 nm) and long (~2–3 μm) rigid structures. This picture confirmed the efficient functionalization of MWCNTs, as it could be observed that the PLA chains completely covered the surface of carbon nanotubes [148,149].

In an approach different than that of Biela and coworkers [148,149]. Stereocomplex PLA-functionalized CNT nanocomposites were also prepared using a commercial PLLA blended with MWCNT-*g*-PDLA, obtained by ROP using the MWCNT-OH/$Sn(Oct)_2$ initiating system [32]. Unfortunately the solution cast stereocomplex films were a mixture of PLA homocrystallites and PLA stereocomplex crystallites even in the first DSC heating run [32]. The amount of PLA stereocomplex crystallites increased with the higher content of MWCNT-*g*-PDLA in contrast to the melt cooled samples, for which the amount of PLA homocrystallites was very small and depended on the heating rate and the amount of PDLA functionalized MWCNTs. The presence of homocrystallites is probably due to the difference in molecular weight of commercially available PLLA (M_n = 130 K) and MWCNT-*g*-PDLA (M_n = 6 K). Nevertheless, a significant enhancement in modulus and hardness of the stereocomplex nanocomposite MWCNT-*g*-PDLA/PLLA in comparison to PDLA/PLLA control sample was observed, discussed further in Section 4 [32]. In addition to POSS and CNT, graphene oxide (GO) has also been grafted onto PLA via a "grafting from" method that involved ring-opening polymerization using modified GO as the initiator to produce GO-*g*-PDLA [30]. FT-IR, DSC and XRD studies showed that a stereocomplex crystal could be formed between PLLA and GO-*g*-PDLA. The incorporation of GO nanofillers leads to a lower crystallization activation energy of stereocomplex and a higher crystallinity in solution casting samples, mainly due to the heterogeneous nucleating effect of the well-dispersed covalently bonded GO sheets, while in cold crystallized samples, the crystallinity was low owing to exfoliated GO sheets that may reduce chain mobility and hinder crystal growth, as illustrated in Fig. 21 [30].

To close this section, it may be noted that throughout the years, there have been many different approaches used to prepare enantiomeric PLA-based copolymers and modulate their stereocomplex properties. Block copolymerization is fascinating in manipulating the architectures of enantiomeric PLA copolymers such as di-, tri-, multi-, star-shape, comb-shape and many other new structures. The stereocomplex formation in these newly designed enantiomeric PLA-based block copolymers has proven to be an efficient strategy to modulate a range of accessible stereocomplex properties including crystallinity, hydrophilicity, mechanical properties and degradation rate. Through

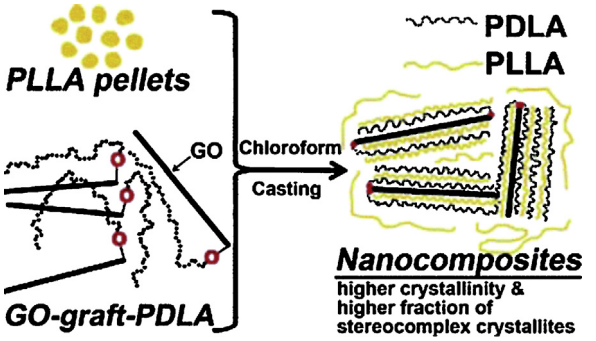

Fig. 21. Schematic representation of the nanocomposites formation when commercial PLLA is blended with graphene oxide-g-PDLA in chloroform solutions [30].
Copyright 2012. Reproduced with permission from the American Chemical Society.

tailoring different chemical structures and adjusting the ratio of constituting blocks, stereocomplex PLA-based block copolymers from soft colloidal systems to the toughened high performance materials have been successfully developed and expanded the applications of PLA to more advanced areas, ranging from biomedical systems to engineered plastic resins. In contrast, graft copolymerization stands out for its ease incorporation of PLA with natural polymers that have unique and intrinsic properties to advance the field of PLA stereocomplexation. Most natural polymers have reactive functional groups on the surface that can be further used for PLA grafting modification with great flexibility in chain length control and grafting density. In addition, the successful grafting of PLA onto the natural polymers often precedes stereocomplexation of PLA itself regardless of the stereocomplexation methods. Considering the good biodegradability and biocompatibility of both natural polymers and PLA, the resulting stereocomplex PLA/natural polymers grafts have great potential for use as implantable biomaterials. A summary of the synthetic methods of different types of enantiomeric PLA-based copolymers is given in Table 1, highlighting and comparing the materials characteristic features of various stereocomplex PLA copolymers as showcased in respective block and graft types. Typically, Table 1 shows that the molecular architecture and chain length of the compositional units have significant impact in the modulation of the strength of stereocomplexation in enantiomeric PLA-based copolymers. For example, the presence of stereocomplex interaction between PLLA and PDLA segments in amphiphilic PLA systems could provide a driving force for the self-assembly of the copolymers into respective micelles or hydrogels in aqueous solution. In contrast to the stereocomplex films, the PLA stereocomplex induced assemblies in solution showed enhanced colloidal stability, as revealed by the lower CMC for micelles, lower CGC and stronger modulus strength for hydrogel systems. As for drug delivery, the more hydrophobic stereocomplex PLA in the micelle core facilitated higher drug encapsulation efficiency due to the stronger interaction with drug molecules. Moreover, PLA stereocomplexation could be used to trigger the morphology transition of the self-assemblies such

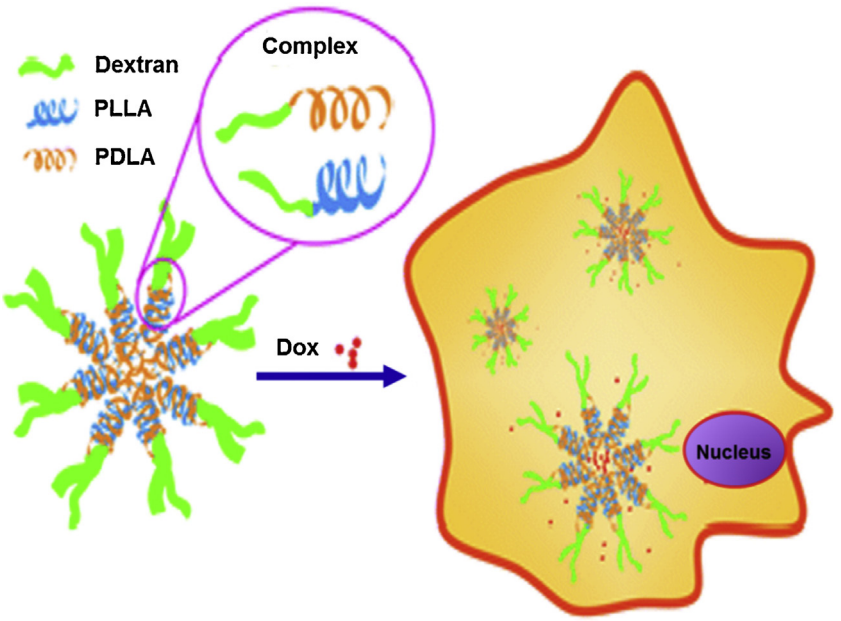

Fig. 22. Schematic illustration of DOX loading and release from DOX-Loaded stereocomplex PLA-dextran block copolymer micelles [10]. Copyright 2013. Reproduced with permission from the American Chemical Society.

as from sol to gel or induce the micelle morphology change from cylindrical to spherical shape. All these unique characteristics of stereocomplex PLA copolymers have aided in the design of functional materials and further directed many potential applications. In the following sections, the stereocomplex-orientated applications of PLA stereocomplex copolymers will be reviewed in three active domains, including biomedical applications, colloidal system stabilization and materials toughening for high performance applications.

4. Applications

4.1. Stereocomplexation of PLA copolymer system in biomedical applications

Particles fabricated in different size and hydrogel materials mediated by PLA stereocompexation in PLA-based copolymers have been explored as biomaterials, ranging from drug delivery carriers to tissue engineering devices, and they continue to evolve. With the incorporation of a PLA stereocomplex, the materials properties with respect to solubility, degradation behavior and bioavailability can be tailored for specific applications; several such are summarized in this section.

4.1.1. Control release in chemotherapy

PLA homo/hetero-stereocomplex incorporated with different model drugs has been previously fabricated to achieve sustained release of the encapsulated cargoes [160,161]. As for stereocomplex in PLA-based copolymers, it is more versatile to formulate the delivery carriers with various sizes and morphologies. For example, Park et al. demonstrated that enantiomeric PLA-PEG-PLA triblock copolymer mixtures could be fabricated into microspheres by a double-emulsion solvent evaporation method for sustained BSA release [47]. Compared with the microspheres made from PLLA-PEG-PLLA, the stereocomplex microspheres had a smoother surface with a more porous and hollow internal structure, due to the preferred racemic crystallization that occurred upon blending. This unique morphology demonstrated a better BSA release characteristics [47]. In another approach, porous spherical particles in the size range of 5–7 μm were formed from the PLA-PSA-PLA stereocomplex by solvent evaporation method [9]. Triamcinalone was incorporated into stereocomplex particle as representative hydrophobic drug. The drug release behavior of the resultant microspheres showed that triamcinalone could be constantly released for one week accompanied by the degradation of the polymer. Chen et al. also described that stereocomplex micelles self-assembled from enantiomeric PLA-PEG diblock copolymers in aqueous solution could be used as drug delivery carriers [4]. These micelles possessed partial crystallized hydrophobic cores with mean hydrodynamic diameters ranging from 40 to 120 nm. When rifampin was encapsulated into the stereocomplex micelles, it showed higher loading capacity and encapsulation efficiency as well as faster rate of drug release compared to the single PLLA-PEG block copolymer micelles, probably due to the higher surface area and small sizes of the stereocomplex micelles [4]. The same research group also demonstrated that these stable micelles self-assembled from stereocomplexation of PLA-dextran block copolymers could be used as efficient drug deliveries (Fig. 22) [10]. The stronger stereocomplex interaction of the micelle cores decreased the drug loading capacity, where DOX was used as the model drug. However, the in vitro release studies exhibited a slower DOX release rate

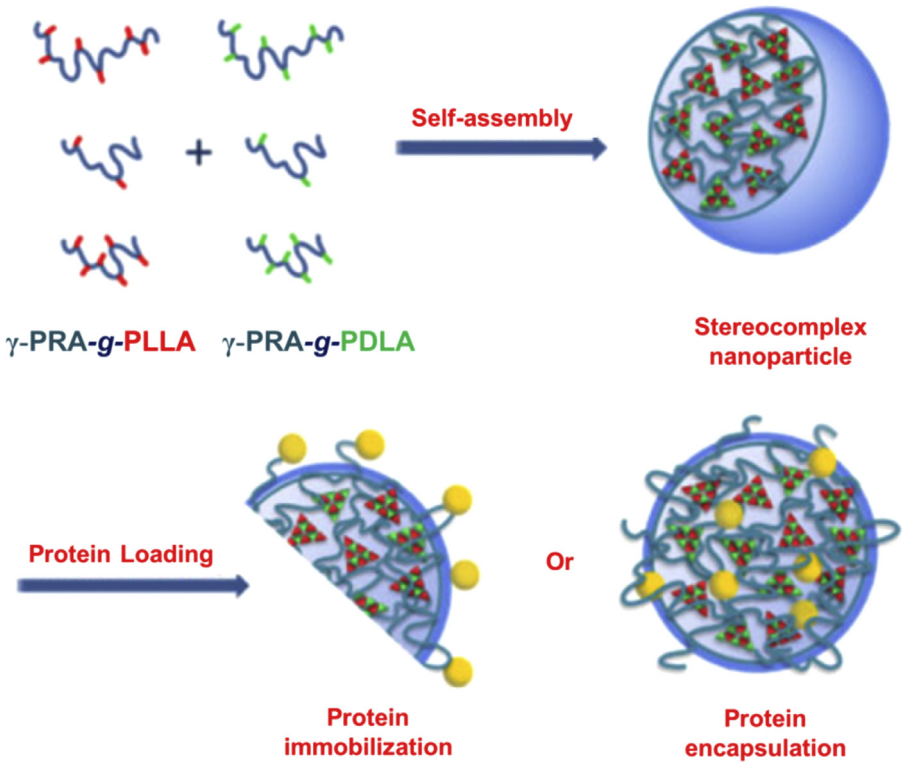

Fig. 23. Schematic illustration of surface-functionalized or protein encapsulated stereocomplex γ-PGA-g-PLA nanoparticles as potential targeting delivery carriers [11].
Copyright 2014. Reproduced with permission from Wiley-VCH.

compared to DOX-loaded unpaired polymer micelles because of the physical cross-linking via stereocomplex interaction, that was in turn an indication of the enhanced stability of the stereocomplex micelles. Moreover, weaker intracellular proliferation inhibition efficacy and lower fluorescence intensity were also achieved for DOX-loaded stereocomplex micelles, suggesting a favorable platform to construct stable and excellent drug delivery systems for cancer therapy [10]. On the other hand, Hedrick's group demonstrated that micelles with narrow size distribution and unique structure could be obtained from stereocomplex miktoarm PEG-PLA-PLA block copolymers, and provided high loading capacity of anticancer paclitaxel drug [8]. No significant initial burst release was observed. Furthermore, these micelles demonstrated sustained and near zero-ordered release of drug, and the stronger interaction between the stereocomplexes and paclitaxel molecules would cause a slower drug release from stereocomplex PEG-PLA-PLA micelles compared to the single PEG-PDLA-PDLA micelles [8].

As for targeted delivery, bio-actives often need to be immobilized on the particles surfaces. For example, the large amount of carboxyl groups on γ-PGA-g-PLA copolymer self-assembled nanoparticles could be potentially applicable for the immobilization of bioactive agents, such as proteins, peptides, targeting ligands and cationic molecules for targeted delivery. Akashi et al. explored the feasibility of protein/peptide immobilization and encapsulation in γ-PGA-g-PLA stereocomplex nanoparticles using ovalbumin (OVA) and RMFPNAPYL (WT1) as model proteins (Fig. 23) [11]. The immobilization of OVA and WT1 peptide on the nanoparticles formed by L- or D-isomers and the equal mixture of the two were successfully achieved by forming amide bonds between the amine group of OVA/WT1 peptide and the carboxyl group on surface of the γ-PGA-g-PLA nanoparticles. As compared to untreated versions, the protein-immobilized nanoparticles did not change their particle size and the amount of protein covalently immobilized onto the nanoparticles increased with increasing initial OVA and WT1 protein concentrations [11]. The loading efficiencies of WT1 peptide in both L- or D-isomer nanoparticles and stereocomplex nanoparticles reached about 50 wt% at 2 mg/mL peptide concentration, that are higher than that of OVA (30 wt%) under the same conditions. The differences may be attributed to the size, molecular weight and number of amino groups on the surface of the proteins. Moreover, at similar hydrophobic content, the inner space of γ-PGA-g-PLA stereocomplex nanoparticles could enhance the protein/peptide immobilization efficiency significantly compared with OVA-surface immobilized nanoparticles formed from γ-PGA-Phe copolymer, showing the advantage of using PLA stereocomplex for particle fabrication [146]. In the case of protein encapsulation, the OVA loading efficiency reached approximately 50 wt% at 0.5 mg/mL of protein concentration, and it increased up to 70 wt% when the OVA concentration was 2 mg/mL. The protein surface-functionalized and loaded nanoparticle system could be

applied as specific targeting nanocarriers for drug and protein delivery and immunotherapy [11].

In another aspect, PLA stereocomplex mediated hydrogels are also receiving growing interests for control release in chemotherapy due to their excellent biocompatibility. Because of the continuous formation and destruction of the crosslinks, the PLA stereocomplex hydrogel constitute a dynamic and evolvable system, for physical entrapment of bioactive molecules such as drugs, proteins and growth factors within the hydrogel networks by simple mixing. For example, Li et al. elucidated the drug release behavior of BSA loaded stereocomplex PEG-PLA hydrogels at different conditions [7]. The release profiles were almost constant over time, with little burst release effect. The BSA release rate was dependent on the gelation conditions such as time and temperature, as well as molar mass and concentration of the mixed PLA-PEG copolymers [7].

In a similar approach, Feijen et al. demonstrated that different sizes of proteins could be easily loaded into stereocomplexed hydrogels by mixing protein containing aqueous solutions of star-shaped PEG-$(PLLA)_8$ and PEG-$(PDLA)_8$ block copolymers (Fig. 24(A)) [12]. The in vitro and in vivo protein release from stereocomplexed PEG-$(PLA)_8$ hydrogels under various gel compositions was further evaluated. The results showed that the release of relatively small protein lysozyme (d_h = 4.1 nm) was proportional to the square root of time up to a cumulative release of approximately 80%, irrespective of the copolymer concentration or PLA block length, indicating the first order kinetics release profile (Fig. 24(B)) and (C)). A cumulative release of approximately 90% was obtained in 10 days. More importantly, Bacteria lysis experiments showed that lysozyme activity was retained after release, revealing that the stereocomplex hydrogels preparation was a protein-friendly process [12]. On the contrary, the larger protein IgG (d_h = 10.7 nm) could be released with nearly zero order kinetics for 16 days. The in vivo test showed that stereocomplex PEG-$(PLA)_8$ hydrogels loaded with therapeutic protein rhIL-2 could be easily injected in mice model. Compared with the free rhIL-2, the therapeutic effect of the released rhIL-2 was retarded for approximately 1–2 weeks, probably due to the slow and constant release from the injected hydrogel depot [12]. In another example, Part et al. illustrated the preparation of thermo-sensitive hydrogel system from the stereocomplexed PLA-F127-PLA multiblock copolymers [66,67]. Human growth hormone (hGH) was encapsulated into different hydrogel formulations by varying the blend ratios between F127 and stereocomplexed PLA-F127-PLA copolymers. 3D hydrogel network could be obtained with the stereocomplexed PLA as the crosslinking nodes and F127 as the connecting chains. Hydrophilic hGH molecules were entrapped within the tightly packed hydrogel structure during temperature induced sol–gel transition process. With the degradation of lactide chains, a sustained hGH release was obtained along with the gradual dissolution of the hydrogel into the surrounding medium. Compared to F127 gel, the blended hydrogels showed more sustained release of hGH up to 10 days [66]. Considering the characteristics such as injectable, thermo-responsive and biocompatible, this type of stereocomplex hydrogel would be particularly useful in the delivery of hydrophilic macromolecular drugs such as proteins and genes.

In addition to the PLA stereocomplex microspheres, micelles, nanoparticles and hydrogels, the stereocomplex interaction between PLLA and PDLA is also known as a convenient approach to preparing thin films or coating materials for drug reservoirs through layer-by-layer (LbL) assembly [160,162–164]. One of the superior features of this approach is the easy processing in obtaining PLA stereocomplex materials with nanometer-order uniformity. As a typical example, Akagi and co-workers demonstrated LbL stepwise deposition of PLLA and PDLA together with proteins onto a substrate using inkjet printing method, and the obtained PLA stereocomplex films showed sustained and controlled release of the encapsulated proteins up to 30 days [160]. The same research group has expanded this technology to the stereocomplex formation of enantiomeric PLA/PEG based amphiphilic block copolymers [162]. In their study, PEG-PLLA and PEG-PDLA diblock copolymers were first employed in aqueous media to optimize the stereocomplex film preparation condition. The stereocomplex was adequately formed in acetonitrile/water (1:1, v/v) at 40 °C. In addition, the presence of water could facilitate the stereocomplex film preparation, that previously suffered from clogging when organic solvents were used in the same process. PLLA-PEG-PLLA and PDLA-PEG-PDLA triblock copolymers were then used for square patterning fabrication and thin films were also produced. It showed that the obtained amphiphilic PLA stereocomplex films were able to retain hydrophobic paclitaxel inside and further used as drug-eluting materials (Fig. 25) [162].

The fabrication has been reported of a highly tunable hybrid drug delivery system via a facile LbL stereocomplex self-assembly of enantiomeric PLLA and PDLA in solution using silica-coated magnetite (Fe_3O_4@SiO_2) as template to produce PLA stereocomplex coated nanoparticles (NPs), (Fe_3O_4@SiO_2@SC) [164]. In addition, various stimuli-responsive polymers such as PDLA–PDMAEMA (pH-responsive) and PDLA–PNIPAAm (temperature-responsive) copolymers were incorporated at the outermost coating layer via PLA stereocomplex interaction, while maintaining the superparamagnetic property of Fe_3O_4 (Fig. 26). The well-designed NPs exhibited a core–shell structure with a mean size of 220–270 nm and possessed high magnetization of 70.8–72.1 emu/g [Fe_3O_4]. In order to investigate the effect of different stimuli on the responsiveness of the NPs for drug delivery, the in vitro drug release was evaluated under various conditions using DOX as model drug. The results showed that pH and temperature controlled drug release profiles were obtained by using Fe_3O_4@SiO_2@SC-D and Fe_3O_4@SiO_2@SC-N NPs, respectively, indicating the successful functionalization of the NPs using PLA stereocomplex coating. Moreover, the DOX-loaded NPs showed higher delivery efficiency towards MCF-7 breast cancer cells. Together with the good biocompatibility and strong magnetic sensitivity, the developed hybrid NPs demonstrated a great potential of control over the drug release at a targeted site [164].

As for the PLA grafted copolymers, Hennink et al. developed stable hydrogels from stereocomplexation of

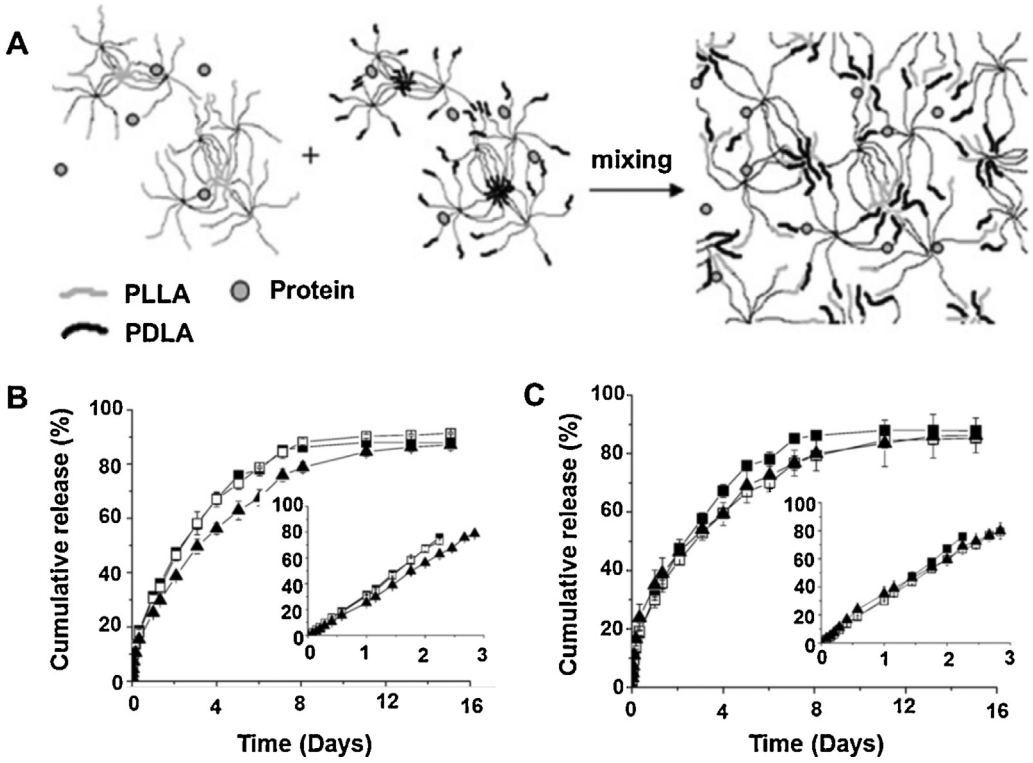

Fig. 24. (A) Preparation of protein loaded stereocomplexed hydrogels by mixing protein containing aqueous solutions of star-shaped PEG-$(PLLA)_8$ and PEG-$(PDLA)_8$ block copolymers. Cumulative release profiles of lysozyme from (B) stereocomplexed PEG-$(PLA_{12})_8$ hydrogels at initial polymer concentrations of 10 (■), 12.5 (□) and 15% w/v (▲); (C) 10% w/v stereocomplexed hydrgeol with different PLA block length: PEG-$(PLA_{12})_8$ (■), PEG-$(PLA_{14})_8$ (□) and PEG-$(PLA_{15})_8$ (▲). The inserts show the cumulative release (%) as a function of the square root of time (days$^{1}/^{2}$) [12].

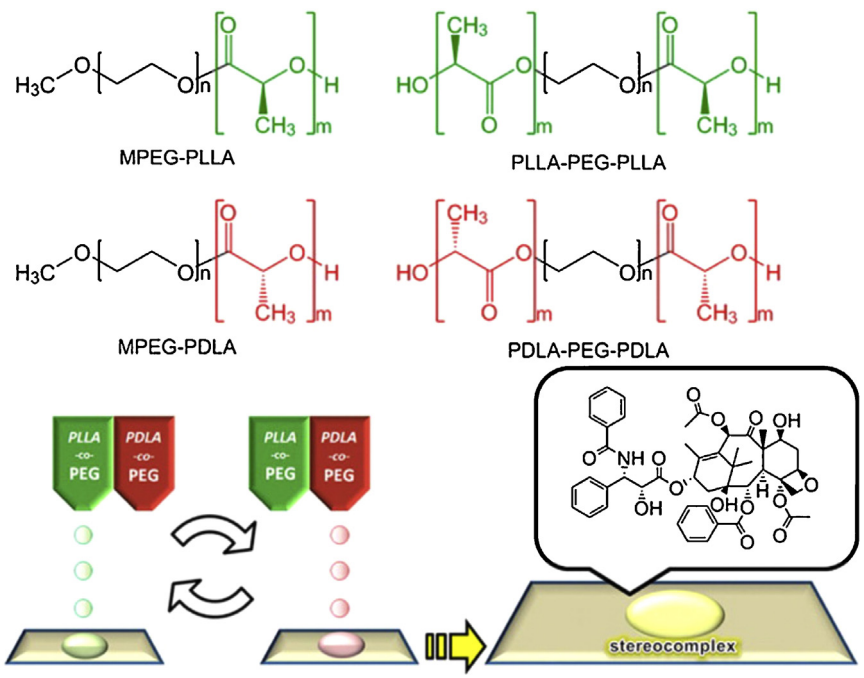

Fig. 25. Schematic illustration of the alternative layer-by-layer approach to prepare PEG-PLLA/PEG-PDLA and PLLA-PEG-PLLA/PDLA-PEG-PDLA stereocomplex films for drug delivery [163].

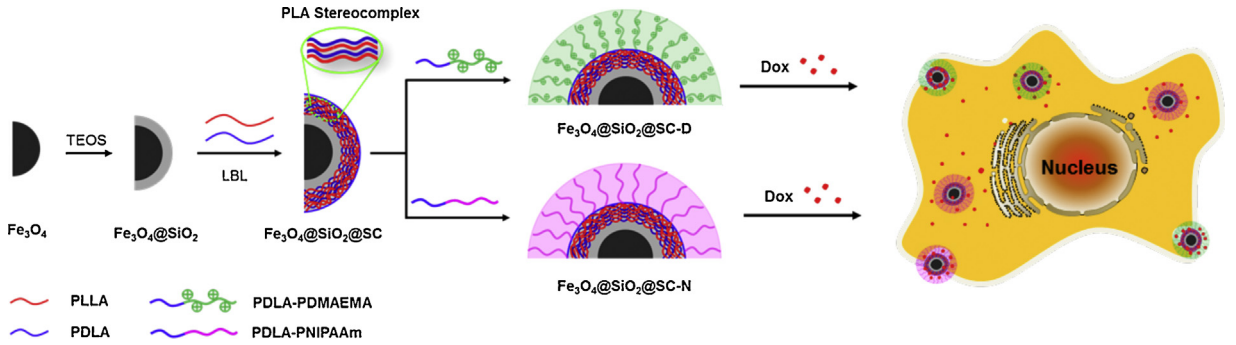

Fig. 26. Schematic illustration showing the design of highly tunable hybrid PLA stereocomplex coated nanoparticles and drug delivery to cells [165]. Copyright 2016. Reproduced with permission from the American Chemical Society.

PLA-*g*-dextran copolymers and demonstrated the loading and release of different model proteins such as IgG and lysozyme [5,136,165]. The hydrogels showed a release of the entrapped model proteins over 6 days and the release kinetics depended on the gel characteristics, such as the polydispersity of the lactate grafts and the initial water content [5]. The smaller lysozyme protein was mainly released by Fickian diffusion, whereas the larger IgC protein was released by diffusion as well as swelling/degradation of the hydrogels. Similar to the stereocomplex PEG-$(PLA)_8$ hydrogel system, the enzymatic activity of lysozyme was fully preserved [12]. This is in contrast to literature reports, where loss of activity of released proteins is frequently reported [166,167]. Protein inactivation occurs during various preparation steps, among that exposure to an organic solvent during loading, adsorption onto various interfaces, and shear forces during the manufacturing process. These factors are absent in our formulation method: hydrogels are prepared in an all-aqueous solution, without addition of any organic reagent, that might explain the retained enzymatic activity. Compared with the hydrogels prepared from PLLA-*g*-dextran copolymers, the stereocomplex hydrogel also showed enhanced stability and longer circulation time of the bioactives loaded in the delivery vehicles [130,133,135,168]. The enhanced stability coupled with the good biocompatibility renders stereocomplex PLA-*g*-dextran hydrogels a suitable candidate for the fabrication of controlled release devices for active proteins [169].

4.1.2. *Tissue engineering in emerging fields*

The biodegradability and biocompatibility of stereocomplex PLA nanofibers were previously evaluated in vitro with proteinase K, as well as in vivo by subcutaneous implantation in rats [170,171]. It showed that stereocomplex PLA nanofibers exhibited a much slower degradation rate than the nanofibers made from individual PLLA. Moreover, the stereocomplex PLA could make it completely resistant to the action of proteinase K after annealing treatment [170]. The in vivo test showed that the slow degradation of stereocomplex PLA could retain the shape after prolonged implantation. This was correlated to a smaller degree of inflammatory reaction as compared with PLLA, indicating the good biocompatibility of PLA stereocomplex materials as implantation device [171]. As for stereocomplex in PLA-based copolymers, they have shown great importance in expanding PLA applications to some emerging aspects in tissue engineering. For example, when one of the PLA was replaced by PLA-PDMAEMA diblock copolymers, a new type of fibrous material was obtained from the stereocomplex between PLLA-PDMAEMA/PDLA and PDLA-PDMAEMA/PLLA that has smooth surface enriched in tertiary amino groups of PDMAEMA units [17]. The mean diameters of the resultant fibers were in the range of 1400–1700 nm. Due to the specific biological properties of PDMAEMA, these fibers could be useful for certain applications. One example demonstrated the hemostatic activity of the fibers by the electrostatic interactions between the positively charged tertiary amino groups and the negatively charged moieties on the surface of the blood cells. For example, when the fibrous mats were placed in contact with blood, the stereocomplex PLLA-PDMAEMA/PDLA and PDLA-PDMAEMA/PLLA mats were intensively red while the PLLA fibrous mat did not change its color because of the lack of functional groups capable of interacting with the blood (Fig. 27) [17]. SEM analysis showed that single erythrocytes with non-altered shape was observed on the surface of the PLLA fibrous mat (Fig. 27(A)), indicating that the mat did not exhibit hemostatic activity. On the other hand, in the case of fibrous PLLA-PDMAEMA/PDLA (Fig. 27(B)) and PDLA-PDMAEMA/PLLA (Fig. 27(C)) mats, a significant number of adhered red blood cells were detected with aggregated, agglutinated, and highly deformed morphology. The observed significant difference of the red blood cells adhered onto the different mats surfaces was also supported well by the blood cell counting results [17]. In another aspect, the mats containing PDMAEMA also reduced the number of adhered cells on the surface when placed in contact with E. coli, showing the antibacterial activity. All these results demonstrated that enriching the surface of the stereocomplex fibers with tertiary amino groups of PDMAEMA units could impart multi-functionalities to the obtained fibrous materials, that has potential for further use in wound healing and device fabrication with contact of pathogenic microorganisms [17].

Attempts have been made to develop stereocomplexed PLA macroporous scaffold for tissue engineering. It is envisaged that possible insufficiencies of the scaffold materials in mechanics and undesired degradation could be hindered

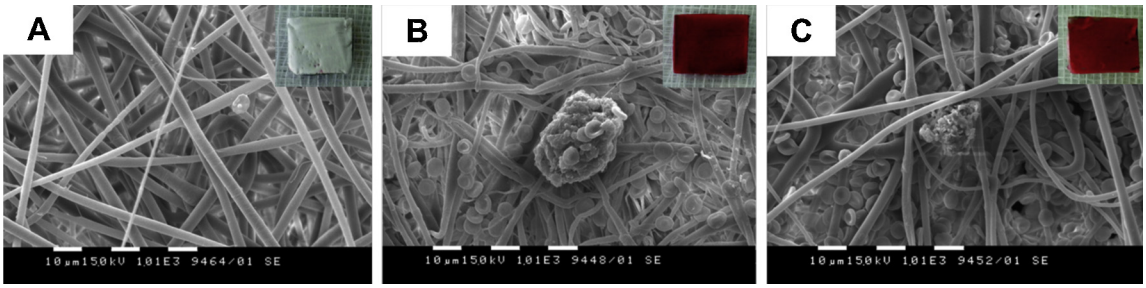

Fig. 27. SEM micrographs of fibrous mats (A) PLLA, (B) stereocomplexed PLLA-PDMAEMA/PDLA and (C) stereocomplexed PDLA-PDMAEMA/PLLA after contact with whole human blood for 1 h. Insert photographs showing the same fibrous mats after stay in human whole blood for 1 h [17].
Copyright 2010. Reproduced with permission from the American Chemical Society.

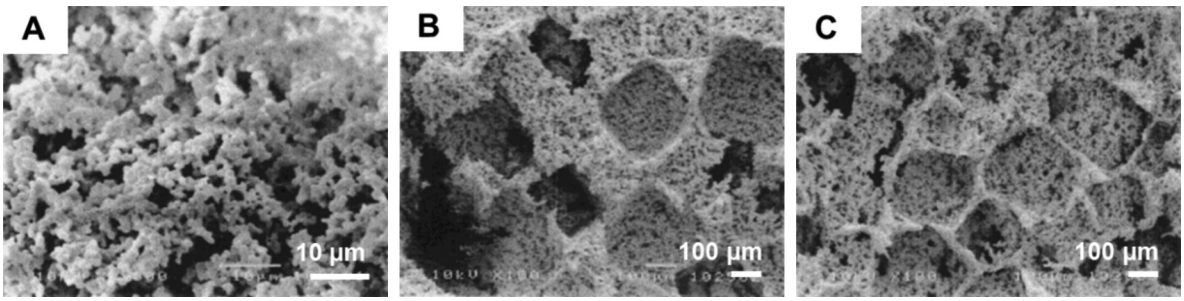

Fig. 28. SEM micrographs of stereocomplex scaffolds obtained from enantiomeric PLA graft-type phospholipid polymers by solvent evaporation: (A) without porogen, (B) with 1:2 weight ratio of polymer/NaCl, (C) with 1:4 weight ratio of polymer/NaCl [16].
Copyright 2002. Reproduced with permission from the American Chemical Society.

by PLA stereocomplexation [13]. For example, Ishihara and co-workers prepared porous stereocomplex PLA scaffold from graft-type copolymers composed of MPC, BMA, and PLA stereocomplex using an extraction procedure with NaCl as water-soluble particles [16,143,144]. The pore size was found to be approximately 200–250 μm, that is necessary for cell intrusion into the scaffold and the adequate surface area in the porous scaffold could allow large number of cells to attach. In addition, smaller pores were also observed by this method due to the aggregation of 2 μm particles (Fig. 28) [16]. The in vitro cell adhesion and morphology of the copolymer coated surface and porous scaffolds were further investigated using Fibroblast cell culture. These studies revealed that the number of adhering cells on the polymer coatings increased with the incorporation of PLLA and PDLA stereocomplexation as compared to the reference copolymer composed only of the MPC that showed low cell adhesion. As for the cell morphology, a round shape was observed as an effect of the MPC units [143]. These results suggested that PLA stereocomplex was effective for cell adhesion, and the cell morphology could be regulated by MPC content. For the cell culture in the scaffold, cell adhesion and intrusion were observed. An increased number of adhered cells was also observed on the porous scaffold when the content of PLA stereocomplex in the scaffold was increased [16,143,144]. The stereocomplex PLA/phospholipid copolymer scaffold could be of great importance as cell-compatible materials for various applications in tissue engineering.

Hedrick and his co-workers described the use of PLA stereocomplexation in PLLA-PEG-PLLA, PDLA-CPC-PDLA (CPC: cationic polycarbonate) and PDLA-PEG-PDLA mixtures to produce thermally sensitive hydrogels [172]. To obtain the cationic CPC triblock copolymer, the pendent propyl chloride chains were quaternized with excess trimethylamine, that further rendered the resultant supramolecular hydrogel antimicrobial functions. These materials were shown to exhibit shear-thinning properties. A typical hydrogel formulation was prepared at a total polymer concentration of 13.2% w/v with PLLA/PDLA molar ratio of 1:1. The antimicrobial activities of the hydrogels were evaluated against various types of pathogenic microbes, including *S. aureus* (Gram-positive), *E. coli* (Gram-negative) and *C. albicans* (fungus). The results indicated that the stereocomplex gels made from PLLA-PEG-PLLA/CPC/PDLA-PEG-PDLA (1:0.15:0.85) completely suppressed bacterial growth and killed the bacteria at 100% efficiency. For C. albicans, an increased amount of CPC was needed in the gel to effectively inhibit the bacteria growth and completely eliminate the fungus. However, CPC alone in the same concentration range and control gel without CPC copolymer showed no antimicrobial activity. The antimicrobial mechanism was proposed to be cell wall/membrane lysis, that was further supported by morphological change observation of incubated bacterial with the gels (Fig. 29). For the untreated microbial cells and cells treated with the control gel, they remained smooth and in their respective healthy shapes. On the other hand, when the cells were cultured with antimicrobial gel, obvious cellular deformation and surface roughness were clearly observed together with lysed cells and debris in treated microbe samples. Specifically, the gel–cell

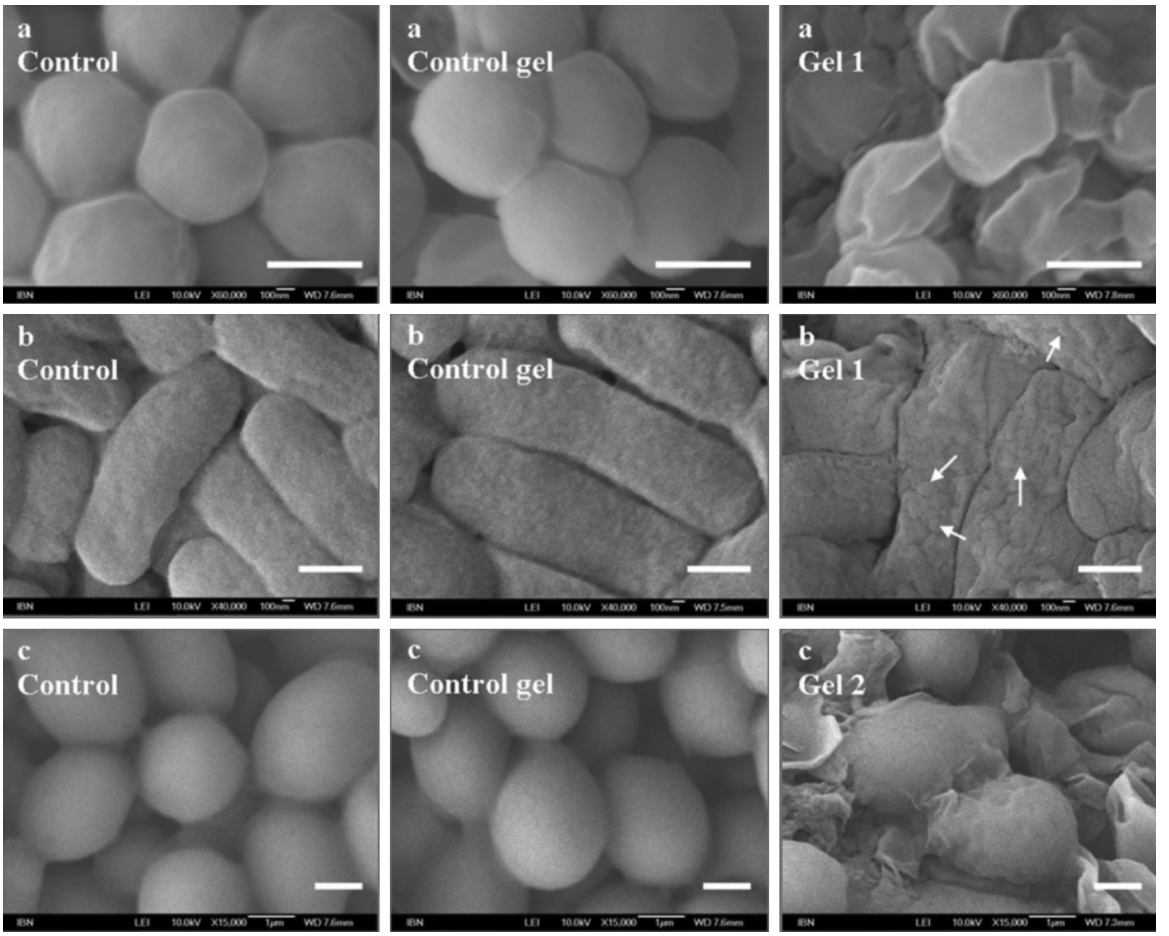

Fig. 29. SEM images showing the morphological changes of (a) *S. aureus*, (b) *E. coli* and (C) *C. albicans* before and after incubation with different gels for 2 h. Scale bar for a, b: 500 nm; c: 1 μm; Control gel: PLLA in PLLAPEG-PLLA and PDLA in PDLA-PEG-PDLA at 1:1 molar ratio; Gel 1: PLLA in PLLA-PEG-PLLA, PDLA in PDLA-CPC-PDLA, and PDLA in PDLA-PEGPDLA at 1:0.15:0.85 [172].

membrane integration caused numerous vesicle-like structures in *E. coli*, while the released cytoplasts from *C. albicans* indicated a catastrophic membrane failure mechanism (Fig. 29). Together with low hemolysis towards mammalian cells and excellent skin biocompatibility, the antimicrobial hydrogels showed high potential in injectable, topical, and coating applications [172].

4.2. Stereocomplexation of PLA copolymers for stabilization of colloidal systems

Another unique application of PLA stereocomplexation is in the stabilization of colloidal systems that has opened up opportunities to fabricate various stable nanoparticles with optimized properties [8,15,19–27,82]. For example, stereocomplexation of poly(L-lactide)-poly(ethylene glycol) (PLLA-PEG) and PDLA-PEG diblock copolymers resulted in enhanced stability of the resultant micellar constructs [19]. Furthermore, the stereocomplex micelles prepared from Y-shaped PEG-PLLA-PLLA and PEG-PDLA-PDLA miktoarm copolymers showed high loadings of paclitaxel and enhanced stability [8]. Another approach, in which the stability has been predicted by theoretical simulations [173,174], uses a mixed micelle approach where block copolymers with complementary blocks that have selective interactions between either the core or shell-forming blocks enabled the access to a range of morphologies. This concept has also been applied to PLA containing materials, for example, Hedrick and co-workers obtained stable patchy polymeric micelles through the stereocomplexation of poly(L-lactide)-poly(N-isopropylacrylamide) (PLLA-PNIPAAM) and PDLA-PEG diblock copolymers [82], whereas Bouteiller and researchers observed stable cylindrical micelles by mixing poly(L-lactide)-poly(ε-caprolactone) and poly(D-lactide)-poly(ecaprolactone) in tetrahydrofuran (THF) [23,24]. Our group also reported that the size and stability of hybrid micelles and nanoparticles are highly dependent on the synergistic effect between stereocomplex PLA and the block length of inorganic P(MA-POSS) that was also supported by the density functional theory (DFT) simulation [25]. O'Reilly and coworkers recently discovered that two homochiral cylinders

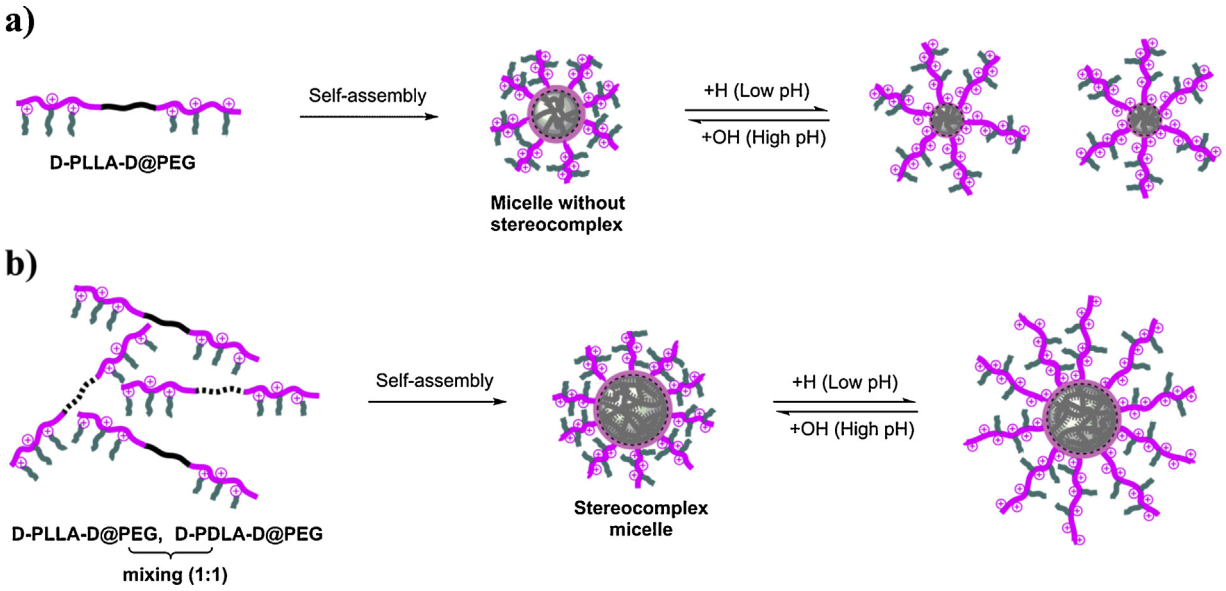

Fig. 30. Illustration of (a) the proposed self-assembly mechanism of pH responsive D-PLLA-D@PEG copolymer in aqueous solution. The increased electrostatic repulsion at lower pH between charged PDMAEMA overcomes the hydrophobic interaction between PLLA, resulting in formation of micelles with lower aggregation number; (b) the proposed self-assembly mechanism of D-PLLA-D@PEG and D-PDLA-D@PEG mixture at molar ratio of 1:1 in aqueous solution. Formation of stereocomplex between PLLA and PDLA in the micelle core enhances the micelle stability even at low pH, thus no significant change in the aggregation number is observed [20].

that were formed from individual PLLA-PAA and PDLA-PAA diblock copolymers, could undergo a morphological transition into spherical micelles with stereocomplex cores when the two enantiomeric block copolymers were mixed together in solution [15]. Such a morphological transition was not observed when enantiopure PLLA-PAA cylinders were exposed to the same self-assembly conditions without the presence of the opposite enantiopure PDLA-PAA cylinders [15,18]. Only by being present as unimers in solution could the components of different stereochemistry interact sufficiently to form stereocomplex micelles that display a higher stability owing to the improved packing and strong interactions of the helical chains of opposite configurations [3,107]. Due to the formation of highly stable micelles, such stereocomplexation triggered reorganization may have potential applications in delivery/controlled release. As reported in Section 2.1.2.1, polyelectrolyte micelles exhibited enhanced stability in aqueous solution, induced by PLA stereocomplexation of enantiomeric PDMAEMA-PLA-PDMAEMA triblock copolymers (D-PLA-D) conjugated with PEG (D-PLLA-D@PEG and D-PDLA-D@PEG) [20]. The micelles formed by 1:1 D/L mixtures showed larger swelling ratios and hydrodynamic radius that did not change significantly with pH and dilution, as compared to micelles formed from individual D or L forms of the copolymers, as illustrated in Fig. 30. The simple and versatile dissolution in the micelle preparation and enhanced kinetic stability of such stereocomplex micelles bearing polyelectrolyte groups could make D-PLA-D@PEG copolymer more attractive in application of biomedicine [20].

4.3. Stereocomplexation of PLA copolymer systems for PLA toughening

PLA's biorenewability as well as its high modulus and strength has made it a promising alternative to petroleum-derived polymers to produce fibers, films, vehicle interiors, food wares and food/beverage packages [3]. However, PLA has drawbacks, such as poor impact strength (~5 kJ/m^2), small elongation at break (<10%), and low heat deflection temperature (HDT; <60 °C), that greatly hinder its large scale commercial applications [3,175]. Rubber toughening is a frequently used strategy to overcome the normal brittle response of PLA to deformation. One important strategy that has proven useful is to enhance the toughening effect of rubber particles is to improve the interfacial adhesion between the matrix and rubber [176,177] via formation of stereocomplex between PLLA and PDLA [31,153,177]. In previous work [177], the synthesized poly(n-butyl acrylate)-*graft*-PLA (PBA-*g*-PLA) copolymer was used to toughen brittle PLLA and a great increase in elongation at break (elongation at break increased from 4.2% to around 25%) was obtained by blending PLLA with PBA-*g*-PDLA while the blending of PLLA with PBA-*g*-PLLA resulted in only a slight increase in elongation at break (increased from 4.2 to 7%). In addition to the synthetic non-biodegradable PBA-*g*-PLA fully biodegradable PLA rubber-like particles, POSS-rubber-D [31] and lig-rubber-D have been developed for toughening the PLLA matrix while maintaining other mechanical properties such as Young's modulus and tensile strength [31,153]. The resulting fully biodegradable nanocomposites, i.e., 10%-POSS rubber-D/PLLA [31]

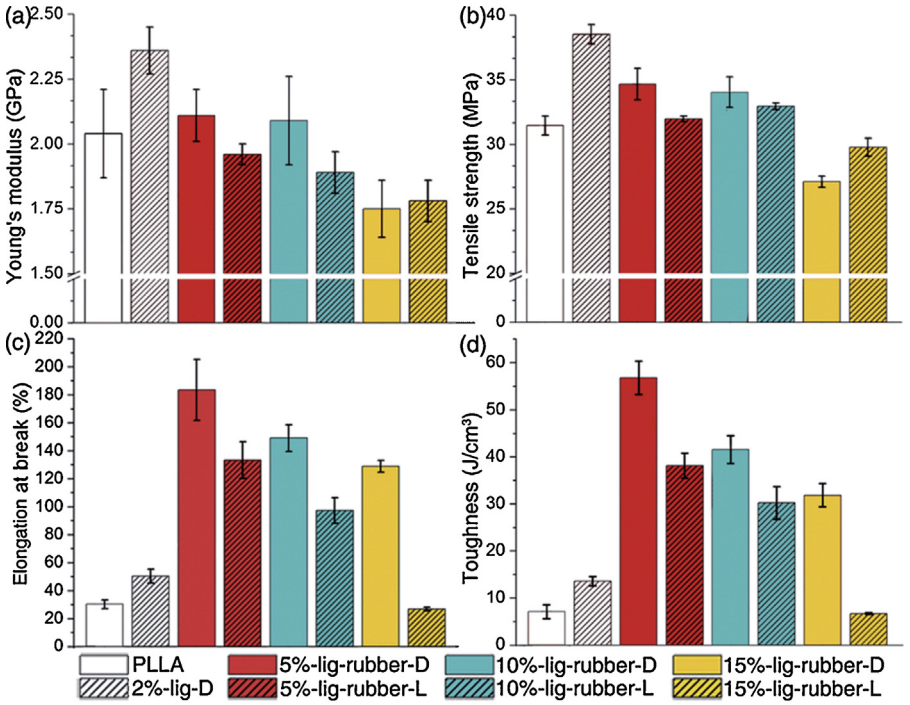

Fig. 31. Mechanical properties of the renewable and biodegradable PLA nanocomposites. (a) Young's modulus. (b) Tensile strength. (c) Elongation at break. (d) Toughness, calculated by integrating the stress–strain curves of the nanocomposites [154].

and 5%-lig-rubber-D/PLLA [153] exhibited a ten-fold and six-fold increase in elongation at break, respectively, compared with neat PLLA, that is considerable noting that the rubber phase content in both the nanocomposites are only ~3–4 wt% [31,153]. For example, the tensile strength, Young's modulus and elongation at break for neat commercial PLLA are 32 MPa, 2.0P GPa and 30%, respectively, as depicted in Fig. 31 [153]. When 5% lig-rubber-D was introduced into neat PLLA, the resulting nanocomposites (PLLA/5%-lig-rubber-D) exhibited an elongation at break of 180%, equivalent to a six-fold enhancement in toughness (calculated by integrating the stress–strain curves) compared with neat PLLA. To demonstrate the effect of stereocomplexation, the authors measured the mechanical properties of nanocomposites without the presence of stereocomplex (PLLA/5%-lig-rubber-L) and reported that the resulting elongation at break is reduced to 130%. The stereocomplex interaction between PDLA in lig-rubber-D and commercial PLLA facilitates better dispersion of lig-rubber-D particles in the nanocomposite system compared with the PLLA/lig-rubber-[153].

Similarly, the blending of 10% POSS-rubber-D with commercial PLLA resulted in fully biodegradable nanocomposites having a ten-fold increase in elongation at break compared with neat PLLA [31]. By analyzing the crystallinities of nanocomposites before and after tensile tests, one can see that deformation and orientation lead to rearrangement of polymer chains and breakdown of homocrystallites while stereocomplex crystallites are hardly changed during the tensile deformation [31,153]. This suggests that under tensile forces the stereocomplex structure is more stable than homocrystallites phase crystallites, possibly due to extra hydrogen bonds in the formation of sc-crystallites [41], that ensures strong rubber/matrix interactions and thus contributes to the mechanical enhancement of the nanocomposites. Detailed morphology analysis of the fractured samples after tensile tests via TEM revealed that the PLLA's deformed part consists of grain-like areas with a boundary composed of microcracks [31] (inset of Fig. 32(a)), thus, energy absorption being low and the material being brittle. By contrast in the PLLA/POSS-rubber-D nanocomposites, rubber particles may act as craze initiators and crazing to provide the main toughening mechanism [178]. The number of craze nucleation sites increases with POSS-rubber-D content and crazes are visible in the deformed part of the rubber reinforced nanocomposites, as pointed out by the small arrows in Figs. 32(b)–(e). At reasonable POSS-rubber-D contents (e.g., 5 and 10 wt%), each craze nucleus was able to fully develop into a mature craze, that is the source of energy absorption and thus improves the toughness of the nanocomposites. Consequently, 10%-POSS-rubber-D shows a much rougher fracture surface than neat PLLA (Figs. 32(f) and (g)). On the other hand, crazes are also the source of polymer breakdown [178]. When the number of craze nucleation sites is too large with excess POSS-rubber-D (e.g., 15 and 20 wt%), the interparticle (or intercraze) distance may not be large enough for the craze to fully develop; as a result, the multicrazes will merge and form cracks and, hence, the toughening effect is reduced. In contrast, when commercial PLLA was blended with POSS-PDLA without rubber phases as the craze initiators, the

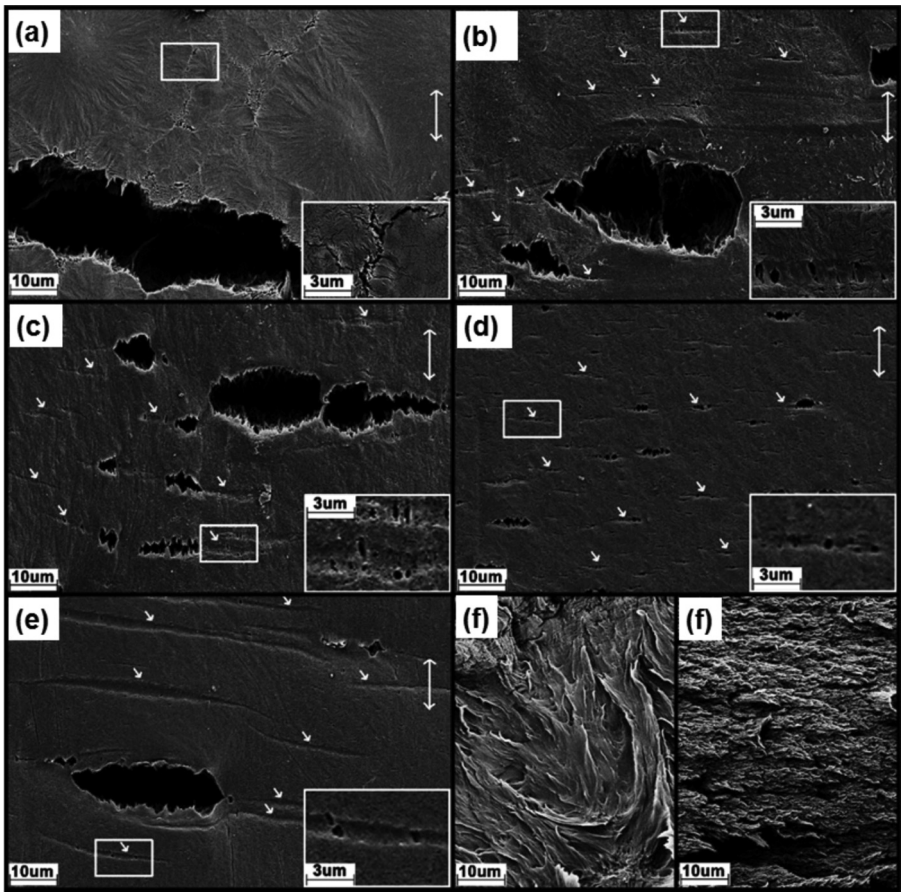

Fig. 32. SEM images of fractured samples after tensile tests: (a–e) surfaces of the deformed part, where the double-head arrows show the tensile direction and (f, g) facture surfaces. (a) PLLA; (b) 5%-POSS-rubber-D; (c) 10%-POSS-rubber-D; (d) 15%-POSS-rubber-D; (e) 20%-POSS-rubber-D; (f) PLLA; (g) 10%-POSS-rubber-D. The insets of (a–e) are enlargements of the corresponding areas in the rectangles [31].

resulting control sample became even more brittle than neat PLLA, with an elongation at break of only ~5% [31]. The strong enhancement in mechanical property could be attributed to the existence of strong stereocomplex interaction between the matrix and rubber particles, good particle dispersion, rubber initiated crazing, stereocomplex cross-linking, and low rubber content in the system [31,153]. The merits of neat PLLA in terms of mechanical properties like Young's modulus, tensile strength, and tensile stress at break are not impaired by the addition of POSS rubber-D [31] and lig-rubber-D [153] that endow the PLA nanocomposites with a good potential in real applications, for example, food packaging and medical device fabrication.

In addition to rubber toughening to enhance the toughness of stereocomplex PLA, significant enhancement has been observed in the modulus and hardness of the PLA stereocomplex nanocomposite via covalent grafting of CNTs in comparison to the control samples without CNTs [32]. For example, the modulus and hardness values for the PLA stereocomplex nanocomposites (having 20 wt% PDLA loadings) without covalently grafted CNTs are approximately 1.5 and 0.1 GPa, respectively, that increased to 5.5 and 0.4 GPa, respectively, when only 0.2 wt% of CNT is grafted onto PDLA. This enhancement in mechanical properties reveals the superior strengthening effect of CNTs within the matrix, where the CNT-PDLA covalent bonds and PDLA/PLLA stereocomplex interaction ensure an efficient load transfer as well as a good CNT-dispersion, as depicted in Fig. 33. In addition, CNTs could also act as pinning spots, that more effectively immobilize PDLA molecules and hence counteract the potential plasticizing effect as revealed by the higher T_g value of the stereocomplex nanocomposites compared to that of the control samples [32].

Nanoclays have also been used to toughen PLA stereocomplex nanocomposites [29] and cellulose nanowhiskers (CNWs) [179]. The stereocomplex directly obtained by melt blending PDLA-graft-clay with commercial PLA has both enhanced melting temperature (more than 40 °C) and storage modulus (higher than 60%) than those of commercial PLA. This could be ascribed to the grafting of PDLA to clay that enhances the dispersion of nanoclays within the PLA matrix via stereocomplexation, resulting in an efficient stress transfer at the interface and efficient dispersion of the nanoclays [29]. Purnama and Kim

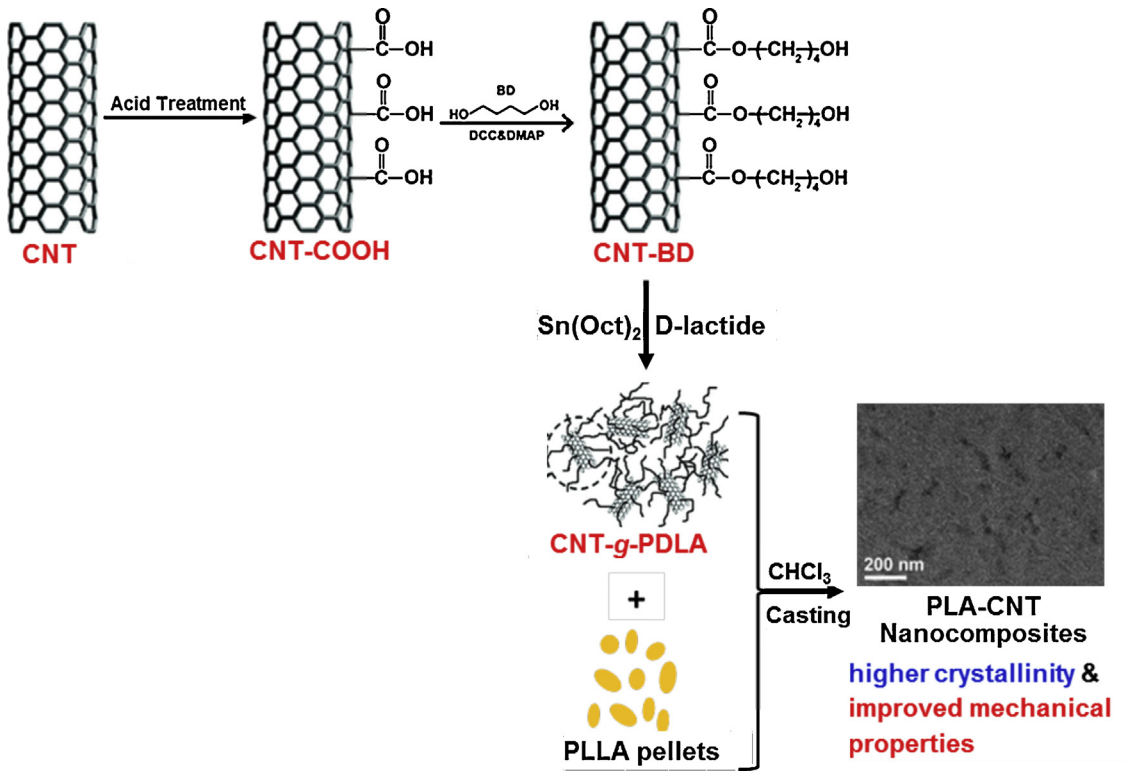

Fig. 33. Schematic representation of fabrication of toughened PLA-CNT nanocomposites showing well dispersed CNTs within the PLA matrix [32]. Copyright 2013. Reproduced with permission from the Royal Society of Chemistry.

fabricated bio-stereocomplex-nanocomposite materials by stereocomplexation of PLA grafted acetylated-cellulose nanowhiskers (PLA-CNWs) that led to improved mechanical strength and thermal stability. For example, the Young's modulus and tensile strength were about 2.70 GPa and 62.96 MPa, respectively, that is about 25% higher than that of neat homopolymers. In addition, the presence of CNW particle in stereocomplex matrix could act as a superior insulator that is an important heat transport barrier during thermal degradation process [179].

The above examples demonstrate that PLA stereocomplexation promotes good dispersion and adhesion of the toughing modifiers within the PLA matrix, that is an important factor that influences the toughening mechanism and subsequently the enhancement in mechanical properties of PLA. Further studies should focus on the development of fully bio-based and biodegradable PLA copolymers for toughening of PLA materials with a balance of outstanding mechanical properties for potential in food packaging and medical device fabrication.

5. Conclusions and outlook

PLA is biodegradable polyester derived from renewable resources. The unique properties such as good biocompatibility, degradation under physiological conditions and formation of non-toxic degradation products have made PLA an extremely attractive material particularly in the field of biomedicine. Although the commercial available PLLA exhibits a broad range of physical properties, the poor thermal and mechanical properties are still not fulfilling the criteria needed for ordinary structural materials. PLA stereocomplexation has opened a new way to modulate the wide range of properties that could not be attained with unmodified PLA alone. The recent advanced development in polymerization techniques has diversified a large array of new functional PLA-based copolymers having various architectures and the stereocomplexation between the enantiomeric PLLA and PDLA segments in these newly developed PLA based copolymers has provided access to many new materials features, such as novel chemical functionalities, bioactivities, as well as smart properties tailored for specific applications. In this review, the recent advances in the synthesis of PLA-based copolymers were addressed with respect to block- and graft-architectures, with special focus on the significant impact of PLA stereocomplex formation on improving material properties. The much enhanced performance of PLA copolymer stereocomplex materials has also shown great value in expanding PLA applications to more advanced areas, including the chemotherapy delivery carriers and tissue engineering devices in biomedical fields, colloidal system stabilization (e.g., microparticles, micelles, and hydrogels etc.), and PLA toughening in different composites as high performance materials. The reduced cost of PLLA and PDLA from renewable resources could further enlarge the field of applications of stereocomplex PLA to new areas at an increasing speed. Are there still undiscovered

"treasures" related to PLA stereocomplexation that could be exploited to cope with the increasing demands of the industry? It is well-known that in the racemic PLLA/PDLA blends with high molecular weight (>80 kDa), the stereocomplex crystallization is significantly suppressed and the homo crystallization of individual PLLA and PDLA becomes predominant in conventional melt crystallization. Since only the high molecular weight PLA has the good mechanical properties and processing ability, more effort is needed to selectively promote stereocomplex crystallization by manipulating the PLLA/PDLA blending conditions and adopting simple methods such as incorporation of additives and nucleating agents. Although PLA stereocomplexes has slower hydrolytic degradation rates, it is accompanied by a more acidic degradation pattern due to shorter degradation products as compared to PLA homopolymers, that may slightly hinder the utilization of PLA stereocomplexes in certain applications, particularly in biomedical devices. Nevertheless, the ability to design new architectures of PLA copolymers such as branched, cyclic, star, dendritic and comb-shaped structures may further offer hope in tackling the current challenges in the utilization of PLA stereocomplexation for the development of improved materials useful to the industry.

Acknowledgements

The authors gratefully acknowledge financial support from the Institute of Materials Research and Engineering (IMRE) under the Agency for Science, Technology, and Research (A*STAR) and National University of Singapore.

References

[1] Fukushima K, Kimura Y. Stereocomplexed polylactides (Neo-PLA) as high-performance bio-based polymers: their formation, properties, and application. Polym Int 2006;55:626–42.
[2] Oh JK. Polylactide (PLA)-based amphiphilic block copolymers: synthesis, self-assembly, and biomedical applications. Soft Matter 2011;7:5096–108.
[3] Tsuji H. Poly(lactide) stereocomplexes: formation, structure, properties, degradation, and applications. Macromol Biosci 2005;5:569–97.
[4] Chen L, Xie Z, Hu J, Chen X, Jing X. Enantiomeric PLA-PEG block copolymers and their stereocomplex micelles used as rifampin delivery. J Nanopart Res 2007;9:777–85.
[5] de Jong SJ, van Eerdenbrugh B, van Nostrum CF, Kettenes-van den Bosch JJ, Hennink WE. Physically crosslinked dextran hydrogels by stereocomplex formation of lactic acid oligomers: degradation and protein release behavior. J Control Release 2001;71:261–75.
[6] Hiemstra C, Zhong Z, Li L, Dijkstra PJ, Feijen J. In-situ formation of biodegradable hydrogels by stereocomplexation of PEG–(PLLA)8 and PEG–(PDLA)8 star block copolymers. Biomacromolecules 2006;7:2790–5.
[7] Li S, El Ghzaoui A, Dewinck E. Rheology and drug release properties of bioresorbable hydrogels prepared from polylactide/poly(ethylene glycol) block copolymers. Macromol Symp 2005;222:23–36.
[8] Nederberg F, Appel E, Tan JPK, Kim SH, Fukushima K, Sly J, Miller RD, Waymouth RM, Yang YY, Hedrick JL. Simple approach to stabilized micelles employing miktoarm terpolymers and stereocomplexes with application in paclitaxel delivery. Biomacromolecules 2009;10:1460–8.
[9] Slivniak R, Domb AJ. Stereocomplexes of enantiomeric lactic acid and sebacic acid ester–anhydride triblock copolymers. Biomacromolecules 2002;3:754–60.
[10] Zhao Z, Zhang Z, Chen L, Cao Y, He C, Chen X. Biodegradable stereocomplex micelles based on dextran-block-polylactide as efficient drug deliveries. Langmuir 2013;29:13072–80.
[11] Zhu Y, Akagi T, Akashi M. Self-assembling stereocomplex nanoparticles by enantiomeric poly(γ-glutamic acid)-poly(lactide) graft copolymers as a protein delivery carrier. Macromol Biosci 2014;14:576–87.
[12] Hiemstra C, Zhong Z, Van Tomme SR, van Steenbergen MJ, Jacobs JJL, Otter WD, Hennink WE, Feijen J. In vitro and in vivo protein delivery from in situ forming poly(ethylene glycol)-poly(lactide) hydrogels. J Control Release 2007;119:320–7.
[13] Bertin A. Emergence of polymer stereocomplexes for biomedical applications. Macromol Chem Phys 2012;213:2329–52.
[14] Spasova M, Mespouille L, Coulembier O, Paneva D, Manolova N, Rashkov I, Dubois P. Amphiphilic poly(D- or L-lactide)-b-poly(N,N-dimethylamino-2-ethyl methacrylate) block copolymers: controlled synthesis, characterization, and stereocomplex formation. Biomacromolecules 2009;10:1217–23.
[15] Sun L, Pitto-Barry A, Kirby N, Schiller TL, Sanchez AM, Dyson MA, Sloan J, Wilson NR, O'Reilly RK, Dove AP. Structural reorganization of cylindrical nanoparticles triggered by polylactide stereocomplexation. Nat Commun 2014;5:5746–55.
[16] Watanabe J, Eriguchi T, Ishihara K. Stereocomplex formation by enantiomeric poly(lactic acid) graft-type phospholipid polymers for tissue engineering. Biomacromolecules 2002;3:1109–14.
[17] Spasova M, Manolova N, Paneva D, Mincheva R, Dubois P, Rashkov I, Maximova V, Danchev D. Polylactide stereocomplex-based electrospun materials possessing surface with antibacterial and hemostatic properties. Biomacromolecules 2010;11:151–9.
[18] Sun L, Petzetakis N, Pitto-Barry A, Schiller TL, Kirby N, Keddie DJ, Boyd BJ, O'Reilly RK, Dove AP. Tuning the size of cylindrical micelles from poly(L-lactide)-b-poly(acrylic acid) diblock copolymers based on crystallization-driven self-assembly. Macromolecules 2013;46:9074–82.
[19] Kang N, Perron MÈ, Prud'homme RE, Zhang Y, Gaucher G, Leroux JC. Stereocomplex block copolymer micelles: core–shell nanostructures with enhanced stability. Nano Lett 2005;5:315–9.
[20] Li Z, Yuan D, Fan X, Tan BH, He C. Poly(ethylene glycol) conjugated poly(lactide)-based polyelectrolytes: synthesis and formation of stable self-assemblies induced by stereocomplexation. Langmuir 2015;31:2321–33.
[21] Nagahama K, Mori Y, Ohya Y, Ouchi T. Biodegradable nanogel formation of polylactide-grafted dextran copolymer in dilute aqueous solution and enhancement of its stability by stereocomplexation. Biomacromolecules 2007;8:2135–41.
[22] Portinha D, Belleney J, Bouteiller L, Pensec S, Spassky N, Chassenieux C. Formation of nanoparticles of polylactide-containing diblock copolymers: is stereocomplexation the driving force? Macromolecules 2002;35:1484–6.
[23] Portinha D, Boué F, Bouteiller L, Carrot G, Chassenieux C, Pensec S, Reiter G. Stable dispersions of highly anisotropic nanoparticles formed by cocrystallization of enantiomeric diblock copolymers. Macromolecules 2007;40:4037–42.
[24] Portinha D, Bouteiller L, Pensec S, Richez A, Chassenieux C. Influence of preparation conditions on the self-assembly by stereocomplexation of polylactide containing diblock copolymers. Macromolecules 2004;37:3401–6.
[25] Tan BH, Hussain H, Leong YW, Lin TT, Tjiu WW, He C. Tuning self-assembly of hybrid PLA-P(MA-POSS) block copolymers in solution via stereocomplexation. Polym Chem 2013;4:1250–9.
[26] Tan BH, Hussain H, Lin TT, Chua YC, Leong YW, Tjiu WW, Wong PK, He CB. Stable dispersions of hybrid nanoparticles induced by stereocomplexation between enantiomeric poly(lactide) star polymers. Langmuir 2011;27:10538–47.
[27] Wolf FK, Hofmann AM, Frey H. Poly(isoglycerol methacrylate)-b-poly(D- or L-lactide) copolymers: a novel hydrophilic methacrylate as building block for supramolecular Aggregates. Macromolecules 2010;43:3314–24.
[28] Zhang X, Tan BH, He C. Tailoring the LCST of PNIPAAM-b-PLA-b-PNIPAAM triblock copolymers via stereocomplexation. Macromol Rapid Commun 2013;34:1761–6.
[29] Re GL, Benali S, Habibi Y, Raquez JM, Dubois P. Stereocomplexed PLA nanocomposites: from in situ polymerization to materials properties. Eur Polym J 2014;54:138–50.
[30] Sun Y, He C. Synthesis and stereocomplex crystallization of poly(lactide)-graphene oxide nanocomposites. ACS Macro Lett 2012;1:709–13.
[31] Sun Y, He C. Biodegradable "Core–Shell" rubber nanoparticles and their toughening of poly(lactides). Macromolecules 2013;46:9625–33.
[32] Sun Y, He C. Synthesis stereocomplex crystallization, morphology and mechanical property of poly(lactide)-carbon nanotube nanocomposites. RSC Adv 2013;3:2219–26.

[33] Cartier L, Okihara T, Ikada Y, Tsuji H, Puiggali J, Lotz B. Epitaxial crystallization and crystalline polymorphism of polylactides. Polymer 2000;41:8909–19.
[34] Eling B, Gogolewski S, Pennings AJ. Biodegradable materials of poly(L-lactic acid): 1, Melt-spun and solution-spun fibres. Polymer 1982;23:1587–93.
[35] Puiggali J, Ikada Y, Tsuji H, Cartier L, Okihara T, Lotz B. The frustrated structure of poly(L-lactide). Polymer 2000;41:8921–30.
[36] Sasaki S, Asakura T. Helix distortion and crystal structure of the α-form of poly(L-lactide). Macromolecules 2003;36:8385–90.
[37] Pan P, Inoue Y. Polymorphism and isomorphism in biodegradable polyesters. Prog Polym Sci 2009;34:605–40.
[38] Ikada Y, Jamshidi K, Tsuji H, Hyon SH. Stereocomplex formation between enantiomeric poly(lactides). Macromolecules 1987;20:904–6.
[39] Lin T, Liu XY, He C. Ab initio elasticity of poly(lactic acid) crystals. J Phys Chem B 2010;114:3133–9.
[40] Lin T, Liu XY, He C. Calculation of Infrared/Raman spectra and dielectric properties of various crystalline poly(lactic acid)s by density functional perturbation theory (DFPT) method. J Phys Chem B 2012;116:1524–35.
[41] Lin TT, Liu XY, He C. A DFT study on poly(lactic acid) polymorphs. Polymer 2010;51:2779–85.
[42] Slager J, Brizzolara D, Cantow HJ, Domb AJ. Crystallization and stereocomplexation governed self- assembling of poly(lactide)-b-poly(ethylene glycol) to mesoscale structures. Polym Adv Technol 2005;16:667–74.
[43] Nakajima M, Nakajima H, Fujiwara T, Kimura Y, Sasaki S. Nano-ordered surface morphologies by stereocomplexation of the enantiomeric polylactide chains: specific interactions of surface-immobilized poly(D-lactide) and poly(ethylene glycol)-poly(L-lactide) block copolymers. Langmuir 2014;30:14030–8.
[44] Pitto-Barry A, Kirby N, Dove AP, O'Reilly RK. Expanding the scope of the crystallization-driven self- assembly of polylactide-containing polymers. Polym Chem 2014;5:1427–36.
[45] Saffer EM, Tew GN, Bhatia SR. Poly(lactic acid)-poly(ethylene oxide) block copolymers: new directions in self-assembly and biomedical applications. Curr Med Chem 2011;18:5676–86.
[46] Stevels WM, Ankone MJ, Dijkstra PJ, Feijen J. Stereocomplex formation in ABA triblock copolymers of poly (lactide)(A) and poly (ethylene glycol)(B). Macromol Chem Phys 1995;196:3687–94.
[47] Lim DW, Park TG. Stereocomplex formation between enantiomeric PLA-PEG-PLA triblock copolymers: characterization and use as protein-delivery microparticulate carriers. J Appl Polym Sci 2000;75:1615–23.
[48] Bishara A, Kricheldorf HR, Domb AJ. Stereocomplexes of triblock poly(lactide- PEG2000-lactide) as carrier of drugs. Macromol Symp 2005;225:17–30.
[49] Liu Y, Shao J, Sun J, Bian X, Feng L, Xiang S, Sun B, Chen Z, Li G, Chen X. Improved mechanical and thermal properties of PLLA by solvent blending with PDLA-b-PEG-b-PDLA. Polym Degrad Stab 2014;101:10–7.
[50] Li Z, Yin H, Zhang Z, Liu KL, Li J. Supramolecular anchoring of DNA polyplexes in cyclodextrin-based polypseudorotaxane hydrogels for sustained gene delivery. Biomacromolecules 2012;13:3162–72.
[51] Li Z, Zhang Z, Liu KL, Ni X, Li J. Biodegradable hyperbranched amphiphilic polyurethane multiblock copolymers consisting of poly(propylene glycol), poly(ethylene glycol), and polycaprolactone as in situ thermogels. Biomacromolecules 2012;13:3977–89.
[52] Li Z, Li J. Control of hyperbranched structure of polycaprolactone/poly(ethylene glycol) polyurethane block copolymers by glycerol and their hydrogels for potential cell delivery. J Phys Chem B 2013;117:14763–74.
[53] Buwalda SJ, Boere KW, Dijkstra PJ, Feijen J, Vermonden T, Hennink WE. Hydrogels in a historical perspective: from simple networks to smart materials. J Control Release 2014;190:254–73.
[54] Nouailhas H, El Ghzaoui A, Li S, Coudane J. Stereocomplex-induced gelation properties of polylactide/poly(ethylene glycol) diblock and triblock copolymers. J Appl Polym Sci 2011;122:1599–606.
[55] Fujiwara T, Mukose T, Yamaoka T, Yamane H, Sakurai S, Kimura Y. Novel thermo-responsive formation of a hydrogel by stereocomplexation between PLLA-PEG-PLLA and PDLA-PEG-PDLA block copolymers. Macromol Biosci 2001;1:204–8.
[56] Abebe DG, Fujiwara T. Controlled thermoresponsive hydrogels by stereocomplexed PLA-PEG-PLA prepared via hybrid micelles of premixed copolymers with different PEG lengths. Biomacromolecules 2012;13:1828–36.
[57] Li S. Bioresorbable hydrogels prepared through stereocomplexation between poly(L-lactide) and poly(D-lactide) blocks attached to poly(ethylene glycol). Macromol Biosci 2003;3:657–61.
[58] Li S, Vert M, Synthesis. Characterization, and stereocomplex-induced gelation of block copolymers prepared by ring-opening polymerization of l(d)-lactide in the presence of poly(ethylene glycol). Macromolecules 2003;36:8008–14.
[59] Mukose T, Fujiwara T, Nakano J, Taniguchi I, Miyamoto M, Kimura Y, Teraoka I, Lee CW. Hydrogel formation between enantiomeric B-A-B-type block copolymers of polylactides (PLLA or PDLA: A) and polyoxyethylene (PEG: B); PEG-PLLA-PEG and PEG-PDLA-PEG. Macromol Biosci 2004;4:361–7.
[60] Jeong B, Bae YH, Lee DS, Kim SW. Biodegradable block copolymers as injectable drug-delivery systems. Nature 1997;388:860–2.
[61] Li F, Li S, El Ghzaoui A, Nouailhas H, Zhuo R. Synthesis and gelation properties of PEG−PLA−PEG triblock copolymers obtained by coupling monohydroxylated PEG−PLA with adipoyl chloride. Langmuir 2007;23:2778–83.
[62] Liu R, Li D, He B, Xu X, Sheng M, Lai Y, Wang G, Gu Z. Anti-tumor drug delivery of pH-sensitive poly(ethylene glycol)-poly(L-histidine-)-poly(L-lactide) nanoparticles. J Control Release 2011;152:49–56.
[63] Liu R, He B, Li D, Lai Y, Tang JZ, Gu Z. Stabilization of pH-sensitive mPEG-PH-PLA nanoparticles by stereocomplexation between enantiomeric polylactides. Macromol Rapid Commun 2012;33:1061–6.
[64] Ma C, Pan P, Shan G, Bao Y, Fujita M, Maeda M. Core–shell structure, biodegradation, and drug release behavior of poly(lactic acid)/poly(ethylene glycol) block copolymer micelles tuned by macromolecular stereostructure. Langmuir 2015;31:1527–36.
[65] Hiemstra C, Zhong ZY, Jiang X, Hennink WE, Dijkstra PJ, Feijen J. PEG-PLLA and PEG-PDLA multiblock copolymers: synthesis and in situ hydrogel formation by stereocomplexation. J Control Release 2006;116:e17–9.
[66] Park SY, Chung HJ, Lee Y, Park TG. Injectable and sustained delivery of human growth hormone using chemically modified Pluronic copolymer hydrogels. Biotechnol J 2008;3:669–75.
[67] Chung HJ, Lee Y, Park TG. Thermo-sensitive and biodegradable hydrogels based on stereocomplexed Pluronic multi-block copolymers for controlled protein delivery. J Control Release 2008;127:22–30.
[68] Matyjaszewski K, Tsarevsky NV. Nanostructured functional materials prepared by atom transfer radical polymerization. Nat Chem 2009;1:276–88.
[69] Gao H, Matyjaszewski K. Synthesis of functional polymers with controlled architecture by CRP of monomers in the presence of cross-linkers: from stars to gels. Prog Polym Sci 2009;34:317–50.
[70] Pintauer T, Matyjaszewski K. Atom transfer radical addition and polymerization reactions catalyzed by ppm amounts of copper complexes. Chem Soc Rev 2008;37:1087–97.
[71] Jun YJ, Park KM, Joung YK, Park KD, Lee SJ. In situ gel forming stereocomplex composed of four- arm PEG-PDLA and PEG-PLLA block copolymers. Macromol Res 2008;16:704–10.
[72] Buwalda SJ, Calucci L, Forte C, Dijkstra PJ, Feijen J. Stereocomplexed 8-armed poly(ethylene glycol)-poly(lactide) star block copolymer hydrogels: Gelation mechanism, mechanical properties and degradation behavior. Polymer 2012;53:2809–17.
[73] Hiemstra C, Zhong Z, Dijkstra PJ, Feijen J. Stereocomplex mediated gelation of PEG-(PLA)2 and PEG-(PLA)8 block copolymers. Macromol Symp 2005;224:119–32.
[74] Nagahama K, Fujiura K, Enami S, Ouchi T, Ohya Y. Irreversible temperature-responsive formation of high-strength hydrogel from an enantiomeric mixture of starburst triblock copolymers consisting of 8-arm PEG and PLLA or PDLA. J Polym Sci B: Polym Phys 2008;46:6317–32.
[75] Hiemstra C, Zhou W, Zhong Z, Wouters M, Feijen J. Rapidly in situ forming biodegradable robust hydrogels by combining stereocomplexation and photopolymerization. J Am Chem Soc 2007;129:9918–26.
[76] Fukushima K, Pratt RC, Nederberg F, Tan JPK, Yang YY, Waymouth RM, Hedrick JL. Organocatalytic approach to amphiphilic comb-block copolymers capable of stereocomplexation and self-assembly. Biomacromolecules 2008;9:3051–6.
[77] Cho K, Wang X, Nie S, Shin DM. Therapeutic nanoparticles for drug delivery in cancer. Clin Cancer Res 2008;14:1310–6.
[78] Fan X, Wang M, Yuan D, He C. Amphiphilic conetworks and gels physically cross-linked via stereocomplexation of polylactide. Langmuir 2013;29:14307–13.
[79] Geschwind J, Rathi S, Tonhauser C, Schömer M, Hsu SL, Coughlin EB, Frey H. Stereocomplex formation in polylactide multiarm stars and

comb copolymers with linear and hyperbranched multifunctional PEG. Macromol Chem Phys 2013;214:1434–44.
[80] Coulembier O, Kiesewetter MK, Mason A, Dubois P, Hedrick JL, Waymouth RM. A distinctive organocatalytic approach to complex macromolecular architectures. Angew Chem Int Ed 2007;46:4719–21.
[81] Wolf FF, Friedemann N, Frey H. Poly(lactide)-block-poly(HEMA) block copolymers: an orthogonal one-pot combination of ROP and ATRP, using a bifunctional initiator. Macromolecules 2009;42:5622–8.
[82] Kim SH, Tan JPK, Nederberg F, Fukushima K, Yang YY, Waymouth RM, Hedrick JL. Mixed micelle formation through stereocomplexation between enantiomeric poly(lactide) block copolymers. Macromolecules 2009;42:25–9.
[83] Petzetakis N, Dove AP, O'Reilly RK. Cylindrical micelles from the living crystallization-driven self- assembly of poly(lactide)-containing block copolymers. Chem Sci 2011;2:955–60.
[84] Fan X, Wang Z, Yuan D, Sun Y, Li Z, He C. Novel linear-dendritic-like amphiphilic copolymers: synthesis and self-assembly characteristics. Polym Chem 2014;5:4069–75.
[85] Shao J, Xiang S, Bian X, Sun J, Li G, Chen X. Remarkable melting behavior of PLA stereocomplex in linear PLLA/PDLA blends. Ind Eng Chem Res 2015;54:2246–53.
[86] Shao J, Sun J, Bian X, Cui Y, Li G, Chen X. Investigation of poly(lactide) stereocomplexes: 3-armed poly(L-lactide) blended with linear and 3-armed enantiomers. J Phys Chem B 2012;116:9983–91.
[87] Sveinbjörnsson BR, Miyake GM, El-Batta A, Grubbs RH. Stereocomplex formation of densely grafted brush polymers. ACS Macro Lett 2014;3:26–9.
[88] Shin EJ, Jones AE, Waymouth RM. Stereocomplexation in cyclic and linear polylactide blends. Macromolecules 2011;45:595–8.
[89] Biela T, Duda A, Penczek S. Enhanced melt stability of star-shaped stereocomplexes as compared with linear stereocomplexes. Macromolecules 2006;39:3710–3.
[90] Ma Y, Li W, Li L, Fan Z, Li S. Stereocomplexed three-arm PPO-PDLA-PLLA. copolymers: synthesis via an end-functionalized initiator. Eur Polym J 2014;55:27–34.
[91] Shao J, Tang Z, Sun J, Li G, Chen X. Linear and four-armed poly(L-lactide)-block-poly(D-lactide) copolymers and their stereocomplexation with poly(lactide)s. J Polym Sci B: Polym Phys 2014;52:1560–7.
[92] Hirata M, Kobayashi K, Kimura Y. Synthesis and properties of high-molecular-weight stereo di-block polylactides with nonequivalent D/L ratios. J Polym Sci B: Polym Phys 2010;48:794–801.
[93] Hirata M, Kobayashi K, Kimura Y. Enhanced stereocomplexation by enantiomer adjustment for stereo diblock polylactides with non-equivalent D/L ratios. Macromol Chem Phys 2010;211:1426–32.
[94] Masutani K, Lee CW, Kimura Y. Synthesis and thermomechanical properties of stereo triblock polylactides with nonequivalent block compositions. Macromol Chem Phys 2012;213:695–704.
[95] Fukushima K, Hirata M, Kimura Y. Synthesis and characterization of stereoblock poly(lactic acid)s with nonequivalent D/L sequence ratios. Macromolecules 2007;40:3049–55.
[96] Hirata M, Kimura Y. Thermomechanical properties of stereoblock poly(lactic acid)s with different PLLA/PDLA block compositions. Polymer 2008;49:2656–61.
[97] Hu J, Tang Z, Qiu X, Pang X, Yang Y, Chen X, Jing X. Formation of flower- or cake-shaped stereocomplex particles from the stereo multiblock copoly(rac-lactide)s. Biomacromolecules 2005;6:2843–50.
[98] Hirata M, Masutani K, Kimura Y. Synthesis of ABCBA penta stereoblock polylactide copolymers by two-step ring-opening polymerization of L- and D-lactides with poly(3-methyl-1,5-pentylene succinate) as macroinitiator (C): development of flexible stereocomplexed polylactide materials. Biomacromolecules 2013;14:2154–61.
[99] Isono T, Kondo Y, Otsuka I, Nishiyama Y, Borsali R, Kakuchi T, Satoh T. Synthesis and stereocomplex formation of star-shaped stereoblock polylactides consisting of poly(L-lactide) and poly(D-lactide) arms. Macromolecules 2013;46:8509–18.
[100] Sugai N, Yamamoto T, Tezuka Y. Synthesis of orientationally isomeric cyclic stereoblock polylactides with head-to-head and head-to-tail linkages of the enantiomeric segments. ACS Macro Lett 2012;1:902–6.
[101] Isono T, Kondo Y, Ozawa S, Chen Y, Sakai R, Sato Si, Tajima K, Kakuchi T, Satoh T. Stereoblock-like brush copolymers consisting of poly(L-lactide) and poly(D-lactide) side chains along poly(norbornene) backbone: synthesis, stereocomplex formation, and structure–property relationship. Macromolecules 2014;47:7118–28.
[102] Lee HI, Jakubowski W, Matyjaszewski K, Yu S, Sheiko SS. Cylindrical core–shell brushes prepared by a combination of ROP and ATRP. Macromolecules 2006;39:4983–9.
[103] Lee HI, Matyjaszewski K, Yu-Su S, Sheiko SS. Hetero-grafted block brushes with PCL and PBA side chains. Macromolecules 2008;41:6073–80.
[104] Sakamoto Y, Tsuji H. Stereocomplex crystallization behavior and physical properties of linear 1-Arm, 2-Arm, and branched 4-Arm poly(L-lactide)/poly(D-lactide) blends: effects of chain directional change and branching. Macromol Chem Phys 2013;214:776–86.
[105] Yu-Su SY, Sheiko SS, Lee HI, Jakubowski W, Nese A, Matyjaszewski K, Anokhin D, Ivanov DA. Crystallization of molecular brushes with block copolymer side chains. Macromolecules 2009;42:9008–17.
[106] Furuhashi Y, Kimura Y, Yoshie N. Self-assembly of stereocomplex-type poly(lactic acid). Polym J 2006;38:1061–7.
[107] Brizzolara D, Cantow HJ, Diederichs K, Keller E, Domb AJ. Mechanism of the stereocomplex formation between enantiomeric poly(lactide)s. Macromolecules 1996;29:191–7.
[108] Li Z, Tan BH. Towards the development of polycaprolactone based amphiphilic block copolymers: molecular design, self-assembly and biomedical applications. Mater Sci Eng C 2014;45:620–34.
[109] Stevels WM, Ankoné MJK, Dijkstra PJ, Feijen J. Stereocomplex formation in AB DI-block copolymers of poly(ϵ-caprolactone) (a) and poly(lactide)(B). Macromol Symp 1996;102:107–13.
[110] Pensec S, Leroy M, Akkouche H, Spassky N. Stereocomplex formation in enantiomeric diblock and triblock copolymers of poly(ε-caprolactone) and polylactide. Polym Bull 2000;45:373–80.
[111] Kang M, Jung Y, Kim S. Biodegradable stereocomplex polylactide having flexible ε-caprolactone unit. Macromol Res 2013;21:1036–41.
[112] Purnama P, Jung Y, Kim SH. Stereocomplexation of poly(L-lactide) and random copolymer poly(D-lactide-co-ε-caprolactone) to enhance melt stability. Macromolecules 2012;45:4012–4.
[113] Shirahama H, Ichimaru A, Tsutsumi C, Nakayama Y, Yasuda H. Characteristics of the biodegradability and physical properties of stereocomplexes between poly(L-lactide) and poly(D-lactide) copolymers. J Polym Sci B: Polym Phys 2005;43:438–54.
[114] Li Z, Loh XJ. Water soluble polyhydroxyalkanoates: future materials for therapeutic applications. Chem Soc Rev 2015;44:2865–79.
[115] Tsuji H, Shimizu K, Sakamoto Y, Okumura A. Hetero-stereocomplex formation of stereoblock copolymer of substituted and non-substituted poly(lactide)s. Polymer 2011;52:1318–25.
[116] Aluthge DC, Xu C, Othman N, Noroozi N, Hatzikiriakos SG, Mehrkhodavandi P. PLA-PHB-PLA triblock copolymers: synthesis by sequential addition and investigation of mechanical and rheological properties. Macromolecules 2013;46:3965–74.
[117] Jia L, Yin L, Li Y, Li Q, Yang J, Yu J, Shi Z, Fang Q, Cao A. New enantiomeric polylactide-block-poly(butylene succinate)-block-polylactides: syntheses, characterization and in situ self-assembly. Macromol Biosci 2005;5:526–38.
[118] Slivniak R, Langer R, Domb AJ. Lactic and ricinoleic acid based copolyesters stereocomplexation. Macromolecules 2005;38:5634–9.
[119] Xu H, Teng C, Yu M. Improvements of thermal property and crystallization behavior of PLLA based multiblock copolymer by forming stereocomplex with PDLA oligomer. Polymer 2006;47:3922–8.
[120] Wanamaker CL, Bluemle MJ, Pitet LM, O'Leary LE, Tolman WB, Hillmyer MA. Consequences of polylactide stereochemistry on the properties of polylactide-polymenthide-polylactide thermoplastic elastomers. Biomacromolecules 2009;10:2904–11.
[121] Hou X, Li Q, Cao A. In situ aggregates of enantiomeric poly(styrene)-block-poly(lactide) diblock copolymers via stereocomplexation in a non-selective solvent. Macromol Chem Phys 2013;214:1569–79.
[122] Hou X, Li Q, He Y, Jia L, Li Y, Zhu Y, Cao A. Visualization of spontaneous aggregates by diblock poly(styrene)-b-poly(L-lactide)/poly(D-lactide) pairs in solution with new fluorescent CdSe quantum dot labels. J Polym Sci B: Polym Phys 2009;47:1393–405.
[123] Wang F, Lu X, He C. Some recent developments of polyhedral oligomeric silsesquioxane (POSS)-based polymeric materials. J Mater Chem 2011;21:2775–82.
[124] Li Z, Tan BH, Jin G, Li K, He C. Design of polyhedral oligomeric silsesquioxane (POSS) based thermo-responsive amphiphilic hybrid copolymers for thermally denatured protein protection applications. Polym Chem 2014;5:6740–53.
[125] Tan BH, Hussain H, He CB. Tailoring micelle formation and gelation in (PEG-P(MA-POSS)) amphiphilic hybrid block copolymers. Macromolecules 2011;44:622–31.

[126] Hussain H, Tan BH, Seah GL, Liu Y, He CB, Davis TP. Micelle formation and gelation of (PEG–P(MA-POSS)) amphiphilic block copolymers via associative hydrophobic effects. Langmuir 2010;26:11763–73.
[127] Wang Z, Tan B, Hussain H, He C. pH-responsive amphiphilic hybrid random-type copolymers of poly(acrylic acid) and poly(acrylate-POSS): synthesis by ATRP and self-assembly in aqueous solution. Colloid Polym Sci 2013;291:1803–15.
[128] Rathi SR, Coughlin EB, Hsu SL, Golub CS, Ling GH, Tzivanis MJ. Effect of midblock on the morphology and properties of blends of ABA triblock copolymers of PDLA-mid-block-PDLA with PLLA. Polymer 2012;53:3008–16.
[129] Nagahama K, Aoki R, Saito T, Ouchi T, Ohya Y, Yui N. Enhanced stereocomplex formation of enantiomeric polylactides grafted on a polyrotaxane platform. Polym Chem 2013;4:1769–73.
[130] Cai Q, Wan Y, Bei J, Wang S. Synthesis and characterization of biodegradable polylactide-grafted dextran and its application as compatilizer. Biomaterials 2003;24:3555–62.
[131] Nouvel C, Dubois P, Dellacherie E, Six JL. Silylation reaction of dextran: effect of experimental conditions on silylation yield, regioselectivity, and chemical stability of silylated dextrans. Biomacromolecules 2003;4:1443–50.
[132] Nouvel C, Dubois P, Dellacherie E, Six JL. Controlled synthesis of amphiphilic biodegradable polylactide-grafted dextran copolymers. J Polym Sci B: Polym Phys 2004;42:2577–88.
[133] Nouvel C, Frochot C, Sadtler V, Dubois P, Dellacherie E, Six JL. Polylactide-grafted dextrans: synthesis and properties at interfaces and in solution. Macromolecules 2004;37:4981–8.
[134] Nouvel C, Ydens I, Degée P, Dubois P, Dellacherie E, Six JL. Partial or total silylation of dextran with hexamethyldisilazane. Polymer 2002;43:1735–43.
[135] Thanki PN, Dellacherie E, Six JL. Prevailing mechanisms of the hydrolytic degradation of oligo(D,L-lactide)-grafted dextrans. Eur Polym J 2005;41:1546–53.
[136] de Jong SJ, De Smedt SC, Demeester J, van Nostrum CF, Kettenes-van den Bosch JJ, Hennink WE. Biodegradable hydrogels based on stereocomplex formation between lactic acid oligomers grafted to dextran. J Control Release 2001;72:47–56.
[137] de Jong SJ, De Smedt SC, Wahls MWC, Demeester J, Kettenes-van den Bosch JJ, Hennink WE. Novel self-assembled hydrogels by stereocomplex formation in aqueous solution of enantiomeric lactic acid oligomers grafted to dextran. Macromolecules 2000;33:3680–6.
[138] de Jong SJ, van Nostrum CF, Kroon-Batenburg LMJ, Kettenes-van den Bosch JJ, Hennink WE. Oligolactate-grafted dextran hydrogels: detection of stereocomplex crosslinks by X-ray diffraction. J Appl Polym Sci 2002;86:289–93.
[139] Nagahama K, Shimizu K, Ichimura S, Takahashi A, Ouchi T, Ohya Y. Biodegradable stereocomplex materials of polylactide-grafted dextran exhibiting soft and tough properties in dry and wet states. J Polym Sci B: Polym Phys 2012;50:2669–76.
[140] Hennink WE, De Jong SJ, Bos GW, Veldhuis TFJ, van Nostrum CF. Biodegradable dextran hydrogels crosslinked by stereocomplex formation for the controlled release of pharmaceutical proteins. Int J Pharm 2004;277:99–104.
[141] van Nostrum CF, Veldhuis TFJ, Bos GW, Hennink WE. Tuning the degradation rate of poly(2-hydroxypropyl methacrylamide)-graft-oligo(lactic acid) stereocomplex hydrogels. Macromolecules 2004;37:2113–8.
[142] Ishihara K, Tsuji T, Sakai Y, Nakabayashi N. Synthesis of graft copolymers having phospholipid polar group by macromonomer method and their properties in water. J Polym Sci B: Polym Phys 1994;32:859–67.
[143] Ishihara K, Nomura H, Mihara T, Kurita K, Iwasaki Y, Nakabayashi N. Why do phospholipid polymers reduce protein adsorption? J Biomed Mater Res 1998;39:323–30.
[144] Watanabe J, Eriguchi T, Ishihara K. Cell adhesion and morphology in porous scaffold based on enantiomeric poly(lactic acid) graft-type phospholipid polymers. Biomacromolecules 2002;3:1375–83.
[145] Watanabe J, Ishihara K. Higher water intrusion property on novel porous matrix composed of bioinspired polymer stereocomplex for tissue engineering. Chem Lett 2003;32:192–3.
[146] Takami K, Watanabe J, Takai M, Ishihara K. Spontaneous formation of a hydrogel composed of water-soluble phospholipid polymers grafted with enantiomeric oligo(lactic acid) chains. J Biomater Sci Polym Ed 2011;22:77–89.
[147] Buescher JM, Margaritis A. Microbial biosynthesis of polyglutamic acid biopolymer and applications in the biopharmaceutical, biomedical and food industries. Crit Rev Biotechnol 2007;27:1–19.
[148] Zhu Y, Akagi T, Akashi M. Preparation and characterization of nanoparticles formed through stereocomplexation between enantiomeric poly(γ-glutamic acid)-graft-poly(lactide) copolymers. Polym J 2012;45:560–6.
[149] Brzeziński M, Biela T. Polylactide nanocomposites with functionalized carbon nanotubes and their stereocomplexes: a focused review. Mater Lett 2014;121:244–50.
[150] Brzeziński M, Bogusławska M, Ilčíková M, Mosnáček J, Biela T. Unusual thermal properties of polylactides and polylactide stereocomplexes containing polylactide-functionalized multi-walled carbon nanotubes. Macromolecules 2012;45:8714–21.
[151] Purnama P, Jung Y, Kim SH. Melt stability of 8-arms star-shaped stereocomplex polylactide with three-dimensional core structures. Polym Degrad Stab 2013;98:1097–101.
[152] Cordes DB, Lickiss PD, Rataboul F. Recent developments in the chemistry of cubic polyhedral oligosilsesquioxanes. Chem Rev 2010;110:2081–173.
[153] Zhang W, Muller AHE. A "Click Chemistry" approach to linear and star-shaped telechelic POSS-containing hybrid polymers. Macromolecules 2010;43:3148–52.
[154] Sun Y, Yang L, Lu X, He C. Biodegradable and renewable poly(lactide)-lignin composites: synthesis, interface and toughening mechanism. J Mater Chem A 2015;3:3699–709.
[155] Kim YS, Kadla JF. Preparation of a thermoresponsive lignin-based biomaterial through atom transfer radical polymerization. Biomacromolecules 2010;11:981–8.
[156] Chung YL, Olsson JV, Li RJ, Frank CW, Waymouth RM, Billington SL, Sattely ES. A renewable lignin–lactide copolymer and application in biobased composites. ACS Sustain Chem Eng 2013;1:1231–8.
[157] Spitalsky Z, Tasis D, Papagelis K, Galiotis C. Carbon nanotube–polymer composites: chemistry, processing, mechanical and electrical properties. Prog Polym Sci 2010;35:357–401.
[158] Treacy MMJ, Ebbesen TW, Gibson JM. Exceptionally high Young's modulus observed for individual carbon nanotubes. Nature 1996;381:678–80.
[159] Hwang GL, Hwang KC, Shieh YT, Lin SJ. Preparation of carbon nanotube encapsulated copper nanowires and their use as a reinforcement for Y–Ba–Cu–O superconductors. Chem Mater 2003;15:1353–7.
[160] Tseng CH, Wang CC, Chen CY. Functionalizing carbon nanotubes by plasma modification for the preparation of covalent-integrated epoxy composites. Chem Mater 2007;19:308–15.
[161] Akagi T, Fujiwara T, Akashi M. Inkjet printing of layer-by-layer assembled poly(lactide) Stereocomplex With Encapsulated Proteins. Langmuir 2014;30:1669–76.
[162] Slager J, Domb AJ. Stereocomplexes based on poly(lactic acid) and insul formulation release studies. Biomaterials 2002;23:4389–96.
[163] Ajiro H, Kuroda A, Kan K, Akashi M. Stereocomplex film using triblock copolymers of polylactide and poly(ethylene glycol) retain paxlitaxel on substrates by an aqueous inkjet system. Langmuir 2015;31:10583–9.
[164] Kondo K, Kida T, Ogawa Y, Arikawa Y, Akashi M. Nanotube formation through the continuous one-dimensional fusion of hollow nanocapsules composed of layer-by-layer poly(lactic acid) stereocomplex films. J Am Chem Soc 2010;132:8236–7.
[165] Li Z, Yuan D, Jin G, Tan BH, He C. Facile layer-by-layer self-assembly toward enantiomeric poly(lactide) stereocomplex coated magnetite nanocarrier for highly tunable drug deliveries. ACS Appl Mater Interfaces 2016;8:1842–53.
[166] van de Weert M, Hoechstetter J, Hennink WE, Crommelin DJA. The effect of a water/organic solvent interface on the structural stability of lysozyme. J Control Release 2000;68:351–9.
[167] van de Weert M, van't Hof R, van der Weerd J, Heeren RMA, Posthuma G, Hennink WE, Crommelin DJA. Lysozyme distribution and conformation in a biodegradable polymer matrix as determined by FTIR techniques. J Control Release 2000;68:31–40.
[168] Ouchi T, Kontani T, Ohya Y. Modification of polylactide upon physical properties by solution-cast blends from polylactide and polylactide-grafted dextran. Polymer 2003;44:3927–33.
[169] Bos GW, Hennink WE, Brouwer LA, den Otter W, Veldhuis TFJ, van Nostrum CF, van Luyn MJA. Tissue reactions of in situ formed dextran hydrogels crosslinked by stereocomplex formation after subcutaneous implantation in rats. Biomaterials 2005;26:3901–9.
[170] Fundador NGV, Takemura A, Iwata T. Structural properties and enzymatic degradation behavior of PLLA and stereocomplexed PLA nanofibers. Macromol Mater Eng 2010;295:865–71.
[171] Ishii D, Ying TH, Mahara A, Murakami S, Yamaoka T, Lee Wk, Iwata T. In vivo tissue response and degradation behavior of PLLA and stereocomplexed PLA nanofibers. Biomacromolecules 2009;10:237–42.

[172] Li Y, Fukushima K, Coady DJ, Engler AC, Liu S, Huang Y, Cho JS, Guo Y, Miller LS, Tan JP, Ee PL, Fan W, Yang YY, Hedrick JL. Broad-spectrum antimicrobial and biofilm-disrupting hydrogels: stereocomplex-driven supramolecular assemblies. Angew Chem Int Ed 2013;52:674–8.
[173] Han Y, Jiang W. Self-assembly of the AB/BC diblock copolymer mixture based on hydrogen bonding in a selective solvent: a Monte Carlo study. J Phys Chem B 2011;115:2167–72.
[174] Palyulin VV, Potemkin II. Mixed versus ordinary micelles in the dilute solution of AB and BC diblock copolymers. Macromolecules 2008;41:4459–63.
[175] Tsuji H, Ikada Y. Stereocomplexation between enantiomeric poly(lactide)s. In: Yu L, editor. Biodegradable polymer blends and composites from renewable resources. New York: John Wiley & Sons Inc.; 2009. p. 163–90.
[176] Liu H, Chen F, Liu B, Estep G, Zhang J. Super toughened poly(lactic acid) ternary blends by simultaneous dynamic vulcanization and interfacial compatibilization. Macromolecules 2010;43:6058–66.
[177] Ye S, Lin TT, Tjiu WW, Wong PK, He C. Rubber toughening of poly(lactic acid): effect of stereocomplex formation at the rubber–matrix interface. J Appl Polym Sci 2013;128:2541–7.
[178] He C, Donald AM, Butler MF. In-situ deformation studies of rubber toughened poly(methyl methacrylate): influence of rubber particle concentration and rubber cross-linking density. Macromolecules 1998;31:158–64.
[179] Purnama P, Kim SH. Bio-based composite of stereocomplex polylactide and cellulose nanowhiskers. Polym Degrad Stab 2014;109:430–5.